NASA Technical Paper 2258

December 1983

Space Shuttle Exhaust Cloud Properties

B. J. Anderson
and V. W. Keller

NASA

25th Anniversary
1958-1983

NASA
Technical
Paper
2258

1983

Space Shuttle Exhaust Cloud Properties

B. J. Anderson
and V. W. Keller

George C. Marshall Space Flight Center
Marshall Space Flight Center, Alabama

NASA
National Aeronautics
and Space Administration

**Scientific and Technical
Information Branch**

1983

ACKNOWLEDGMENTS

We wish to acknowledge the support and contributions of the numerous personnel and organizations who made this report possible; NASA Headquarters, Kennedy Space Center, Johnson Space Center, the Air Force Space Division, Cape Canaveral A.F.S. Weather Station, the Occupational and Environmental Health Laboratories at Brooks AFB, the A.F. Geophysics Laboratories at Hanscom AFB, the NOAA Research Facilities Center, the NOAA Hurricane Research Division, and the Universities Space Research Association, as well as personnel within the many offices and laboratories of the Marshall Space Flight Center. Special recognition is due to Dr. Al Koller Jr., Dr. Bill Knott, and Mr. Bill Cox of the KSC Bioenvironmental Office and the staff of the Bionetics Corporation for their support of the measurements program at KSC, and to Capt. Jeppie Compton, USAF/SD; Mr. Terry Allen of Martin-Marietta, Vandenberg Operations; Mr. David Bowdle, USRA; Lt. Col. Dennis Naugle and Major Doug Swobota of OEHL for important technical suggestions. Mr. Stan Guest, Harrold Davis and Bruce Glick of MSFC Systems Dynamics Laboratory, Lamar Thompson and staff of MSFC Test Laboratory, and Alice Dorries of MSFC Space Science Laboratory all made significant contributions to the tests and analysis at the Marshall Center.

We gratefully acknowledge the use of a NOAA P-3 cloud physics instrumented aircraft for the STS-3 exhaust cloud study. Dr. C. B. Emmanuel NOAA, RFC, Director and Dr. James McFadden made the aircraft available on short notice. The entire NOAA, RFC staff and crew were most helpful. We owe special thanks to Mr. Terry Schricker and Mr. Brad Patten for insuring that the necessary special instrumentation was installed and operational and to Mr. Fred Werly and Mr. Lowell Genzlinger for ably piloting the aircraft. Thanks are due Dr. Stanley Rosenthal, Mr. Robert Black and Mr. Neal Dorst NOAA Hurricane Research Division for assistance in data acquisition and processing.

This research was initiated and supported by Dr. Andrew Potter of the JSC Space Science Branch and Dr. Paul Wetzel, NASA Headquarters. It was conducted under the direction of Dr. William Vaughan and Dr. Robert E. Smith, MSFC Atmospheric Sciences Division, Systems Dynamics Laboratory. For the support and cooperation of these many personnel and organizations the authors wish to express their gratitude.

TABLE OF CONTENTS

TECHNICAL MEMORANDUM

SPACE SHUTTLE EXHAUST CLOUD PROPERTIES

I. EXECUTIVE SUMMARY

After the initial launch of the Space Transportation System, STS-1, on April 12, 1981, a light fallout of acidic particles was detected as far as 7.4 km from the launch pad by the Kennedy Space Center environment monitoring effort [1]. Prior to this, concerns regarding environmental damage due to the Shuttle's exhaust products centered on possible effects from noxious gases, contamination of nearby lagoons by the deluge and washdown water from the launch pad; and other related land and water quality issues. Two concerns related to weather modification were addressed: (1) acid rain resulting from natural precipitation from higher clouds passing through the stabilized ground cloud and washing out hydrogen chloride, and (2) precipitation enhancement or suppression due to mixing of the exhaust cloud with a natural convective cloud. The Kennedy Space Center environmental impact statement also mentions the possibility that "Depending on atmospheric conditions, the exhaust cloud could entrain enough water to generate a light rain or mist," [2] but the point was not considered in detail, apparently because the impact was expected to be highly local and dependent on the local weather at launch time. The light acidic fallout observed following the launch of STS-1 was not associated with any natural clouds. Thus, this type of deposition was not expected.

This study was undertaken at the request of the Space Environment Office at the Johnson Space Center because of the observations at the STS-1 launch. The primary objective was to define the production mechanism for the fallout from STS-1 and subsequent launches. The secondary objective was to investigate other possible forms of weather modification which could result from the Shuttle exhaust products. The study consists of a field measurement program to define the properties of the exhaust and fallout and an analysis of this data base. An existing two-dimensional cloud model has been utilized to investigate several aspects of the problem but no extensive statistical or numerical modeling has been undertaken. This report summarizes both the data base and the analysis.

A. Measurements and Observations

In the following paragraphs special observations and measurements made for specific launches are listed and the most significant points for each launch are noted. A variety of data recorded on a routine basis at KSC in conjunction with Shuttle launches, especially the KSC Environmental Monitoring effort, have proved exceedingly valuable in this study. Most significant of these are the L-zero meteorological data, cloud photography with time and azimuth recorded, pH papers from the KSC environment monitoring field array, and in-cloud measurements by the Langley Center's instrumented aircraft. These sources provide the only data available on STS-1 effects. On STS-2 through 4 they provide a valuable supplement to the copper plate array, near pad, and aircraft measurements which form the basis of this study.

1. STS-1; April 12, 1981

Significant observations are as follows:

1) Deposition of acidic particulates up to 7.4 km from pad 39A on pH papers and foliage. Damage on leaves covered up to 40 percent of the surface on one species at a site 5 km from the pad [1].

2) Each deposition particle was composed of a cluster of many smaller spherical particles plus an unknown quantity of liquid. The small particles ranged from submicron to about 30 microns [1].

3) Analysis of photographs indicated that the top of the ground cloud rose between 5 and 6 m s^{-1}, indicating updrafts sufficient to lift drops in excess of 1 mm diameter. Falling trails of precipitation were visible under the ground cloud as soon as it lifted above the surface. These were observable for about 8 min.

4) Lift-off photographs showed a definite color difference between the portion of the cloud in the flame trenches and the direct exhaust from the vehicle. This indicates that the deluge water spray had a significant impact on the composition of the cloud.

5) Relative humidity at the pad was 82 percent and there was no precipitation near launch time. Although higher humidities and patches of ground fog were observed at the Shuttle strip and Cape Canaveral A.F.S. weather stations, there was no indication that natural fog or clouds played a role in producing the deposition.

2. STS-2; November 12, 1981

The objective of the STS-2 measurement effort was primarily to become familiar with the KSC launch environment and to test new ideas, preparing the way for a major field study during STS-3. A set of readily available instruments was set up on the north side of the pad near the perimeter fence. Also, about 50 copper clad sampling plates were deployed along with the KSC environment monitoring equipment at their array of field monitoring sites. The plates effectively provided a measure of the wet particle size for the deposition as well as a backup indication of their pH (in addition to the KSC pH papers). The Langley aircraft sampled the cloud using a PMS Inc. 1-D cloud probe to measure particle size distributions in the range 30 to 300 microns diameter.

Significant observations were as follows:

1) A sample of liquid collected from the polyethelene sheet covering the instrument shelter at the pad perimeter site had a pH $\leqslant$ 0.5, verifying that the gaseous HCl from the exhaust is rapidly scavenged by water.

2) STS-2 was launched on a relatively dry day (61 percent RH) with brisk northerly winds, 7.6 m s^{-1} from 320 deg at the surface, 8.5 m s^{-1} from 25 deg at 1000 m. The copper plates detected acidic fallout with a mean diameter of 870 microns, about 0.5 hits cm^{-2}, at 8 km south of the pad. At 20 km, fewer than 0.04 hits cm^{-2} were detected; mean diameter was about 200 microns. At the pad perimeter site it was evident that the deposition was composed of a significant fraction of liquid. The dry, clear conditions preclude the possibility that natural clouds or fog played a role in producing the deposition.

3) Both the pH papers and the copper plates indicated that the pH of the deposition was less than 1. (The pH papers indicated higher values, between 2 and 3.5, at ranges beyond 12 km but this is probably an artifact caused by the drop sizes. The copper plates only indicated that these drops contained a lower fraction of liquid, not that it was less acidic.) No vegetation damage was found in the far field, apparently because of enhanced evaporation due to the high winds and low humidity [3].

3. STS-3; March 22, 1982

The major measurement effort during the STS-3 launch employed NOAA's WP-3D Orion hurricane research aircraft from the Research Facilities Center, Miami, Florida. Penetrations of the exhaust cloud were made to obtain a wide spectrum of cloud microphysical data. In addition to the extensive instrumentation normally available on the aircraft (Table IIc-2), special arrangements were made through the State University of New York at Albany and Universities Space Research Association (USRA) to have Aitken, cloud condensation and ice nuclei measured with instruments provided and operated by Dr. Garland Lala and Dr. Gerhard Langer. On the ground a 3-m platform was erected at the pad perimeter in line with the SRB flame trench and instrumented with wind and temperature recording equipment (MSFC) and three PMS probes for measuring particle size distributions and concentrations (Air Force Geophysical Laboratories, Hanscom Field, MA). Copper plates were deployed as before along with the KSC environmental monitoring equipment.

Significant observations were as follows:

1) The acidic deposition occurred again, very similar to the two previous launches. However, the winds carried the cloud directly out to sea so only the small area near the pad and the beach was affected.

2) The pH of drops sampled by pH paper in the modified foil impactor on the aircraft was under 0.5.

3) Updrafts as high as 4.0 m s^{-1} were detected in the cloud on each of the first three aircraft passes, up to 9 min after launch. A 4.0 m s^{-1} updraft will lift a 900 micron diameter drop.

4) Ice nuclei concentrations measured at -20°C in the cloud were not significantly greater than those measured in the surrounding ambient air.

5) Maximum wind speed in the exhaust measured on the tower at the pad perimeter was 35 m s^{-1}. Maximum temperature was 47.3°C. This implies that damage to vegetation beyond the perimeter fence is due to acid burns, not heat.

4. STS-4; June 27, 1982

Significant observations were as follows:

1) Deposition collected on copper plates and pH papers was similar to prior launches. Again the cloud moved almost directly out to sea so far-field deposition could not be recorded.

2) A sample of the deposition collected under mineral oil on the pad perimeter tower was composed of approximately 30 percent solids and 70 percent liquid by volume. A meter test gave a pH reading of 0.36 which implies an acid concentration of about 0.4 N, but subsequent analysis by titration showed the acid concentration to be 2.36 N. This indicates that pH meters and papers are not adequate methods for measuring the true acidity of the deposition. However, pH papers are very useful for detecting where fallout occurs.

5. 6.4 Percent Model Tests, May 17, 20, 24, and June 4, 1982

Static test firings of a 6.4 percent model of the Shuttle's Solid Rocket Booster were conducted at the Marshall Center in late May and early June 1982. The tests modeled only a single SRB, not the main engines. The pad was configured to model the Western Test Range (Vandenberg) configuration; deluge water was modeled at design flow rate (May 17) and fractions thereof. The exhaust clouds from the tests were observed and recorded with IR sensitive video and 35 mm still photography. Copper clad plates and pH papers were deployed in a field array for detecting fallout.

Significant observations were as follows:

1) Acidic fallout was detected after each firing. The reaction of the copper plates appeared identical to the Shuttle launches, although the spot sizes were generally smaller for the model. The pH papers indicated the fallout pH was under 0.5.

2) On the May 20 test, fallout occurred at least 300 m from the pad. On June 4 it was detected up to 550 m.

3) On the May 17 test (baseline WTR water flowrate, 6:30 p.m. CDT, 24°C ambient temperature, 70 percent RH) the cloud dissipated within 1 min and deposition reached only 160 m from the stand. This demonstrates that the deposition forms very quickly in or near the flame trench.

B. Conclusions

Analysis of these observations and the other supporting data forces the following conclusions concerning the properties of the Shuttle exhaust cloud and the associated production of acidic fallout:

1) The deposition is composed of liquid water (about 70 percent by volume except at extreme distances from the pad where evaporation may become significant), large numbers of small spherical aluminum oxide particles from the Solid Rocket Boosters, sufficient HCl to lower the pH to less than 0.5, plus trace materials.

2) The deluge water spray, atomized by the vehicle exhaust, is the primary source of liquid water in the deposition. This atomization is the controlling mechanism in the formation of the fallout drops.

3) Water from the SRBs and main engines and the vaporized portion of the deluge water primarily serve to raise the humidity in the cloud to saturation; secondarily to increase cloud buoyancy. Thus, it affects the environment of the fallout but it does not enter into its formation in a significant way. Scavenging of small cloud particles may contribute a moderate fraction of the final mass of the fallout.

4) Given the absence of a very strong low level inversion, the exhaust has sufficient bouyancy to lift 1 mm drops (fallout) well into the atmosphere so that ambient winds can carry them moderate distances from the pad. Twenty-two kilometers is the maximum range observed to date (STS-2). Range and azimuth for fallout on a given launch day will depend almost exclusively upon the low level atmospheric stability and winds.

5) Since the fallout drops are produced on the pad by the exhaust – deluge interaction, atomization plus coagulation, one can expect it to occur with each launch. Barring changes in the vehicle or pad configuration, the total quantity of fallout material should remain relatively constant under normal atmospheric conditions.

6) Given adverse atmospheric conditions, a potential exists for the exhaust to mix with a natural precipitating cloud or to develop into a cloud with a sustained precipitation mechanism of its own. The result could be an acid rain event with significant impact. Several properties of the exhaust cloud work against this possibility – the high CCN concentration and low drop concentration in the 20 to 50 micron range, the rapid production and rise of the cloud which does not allow time for effective organization of the air flows – but it should not be assumed that the probability of such an event is negligible without further study. The potential for adverse effects is maximized when there are active convective clouds within a few kilometers of the pad.

7) Ice nucleus concentrations in the exhaust ground cloud are sufficiently low that weather modification by a "cloud seeding" interaction in a natural cloud is quite unlikely.

8) Given a launch into an atmosphere with a strong inversion, the ground cloud may become trapped near the surface.

II. DATA AND OBSERVATIONS

A. STS-1; April 12, 1981

The STS-1 launch pre-dates the initiation of this study. Available information is from the report of the environmental effects study group at KSC, the atmospheric environment (meteorology) report for STS-1 [4], and various photographs and video tapes of the launch. Of course, the most relevant fact is that an acidic fallout did occur. It was possible to map the area affected from vegetation damage on both native shrubs and control plants (radishes and pennywort), and from pH papers set in the field. The detection was complicated by several factors; the generally rough terrain, some of it water covered, a general drought which left the native plants in a relatively poor condition, dew or fog the night before which caused the pH paper dyes to run. However, the results clearly showed (Fig. IIa-1 adapted from Reference 1) a moderately extensive area covered by fallout ranging to over 7 km from the pad. The pH papers showed definite spotting from low pH material, distinct from a reaction to a gas, and so did the vegetation. One species sustained as much as 40 percent leaf damage due to spotting at a location 5 km NW of pad 39A [1].

There was no apparent influence of adverse weather in the production of the fallout. The launch occurred at 1200Z (0700 EST) on a warm, sunny morning; the only clouds were cirrus at 34,000 ft and contrails. Ground observing stations reported patches of ground fog but none is seen in the launch photos so it was apparently quite light or dissipated in the area near the launch pad. The relative humidity measured at the pad at L-0 was 82 percent, 92 and 93 percent at the ground observing stations. The L-0 sounding (Fig. IIa-2) shows dry air aloft and an inversion around 2000 m. Surface winds were southeasterly changing to east northeasterly above 1200 m so the exhaust cloud and fallout followed the coast toward the northwest.

Three other important pieces of information were obtained from STS-1, from photographs and video tape. First, several photos of the lift-off, especially the one reproduced in Figure IIa-3, showed that the portion of the exhaust cloud coming directly from the vehicle was much darker in color than

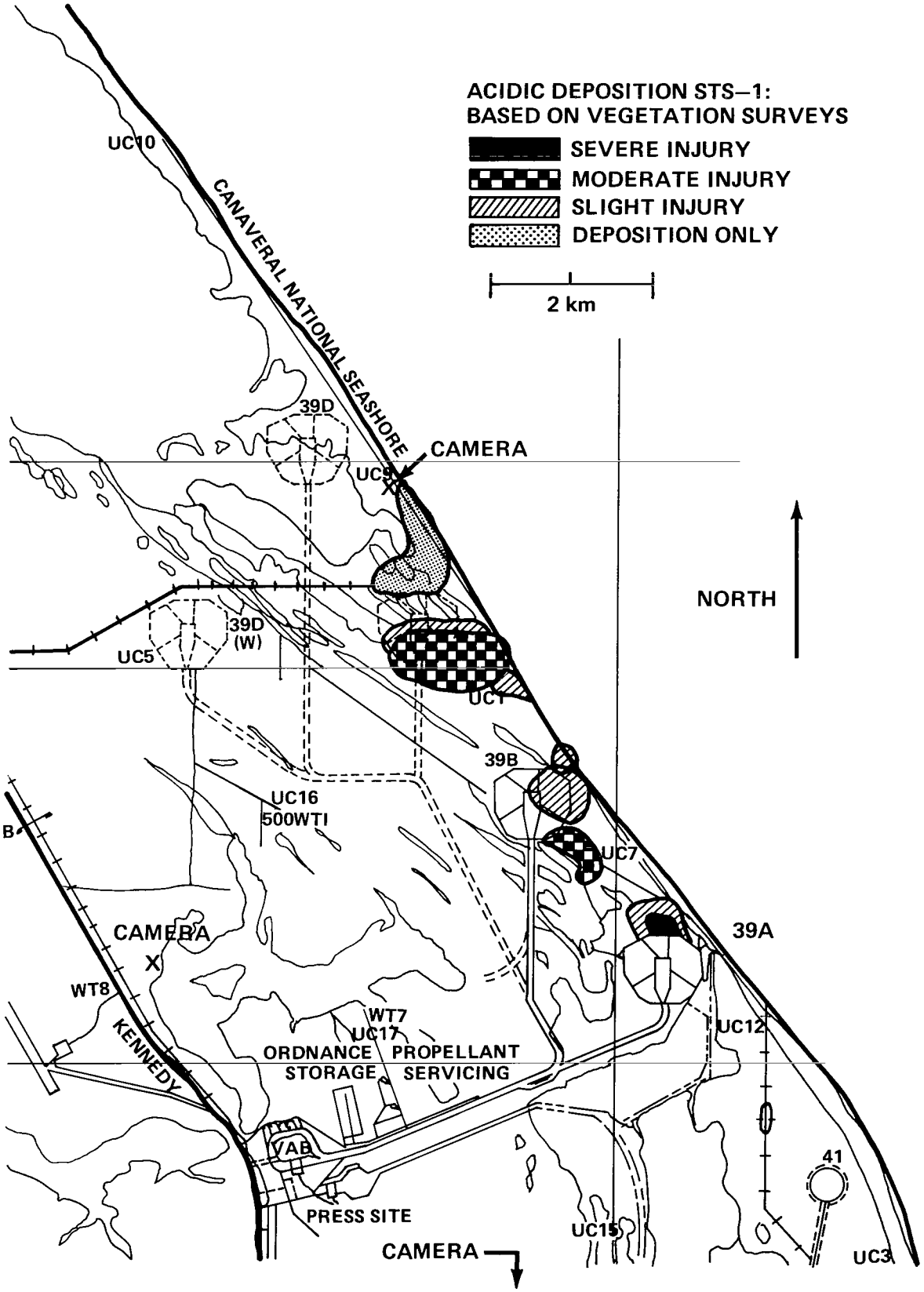

Figure IIa-1. Area of vegetation injury after STS-1 launch (from Ref. 1 with changes).

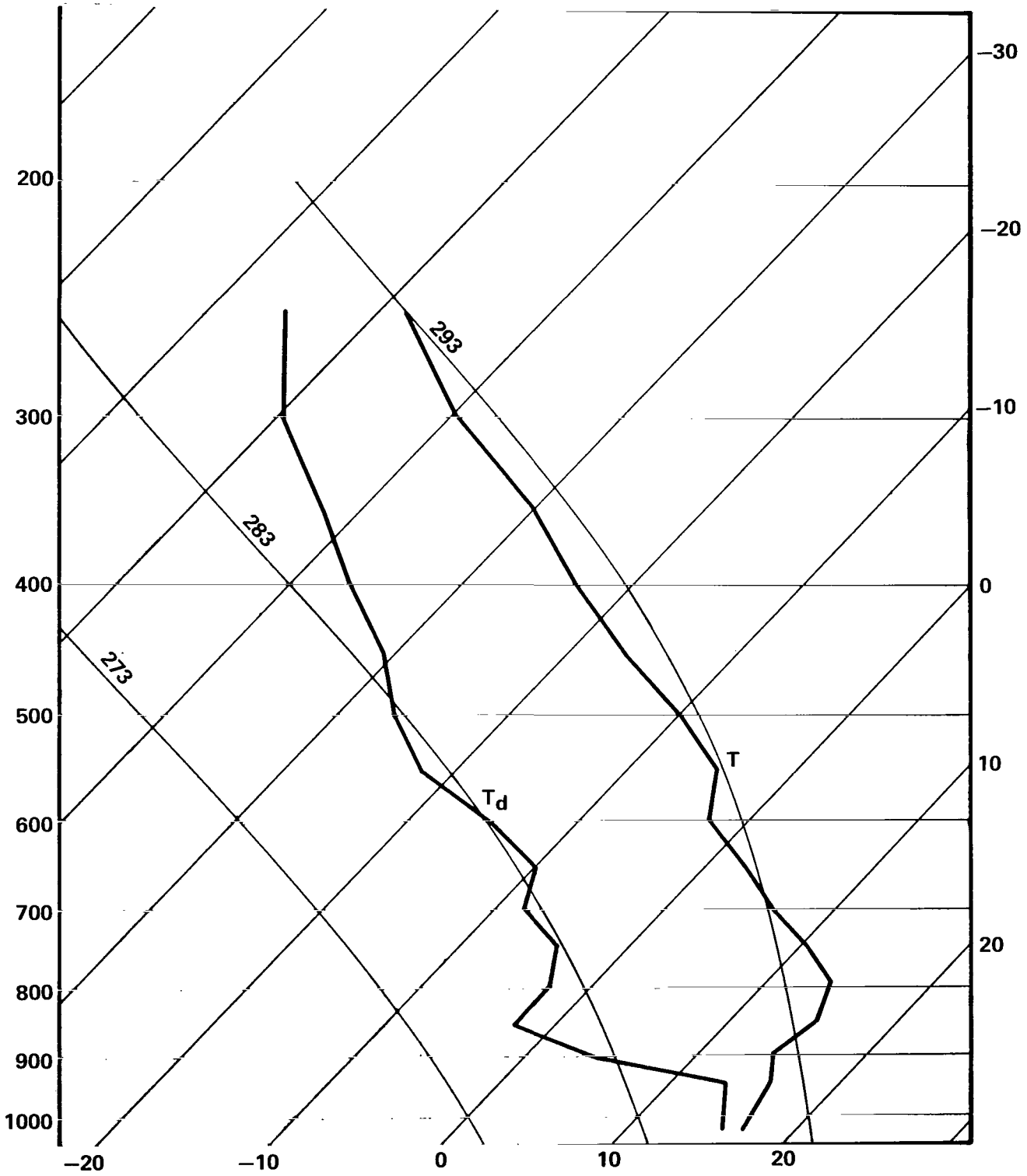

Figure IIa-2. L+0 meteorological sounding for STS-1 launch, April 12, 1981, 1200Z (0700 EST).

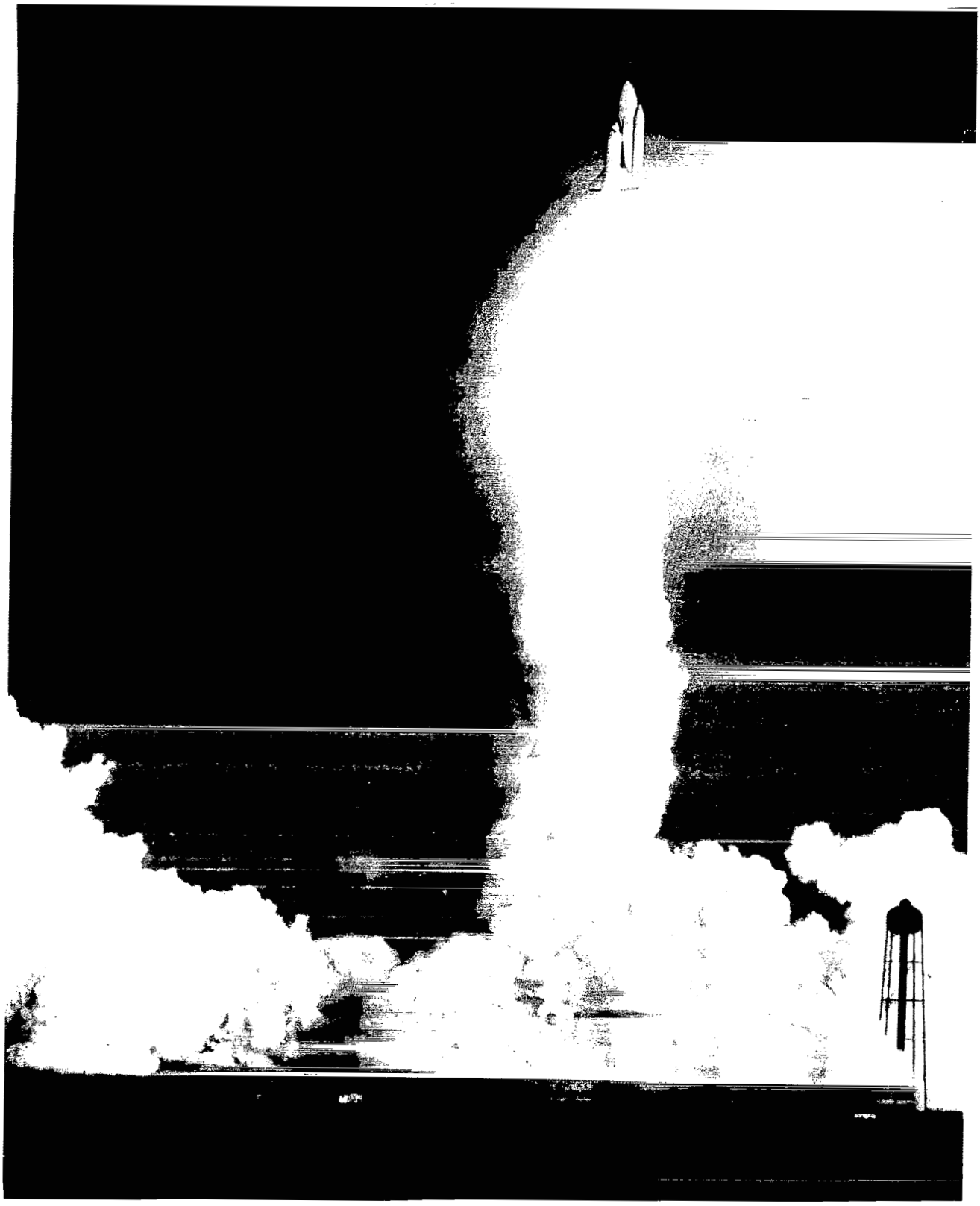

Figure IIa-3. STS-1 launch photo showing color differences in cloud from SSME flame trench (left), direct from vehicle (center), and from SRB flame trench (right).

the portion in or emerging from the flame trenches. The implication is that the deluge water sprayed into the trenches significantly altered the properties of the cloud. Second, from sets of photos taken of the cloud at 30 sec intervals from three widely spaced locations (Fig. IIa-1) it is possible to show that the cloud top rose at 6 to 9 m s^{-1}. Dimensions on the photographs were quantified by two methods, comparison with the height of the gantry on the pad and triangulation using maps and the separation between landmarks. This set showed that the top of the ground cloud rose for about 5 min, to a height of 1800 m. After that it settled slightly to stabilization with a top at about 1300 m and a base at 600 m. Virga was clearly visible under the cloud after the first few minutes. Initially the cloud hung near the surface where the sun angle made observation difficult, so fallout could not be definitely seen until the L+3 min mark. It lasted until about L+10 min.

B. STS-2; November 12, 1981

(with M. T. Reischel)

The measurement efforts for this study were initiated during the STS-2 launch. The objectives were to gain familiarity with the KSC launch working environment, to test some instrumentation and measurement methods, and to obtain data on the behavior of the Shuttle exhaust cloud in order to improve the chances for success during the STS-3 program. The study was composed of two primary efforts: the addition of copper settling plates to the KSC array of field monitoring sites, and instrumentation of a site near the pad with small size range aerosol counters, "maxometers" for measurement of the maximum wind velocity, and temperature and relative humidity sensors. The copper plates were deployed as a new method for obtaining information on the size, number concentration and pH of the acidic fall-out. The other instruments were deployed in the hostile near pad environment to test the feasibility of locating more delicate (and more appropriate) instruments in this area during the STS-3 program. In addition to these efforts, the usual observations of the cloud (visual, video, and photographic) and data collection by the KSC environment monitoring program were repeated. As it turned out, a power outage caused by a transformer failure in the KSC power distribution system at the pad prevented the aerosol counters at that site from operating. However, some information was obtained from the other instruments and from observations of the area. The most significant results from STS-2 came from the field array of copper plates and KSC pH papers. The strong northerly winds of that morning carried the fallout southward along the Banana River so that much of it fell over land within the field array. Since the fallout from launches 3 and 4 was carried directly out to sea, this represents the most complete data set on a fallout pattern.

1. Near-Pad Observations

STS-2 was launched at 10:10 a.m. EST November 12, 1981, a day with clear skies and brisk northerly winds. The relative humidity was only 61 percent at the pad, 63 and 67 percent at nearby observing stations [5]. It was also dry at all levels aloft, as indicated by the sounding (Fig. IIb-1). The surface winds (4.3 m level) were 7.6 m s^{-1} from 320 deg; 1000 m level winds were 8.5 m s^{-1} from 25 deg. The SRB flame trench is directed essentially due north on pad 39A, almost directly into the northerly wind which was blowing that morning. The pad area is level with the trench out to the perimeter fence and the cloud stayed near the ground that far. This is evident from both deposits of residue left on the fence and light poles at the pad perimeter, and from the video tapes taken by automated cameras at the pad. Beyond the perimeter fence the ground level (on the north side) drops abruptly about 2 m to the level of the lagoon. The instruments were located in this lower area, about 50 m from the fence and slightly west of the flame trench centerline. Observations in the instrument area following launch indicated that the strong winds came in under the cloud and kept it from reaching

the ground in this area. An unsheltered hygrothermograph showed only a very small increase in temperature (less than 2°F) and an increase in relative humidity from 73 to 83 percent. Very little, if any, residue was deposited on the side of objects facing the flame trench, but the sides opposite it were heavily coated. This indicates that the material was carried up past the instruments and blown back into the area. This was confirmed by the maxometer (maximum wind speed indicators) which did not show measurable deflections, i.e., wind speed less than 40 mph, indicating that the high velocity jet direct from the flame trench did not strike them.

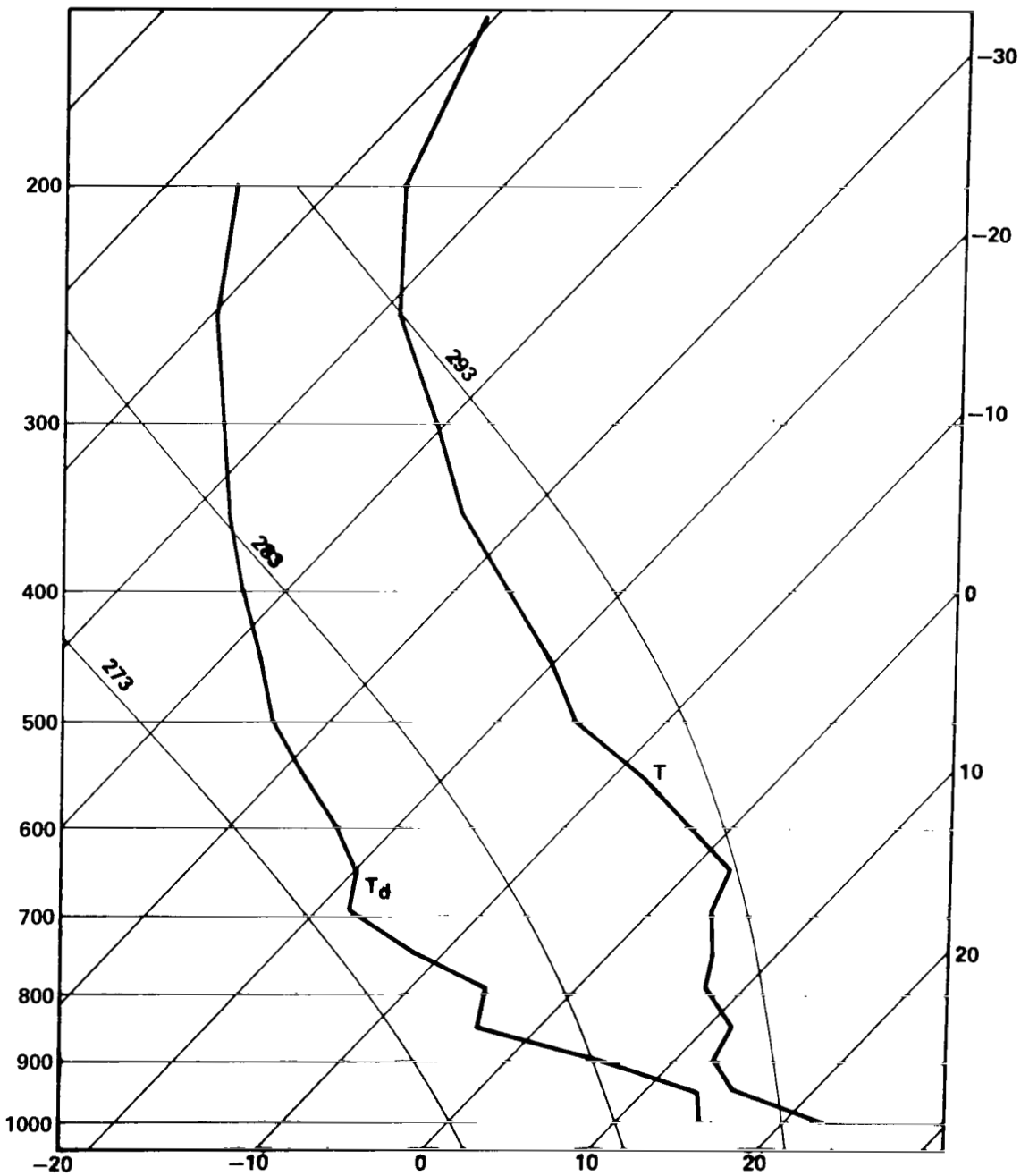

Figure IIb-1. L+0 meteorological sounding for STS-2 launch, November 12, 1981, 1510Z (1010 EST).

Figure IIb-2, a map of the KSC area, shows the area south of pad 39A where acidic fallout was detected by the copper plates. The small circles indicate the locations where the plates did not detect any acid, only some corrosion effects from contact with sea salt spray or background aerosol. Plates at the pad perimeter were uniformly darkened, presumably due to exposure to HCl gas. Small numbered squares indicate locations of plates which were lightly hit by the fallout drops. The numbers indicate the plate identification number; they can be used to index the spot size distributions presented later in this section. The larger square boxes over circles indicate locations of heavily hit plates.

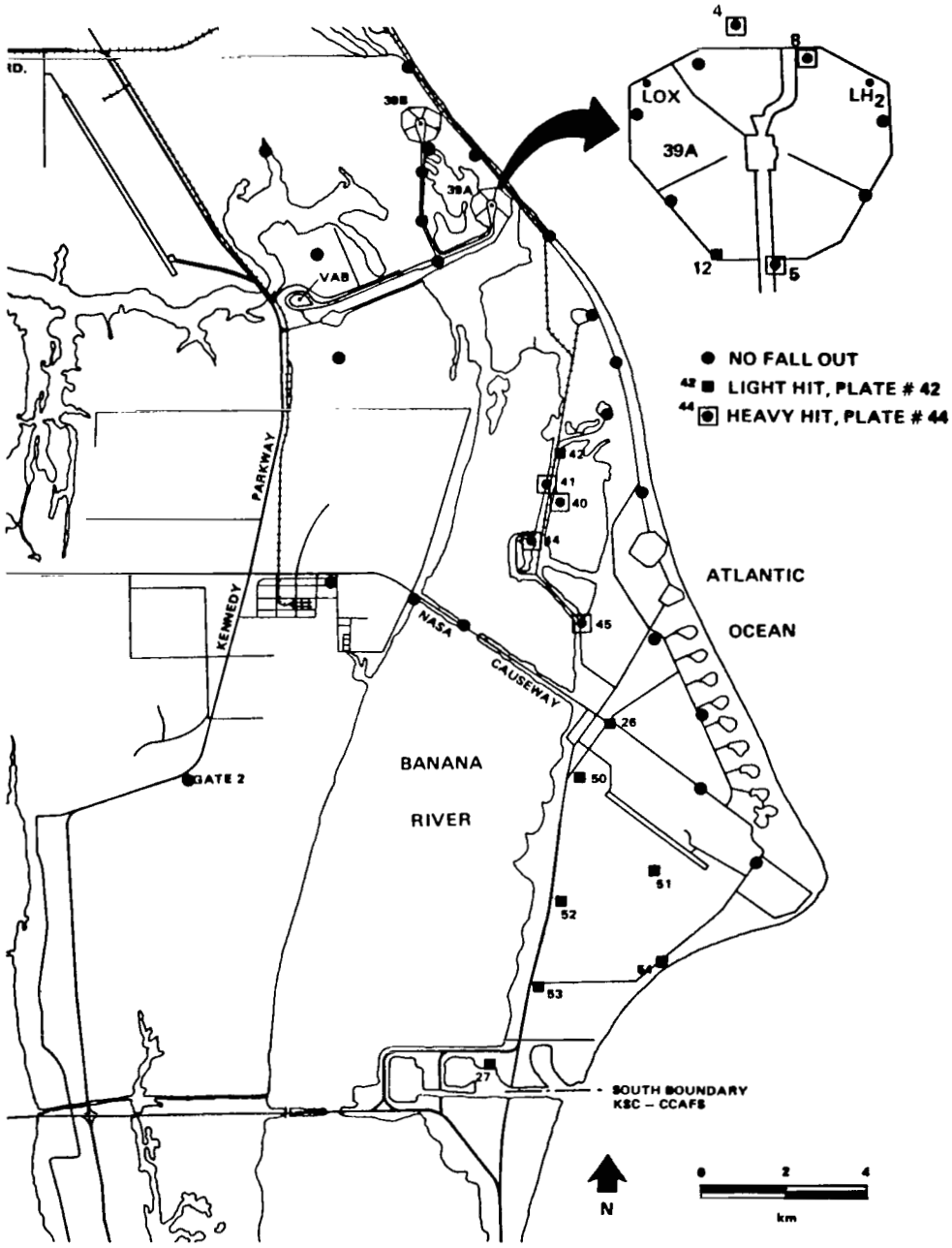

Figure IIb-2. Map of the KSC Cape Canaveral area indicating the acid deposition pattern detected by copper plates after the STS-2 launch.

Figure IIb-3 is a photograph of plate 41 taken at the deployment site in the Cape Canaveral Titan complex shortly after launch. The light colored streaks, or "spots", are the result of direct contact with the acidic liquid. The large halo around each spot is due to attack by vapor from the acid drop coupled with exposure to solar UV radiation. The extent of liquid contact is clearly defined by sharp ringlike features, while the area attacked by vapor is defined by diffuse features. It exceeds the area contacted by liquid by factors from 10 to 40. Nearest the drop the vapor produced mottled green and brown deposits; the mottled appearance is probably due to the secondary influence of the natural background. Beyond that the surface exhibits dark irridescent blues and violets.

Figure IIb-3. Photograph of a copper plate (No. 41) deployed about 7 km south of pad 39A, showing deposition from the STS-2 launch. The diameter of the hole in the center of the plate is 0.6 cm.

Comparison of the plates with the laboratory test samples available at the time revealed significant differences, although subsequent tests resolved most of the anomalies. The coloration in the vapor attacked area is about equivalent to that produced by reagent grade HCl acid having a concentration of 1 N dropped on a plate in full sunshine. Coloration of the field samples degraded rapidly with obvious changes occurring within 24 hr. Coloration of plates exposed in the laboratory is stable for weeks or even months. The difference is probably due to the background of sea salt, other aerosol, and of sulfur compounds in the KSC area. The winds on launch day made the drops flow a short distance across the plates and greatly enhanced their evaporation, thus reducing the available time for chemical reaction with the copper surface. All of these factors complicate the estimation of the acidity of the deposition. However, the extensive halo caused by the vapor forces us to the conclusion that the acid was quite concentrated, 0.1 N or greater in all cases. This corresponds to a pH of not more than 1.

Upon examination under an optical microscope the deposits were found to consist of a streak composed of white globular or spherical material. The deposit of white material was typically greatest at one end of the streak and decreased along the length of the streak. The central whitish deposit was surrounded by a darker ellipsoid shaped area with a well defined boundary. Figure IIb-4 shows a typical photomicrograph of deposits found on Plate 50. The width of the streak is 0.38 mm. The microscopic and visual analysis of the deposits on the plates suggested that the streaks were produced by liquid drops which contained solid material before impact.

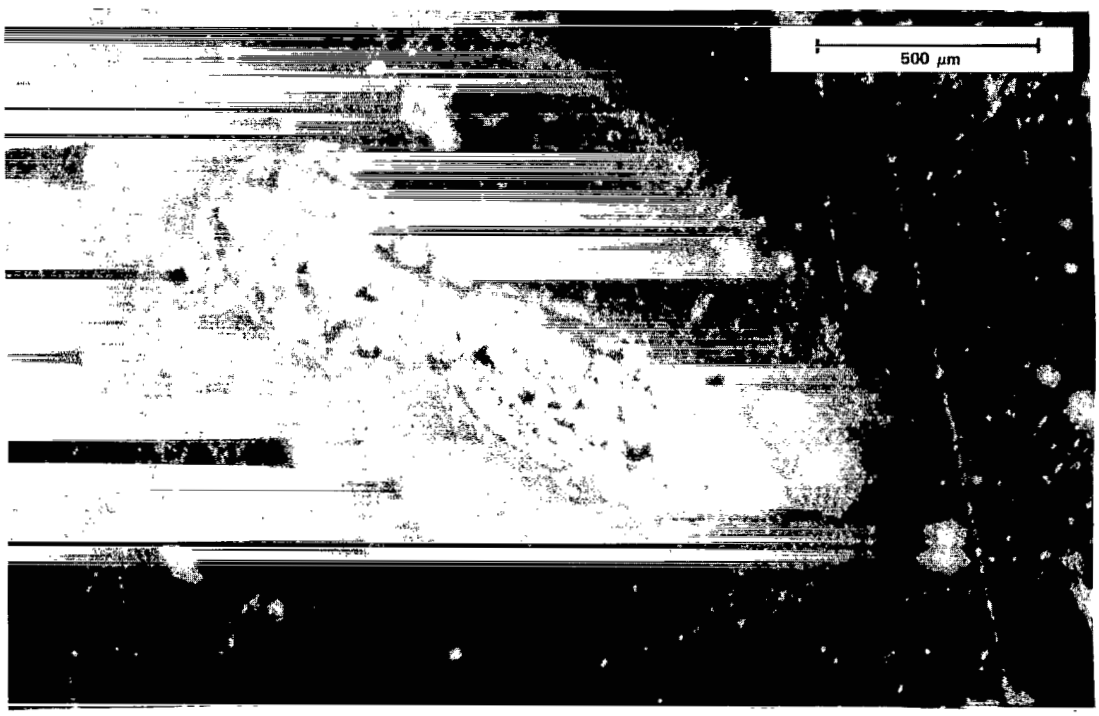

Figure IIb-4. Photomicrograph of deposit on copper plate No. 50 which was located 14.5 km from the pad during the STS-2 launch.

Electron micrographs were taken of plates 50, 27, and 45. An example, in this case from an STS-4 plate, is shown in Figure IIb-5. They show that the central streak is composed of spherical particles. Analysis of these particles using an X-ray energy dispersive spectrometer indicated that they were composed of aluminum or, almost certainly, aluminum compounded with a light element (perhaps oxygen). By performing the X-ray spectrometer analysis using a magnification of 4000 X, the surface

Figure IIb-5. Mosaic electron micrograph of a deposition spot on a plate near the pad perimeter during the STS-4 launch. Spherical particles are Al_2O_3, tetrahedral crystals are copper chloride or a related compound from reaction of HCl with substrate. (Electron microscopy by Alice Dorries)

of the spherical aluminum particles could be analyzed without obtaining background counts from the surface of the copper plate. The size of the spherical aluminum particles observed on the various copper plates typically covered the range from submicron to greater than 50 microns in diameter.

Using high magnification the electron micrographs also showed that the colored rings which define the perimeter of the streaks, Figure IIb-4, are composed of individual particles of tetrahedral form and typical sizes of 3 to 4 microns diameter. The X-ray energy dispersive spectra taken for these particles using a magnification of 10,000 X show that copper and chlorine are the main constituents with some silicon, calcium, and sulfur also being indicated. Silicon, sulfur, chlorine, and calcium were also found on background plates (i.e., plates exposed and collected prior to launch). The absence of background counts of copper from the surface of the plate when looking at the spherical aluminum particles using an analysis magnification of 4000 X, and the presence of copper when using an analysis magnification of 10,000 X is not conclusive evidence that the copper detected was in the particle rather than background. However, the tetrahedral particles are very similar to the reaction products found in the laboratory after evaporation of drops of 1 N reagent HCl from the surface of identically prepared copper plates. Thus we suggest that they are copper chloride crystals which result from the following sequence of events. The HCl acid drops dissolve copper from the copper plate surface to form copper chloride solution. The solution becomes enriched and finally supersaturated with copper chloride as the drop evaporates. Copper chloride crystals nucleate and grow in the enriched solution, their habit (i.e., shape) being primarily determined by the magnitude of the supersaturation existing in the solution. As the crystals grow they deplete the supply of copper chloride in the solution and the crystal habit changes from needles to more equiaxed (i.e., tetrahedral) particles.

Elemental analysis of the various features of the deposits found on Plates 50, 27, and 45 may be summarized as follows:

1) The spherical particles found in the central streak were composed primarily of aluminum and chlorine; some silicon and calcium was also found. (Oxygen is too light to be detected by this method.)

2) The outer rings were typically rich in chlorine with little or no aluminum or silicon present.

3) Sulfur was present primarily in the outer ring material and also appeared on the background plates.

Figures IIb-6 and IIb-7 show the drop size distributions (spot widths) obtained from analysis of five copper plates. The plate locations are given in Figure IIb-2. As one would expect, the general trend is for both the number concentration (hits/area) and mean size to decrease with increasing range from the pad. Two additional plates (distributions not shown) which were located at ranges of 16.2 km (Plate 51) and 20.4 km (Plate 27) only showed 0.034 total hits cm^{-2} (230 micron mean diameter) and 0.033 hits cm^{-2} (220 micron mean diameter) respectively.

C. STS-3; March 22, 1982

STS-3 was launched at 1600 Z (11:00 a.m. EST) on March 22, 1982, in almost perfect weather. The only notable meteorological observation was four-tenths cover of thin strato-cumulus clouds with bases near 550 m located over the pad and to the west. Photography from a NASA T-38 chase plane (Fig. IIc-7) showed that the vehicle passed directly through one of these small clouds. Above this thin layer the atmosphere was dry and stable as the sounding (Fig. IIc-1) illustrates. Winds were light and

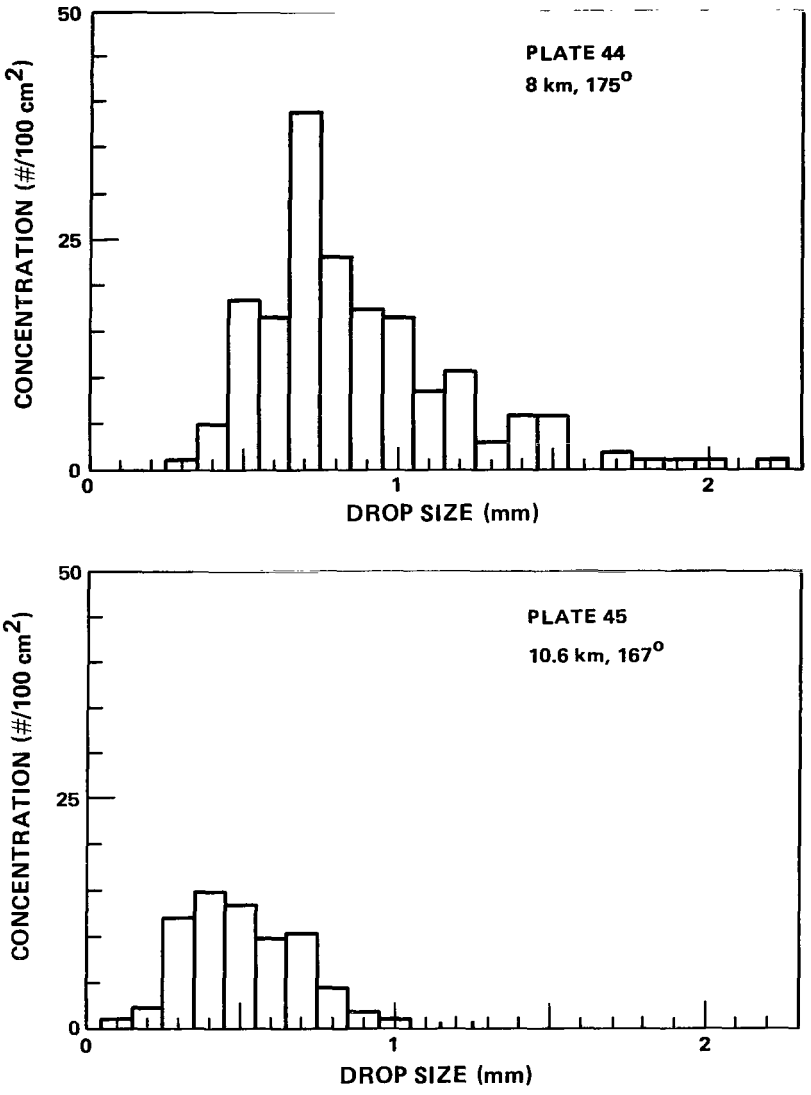

Figure IIb-6. Deposition drop diameters estimated to be equal to the spot width at two far field locations after STS-2.

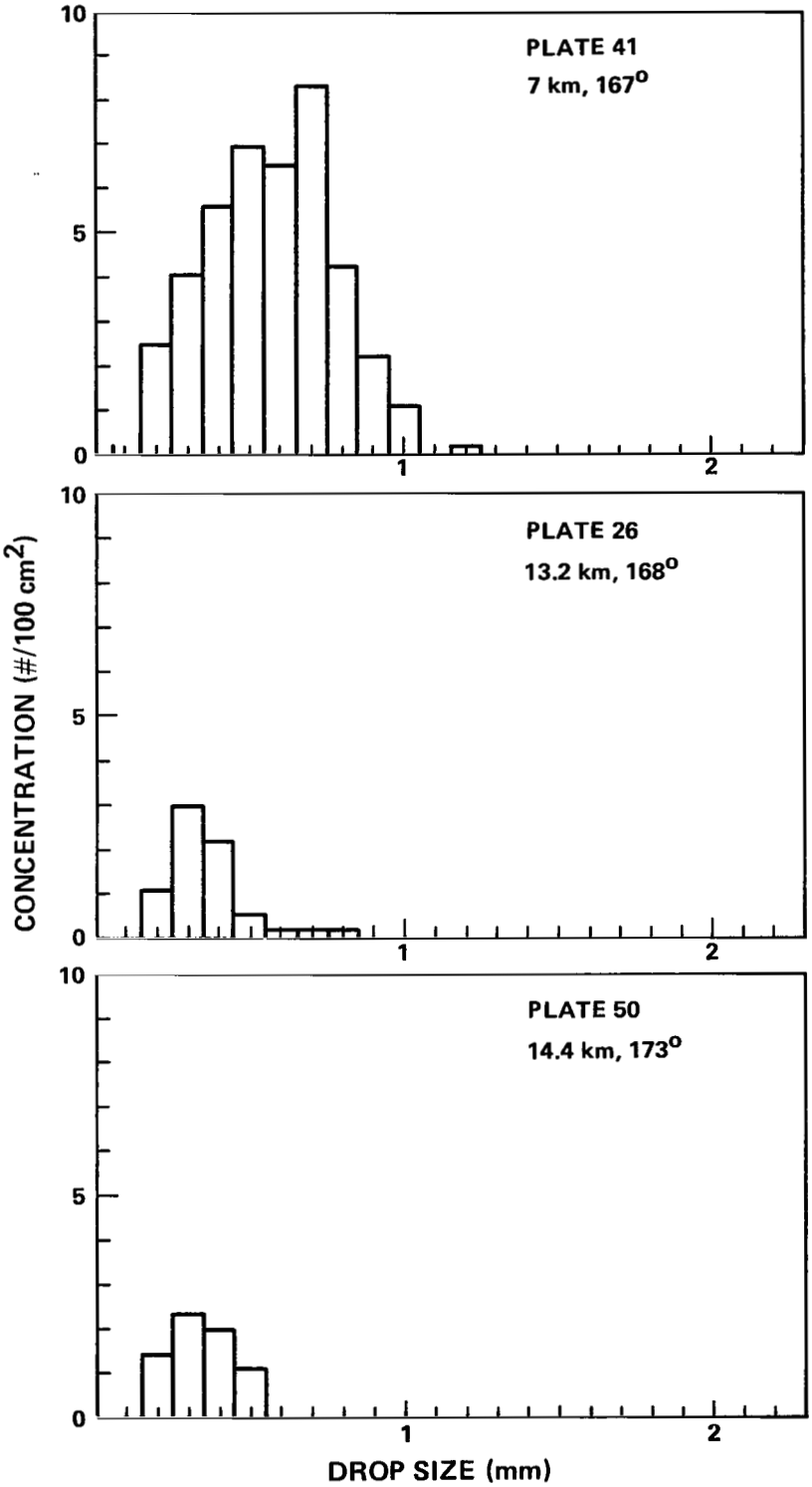

Figure IIb-7. Additional drop diameter distributions from STS-2, plates at greater range.

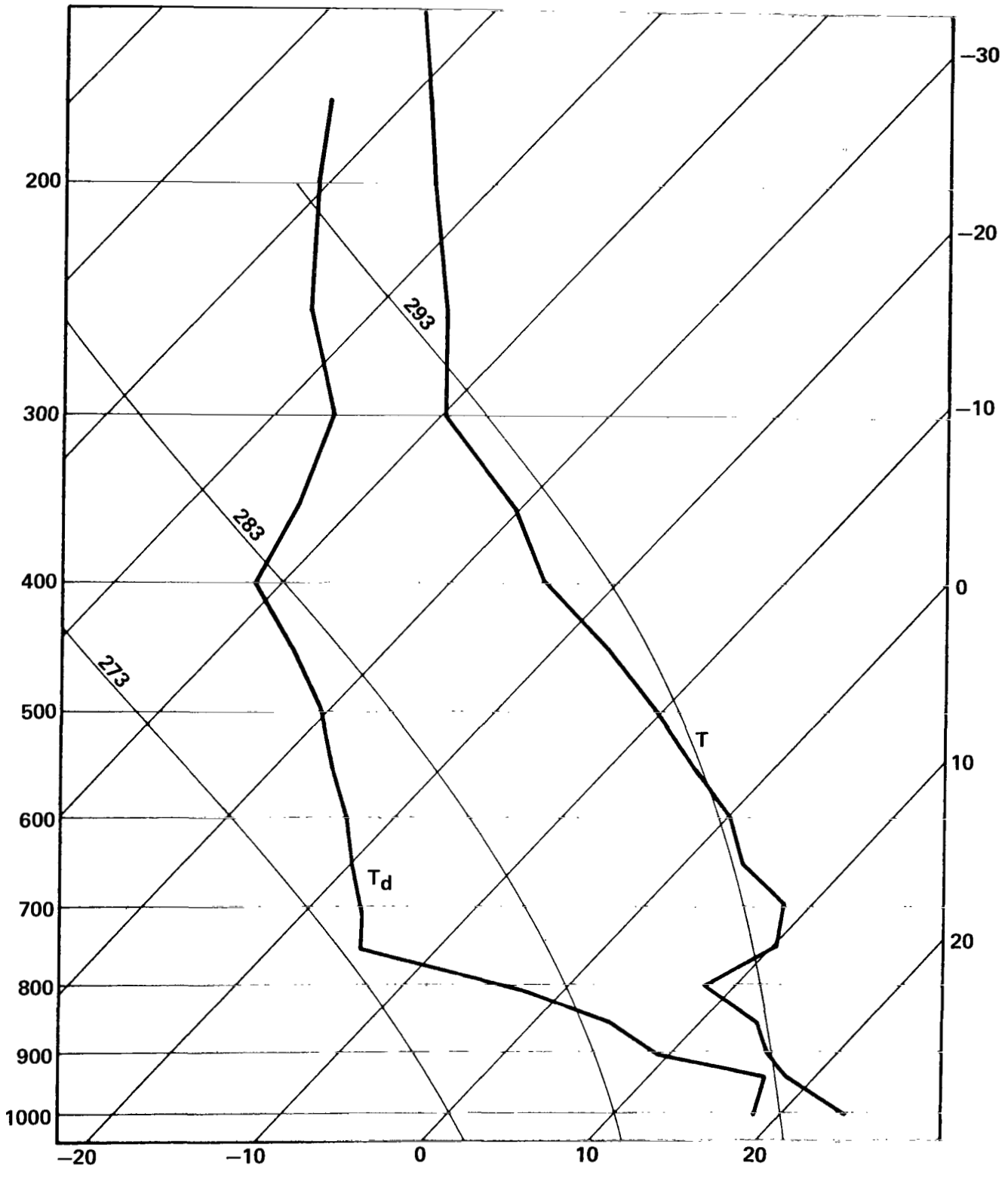

Figure IIc-1. L+0 meteorological sounding for STS-3, March 22, 1982, 1600Z (1100 EST).

westerly for the hours preceding launch. Just a few minutes prior to launch the sea breeze began to set up, so that surface winds (60 m) were turned around to easterly to northeasterly at L–0 [7]. L–0 surface (60 m) winds were 2.1 m s^{-1}. Aloft the speed increased slowly with height. They were about 5.8 m s^{-1} at 1000 m. Wind direction exhibited some variation with height but westerly flow was dominant above 600 m.

1. Ground Observations

Ground instrumentation was required to meet two primary objectives in the STS-3 measurement program: characterize the fallout in terms of size, pH, location and quantity, and characterize the size distribution and other properties of the cloud near the source, before it was extensively modified by the ambient atmosphere and the various microphysical processes occurring within it. Copper plates, along with the KSC environmental monitoring program's pH papers and vegetation survey, were deployed to meet the first objective. To meet the second a 3 m high instrument platform was erected at the pad perimeter and equipped with a variety of devices. The platform was located on the north side of the pad 4.5 m beyond the perimeter fence in direct line with the SRB flame trench. Unfortunately, this location has proved very hostile to instrumentation and the tower measurements were only partially successful.

Acidic fallout occurred again with STS-3 just as with the prior launches. In this case the westerly winds in all but the lowest levels carried the cloud (and fallout) to the east, directly out to sea. The center of the pad is only 700 m from the shoreline so only a limited amount of land was exposed (Fig. IIc-2). Deposits were found in a 1100 m long stretch along the shore. The fallout was easy to trace in this area because the tan granular solids left from the drops are easily seen on the rusted railroad track that parallels the shoreline east of the pad. It was estimated in the field that the greatest concentration on the track was 5 to 8 hits per cm^2 with diameters of the powder patterns ranging up to 4 mm. Figure IIe-1 is an illustration of similar deposits on a rusted metal plate after a model test firing.

As Figure IIc-2 illustrates, light deposits were also detected on copper plates and pH papers west of the pad, along the road to pad 39B. This fallout must have been present in the cloud at low elevations and outside the primary updraft, since it could not have been carried far above 600 m into the westerly air flow and still reach this resting place. The spot patterns on these and the other copper plates hit after STS-3 were essentially the same as found after STS-2. The spots did not show the great elongation that was evident on STS-2, rather they were nearly circular as one would expect in the gentle ambient winds. Because of this circularity the assumptions used on STS-2 to transform spot sizes to drop sizes are not valid for this case. Therefore, the experiments described in section IIF of this report were performed and the transform [equation (II-1)] was obtained. Figure IIc-3 illustrates drop and spot size distributions for a few of the STS-3 plates. The mode size for the plates corresponds closely to the mode size from the STS-3 aircraft measurements described below but the drop sizes are generally smaller than those observed at greater range from STS-2. Since the corresponding near field data is missing from STS-2 (that area south of the pad is a lagoon) and most of the STS-3 fallout was out over the ocean, it seems premature to look for an explanation for this apparent anomaly.

The primary instruments set up on the tower at the pad perimeter, the "flame trench" site, were three Particle Measuring Systems, Inc., probes provided under contract by the Air Force Geophysics Laboratory, Hanscom AFB, Massachusetts. The probes were an ASSP, a 1-D cloud probe, and a 1-D precipitation probe for measurement of cloud particle size distributions and concentration in the ranges from 2 to 30, 20 to 300, and 300 to 4500 microns, respectively. Unfortunately the data from these instruments was lost, apparently because a power transient brought down the recording device. Complementary to this, MSFC installed three thermistor temperature probes and a Belfort Model 5-120

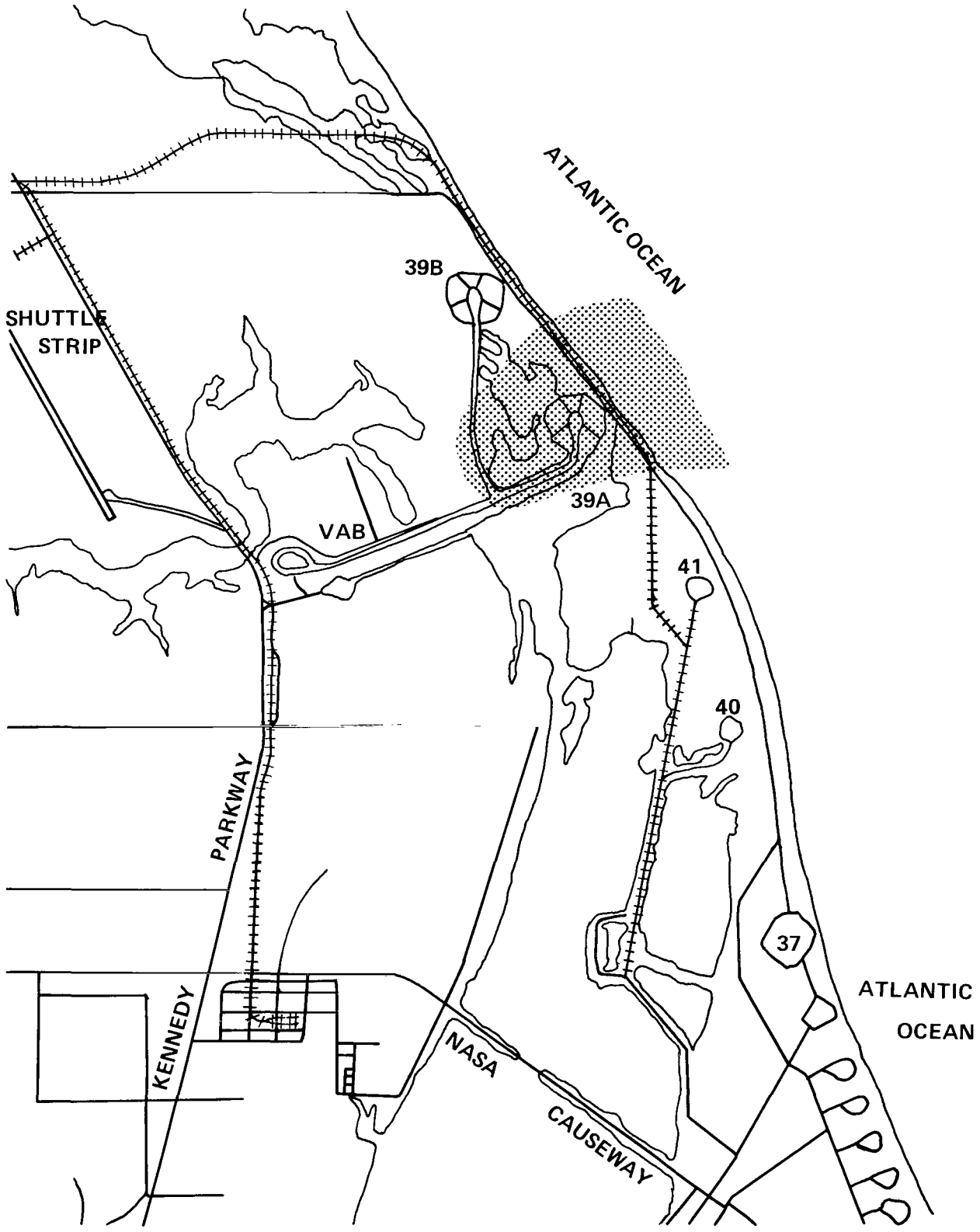

Figure IIc-2. Area exposed to acidic deposition from the launch of STS-3. Even though the primary flow was eastward, over the ocean, there was sufficient westward flow at the surface to carry deposition as far as the road to complex 39B.

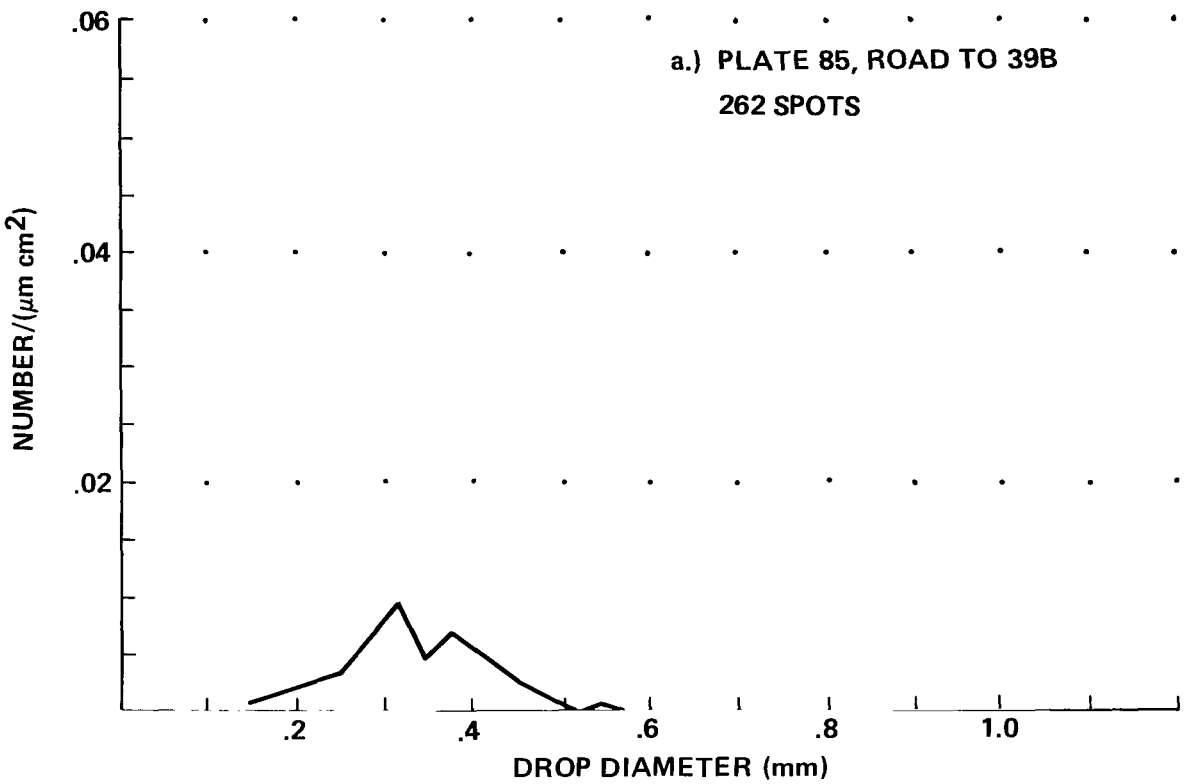

Figure IIc-3. Size spectra of deposition drops deduced by automated image analysis of copper plates deployed during the STS-3 launch. (a) shows the distribution of smaller drops blown inland by the low level westerly winds; plates (b) through (g) were located either at the 39A pad perimeter or along the coast road between the pad and the beach. The automated system misses the small particles and undercounts the large ones. (c) shows an automated image analysis spectrum (heavy line) overlaid on two spectra made manually on the same plate. The two manual counts were made of the same drops, one to the inside (light solid line) and the other to the outside (dashed line) of the broad ring that defines the drop perimeter. The curve for the minimum (inside) drop dimension was artificially truncated at 0.4 mm so the large number of smaller sized drops shows only in the maximum dimension (dashed line) curve. Where two curves are given for the same plate (d and f) they represent a second automated count on the same plate under different illumination (changed polarization).

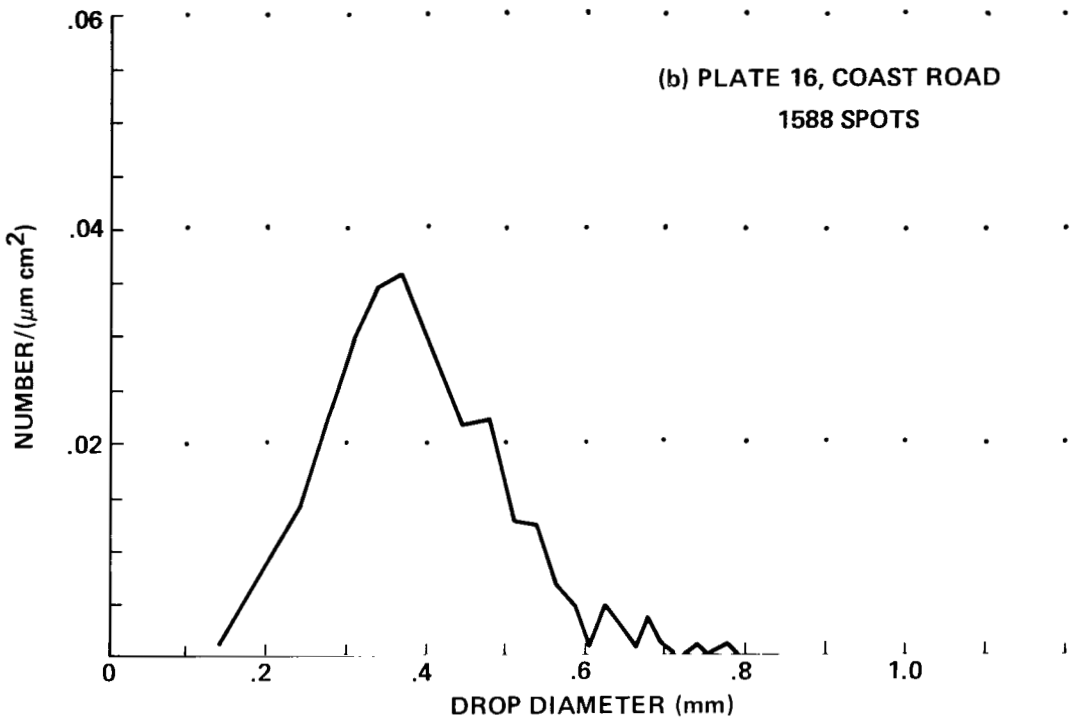

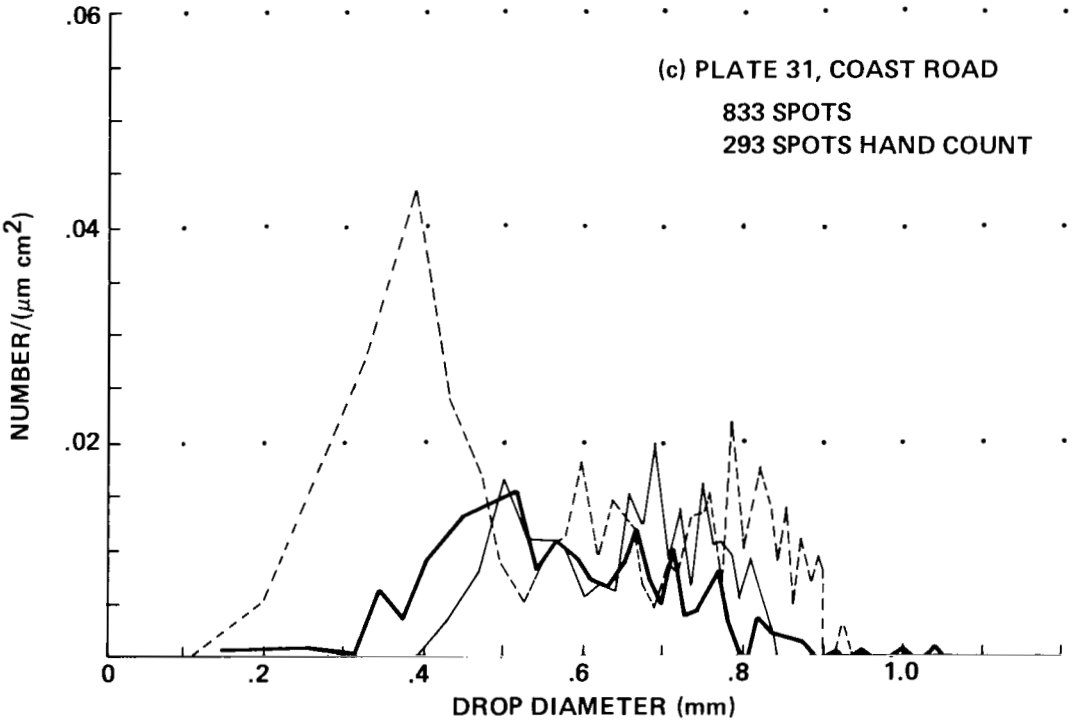

Figure IIc-3. (Continued)

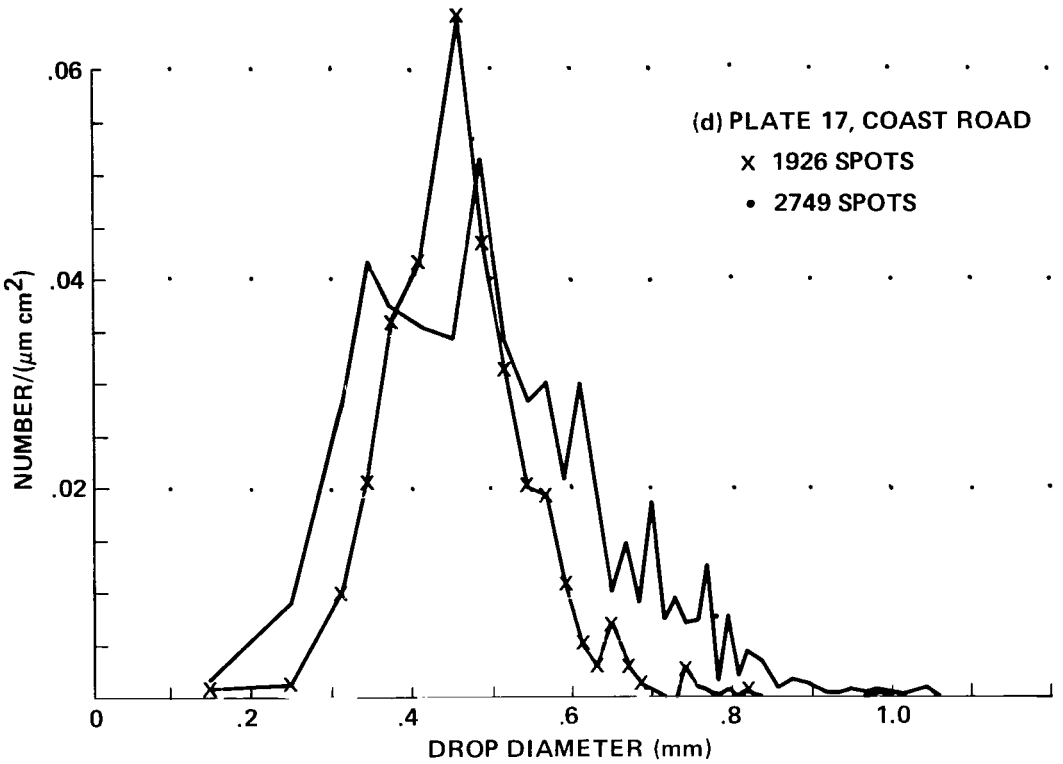

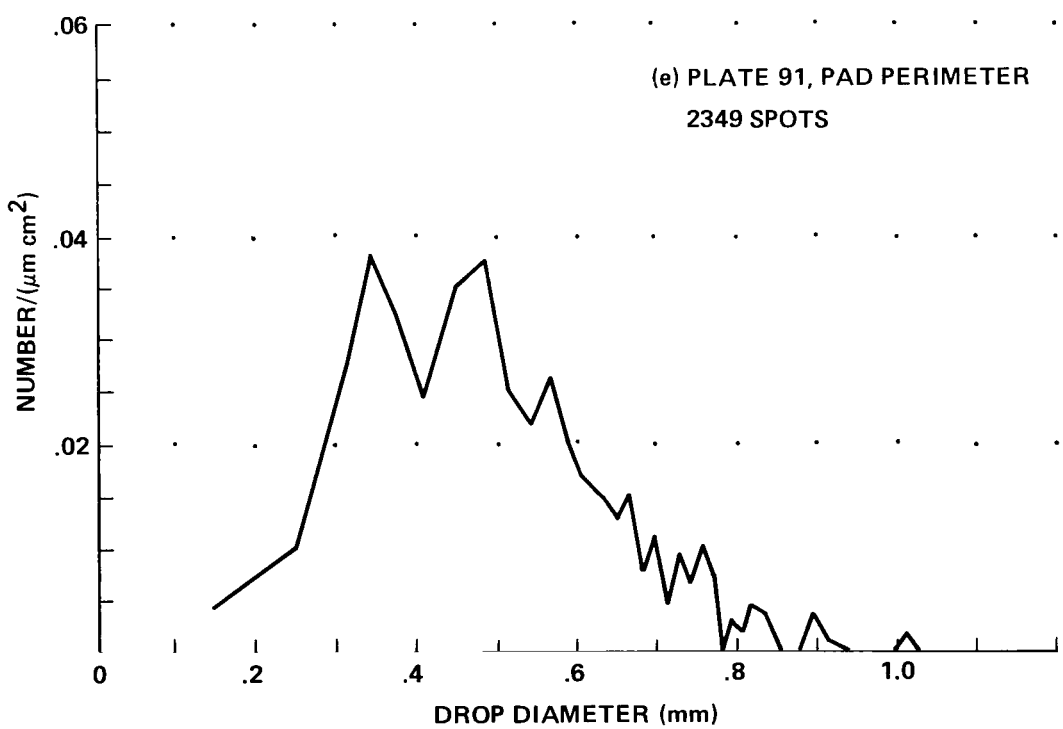

Figure IIc-3. (Continued)

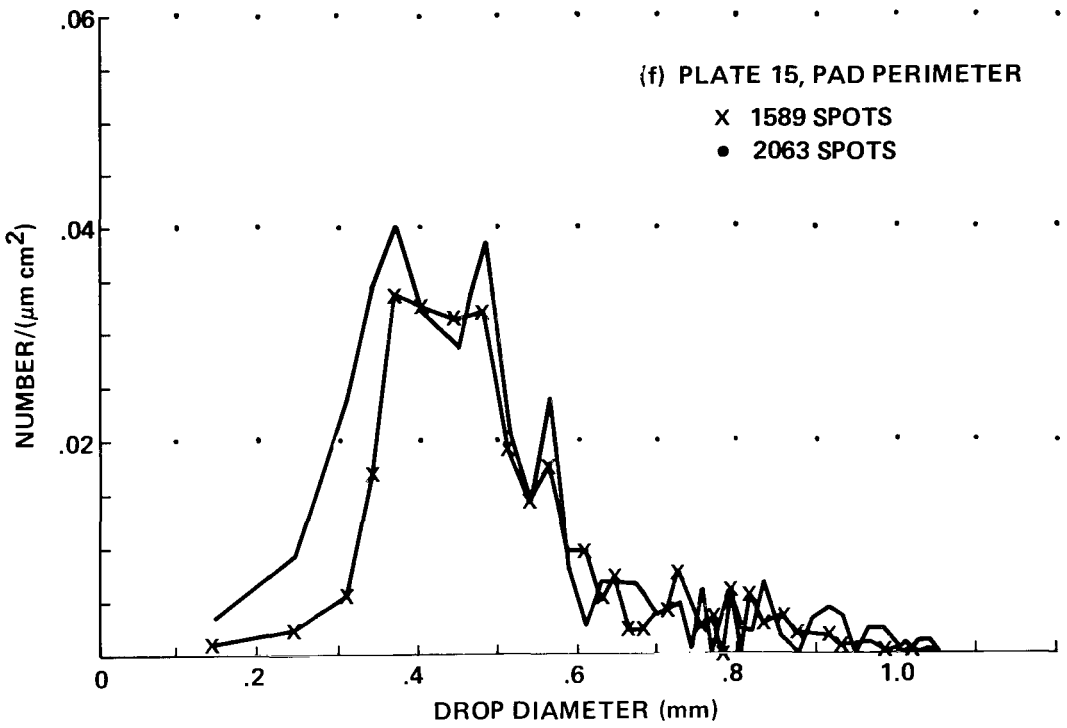

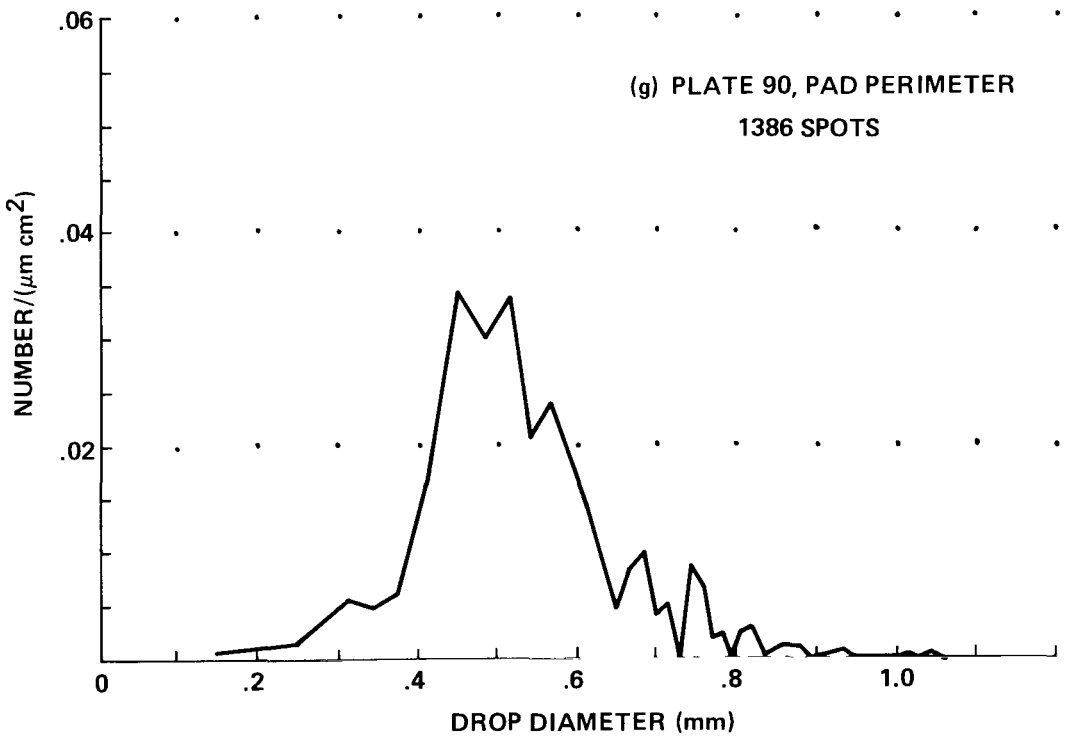

Figure IIc-3. (Concluded)

anemometer with a separate microprocessor based data system. Both recorders failed because of the intense noise levels at the site (140 db estimated) but one survived long enough to record the first 12-sec data block after launch. The data are shown in Table IIc-1. The wind transients were more rapid than expected before launch so the once every 4 sec recording frequency is not really adequate, but it was partially forced by availability of hardware and design constraints set to optimize the chances of success.

TABLE IIc-1. AIR SPEED AND TEMPERATURES FOR STS-3, FLAME TRENCH SITE

Time	L-1s	L+3s	L+7s	L+11s
1 m Temperature (°C)	23.7	23.8	45.5	44.1
3 m Temperature (°C)	23.0	22.6	46.4	44.4
5.5 m Temperature (°C)	24.1	24.0	47.3	45.6
Air Speed (m s^{-1})	2.2	10.9	34.6	9.7
Wind Direction	31	159	214	159

Notes: Temperature locations are above tower base which sits approximately 1 m below the run-out grade from the flame trench. 1 m thermistor was on the north (back) side of the pole; 3 m was in the shade under the instrument platform; 5.5 m was taped to the lightning rod, in open air.

2. Aircraft Observations

For STS-3 a WP-3D Orion cloud physics instrumented aircraft (NOAA 43, Fig. IIc-4) from the National Oceanic and Atmospheric Administration's (NOAA) Research Facilities Center, Miami, Florida, was contracted by MSFC to make in-situ cloud microphysical measurements. A list of the relevant onboard instrumentation is given in Table IIc-2. An air intake system was added specifically for this flight for the aerosol measurements. Outside air was drawn through the cabin and sampled from the aerosol manifold shown in Figure IIc-5. This system was designed to allow sampling from either a continuous flow or from a 70 liter electrically conductive Velostat sampling bag. After passing through the manifold in the cabin the sample air stream was vented to the outside. Extra precautions were taken to prevent rocket exhaust HCl gas from being released inside the aircraft cabin. This system was used for the cloud condensation nucleus (CCN), Aitken nucleus, and ice nucleus (IN) measurements.

Dr. Garland Lala, the State University of New York (SUNY), Albany, New York, under contract to MSFC provided and operated the CCN, Aitken nucleus, and ice nucleus filter sampling instrumentation. SUNY also provided a precipitation water sampler. CCN were measured with the microprocessor controlled thermal gradient-diffusion-cloud chamber developed by SUNY. The principle of the design and performance data for this instrument have been described by Lala and Jiusto, 1977 [8]. This chamber compared very favorably with other CCN instruments at the Third International CCN Workshop in 1980 [9]. The fact that it is small and lightweight greatly simplified its integration onto the aircraft. A Gardner counter was used to count Aitken nuclei. This is a portable expansion type counter capable of detecting particles larger than 0.003 microns diameter.

TABLE IIc-2. AIRCRAFT CLOUD PHYSICS INSTRUMENTATION

Specialized Instrument Parameter	Instrument Type
Cloud condensation nucleus (CCN)	SUNY static diffusion chamber
Aitken particle	SUNY Gardner counter
Ice nucleus (IN)	SUNY membrane filters NCAR continuous counter
Drop size/concentration	PMS FSSP, PMS 2-D cloud probe, PMS 2-D precipitation probe, DRI formvar replicator
Cloud liquid water	Johnson-Williams hot wire; Nimbiometer
pH	Foil impactor with litmus paper SUNY precipitation water sampler
Air temperature	Rosemount total temperature (platinum resistance)
Dewpoint	General Eastern (cooled mirror)
Vertical winds	Accelerometer coupled to pitch and attack angles
Winds	Omega (INS TAS computed)
Pressure	Garrett (static and dynamic)
Altitude	Stabilized radar altimeter
Radar	C-band PPI, 360 deg horizontal scan X-band RHI, 360 deg vertical scan
Electric field	Electric field mills (top and bottom of fuselage)
Cloud size/shape	16 mm photography (nose, sides and downward)
Near pad deposition effects	35 mm photography (handheld)

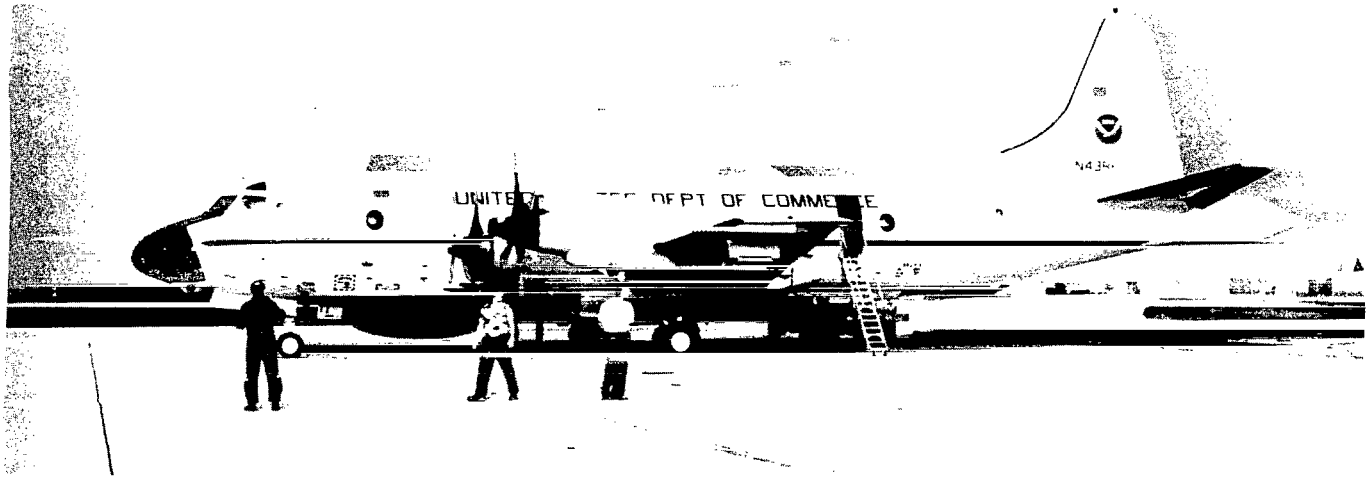

Figure IIc-4. NOAA 43 WP-3D Orion cloud physics instrumented aircraft at Patrick Air Force Base, Florida, the morning of the STS-3 launch.

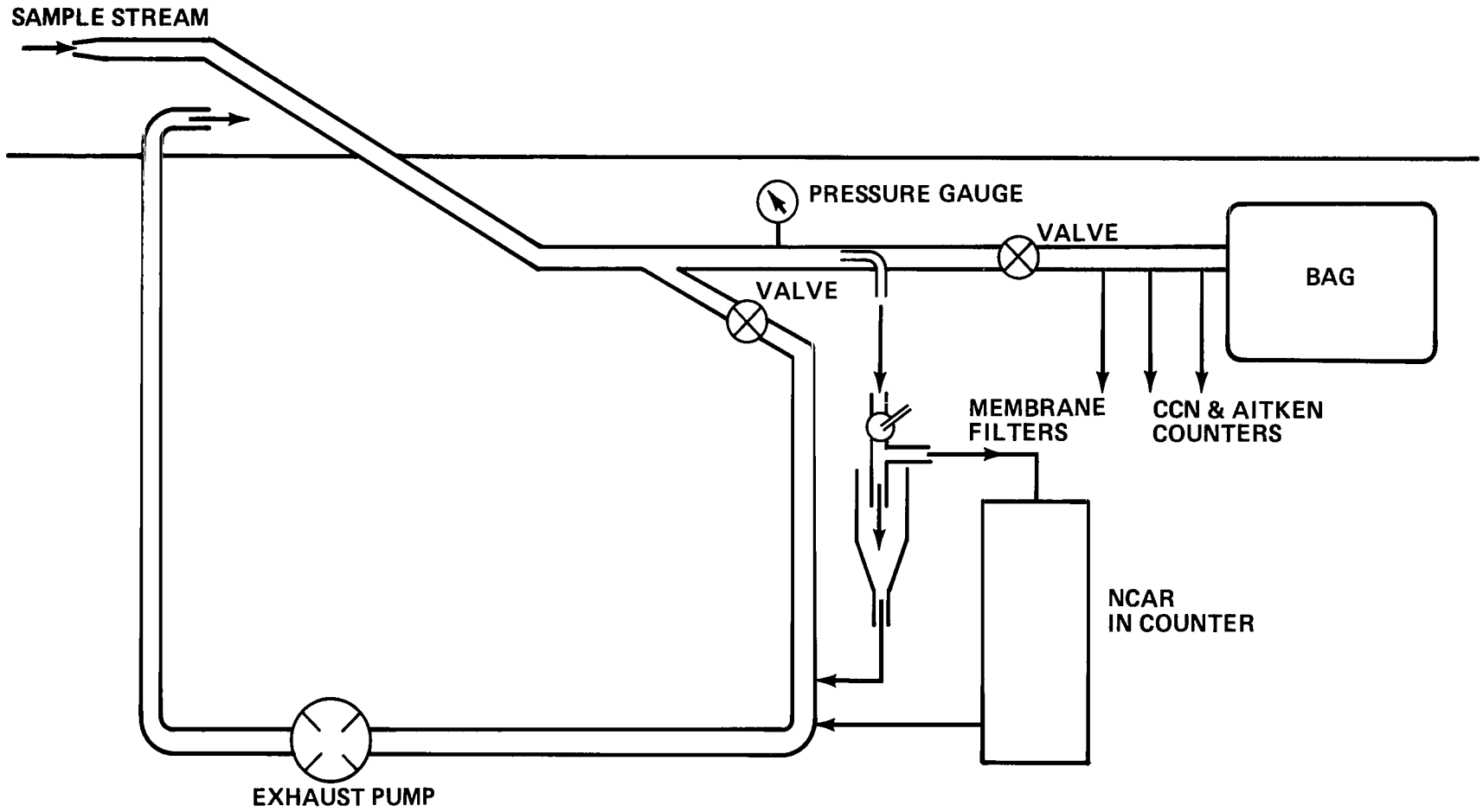

Figure IIc-5. Flow schematic for aerosol sampling aboard P-3.

Ice nuclei were counted by two different methods, the filter technique and an NCAR continuous ice nucleus counter. For the filter measurements two identical Sartorius 47 mm diameter membrane filters having pore sizes of 0.45 μm were mounted in parallel for each bag sample. Care was taken to minimize the effects of high CCN concentrations on the ice nucleus counts. The flow rate through each filter was 20 l min^{-1} and the total volume sampled per filter was 20 l. One set of filters was processed at SUNY and the other set at the National Center for Atmospheric Research Laboratory (NCAR) in Boulder, Colorado. The processing scheme provides for the humidification of the filter at 100 percent relative humidity (with respect to water) and a temperature of -20°C. Ice nuclei in the sample activated under these conditions grow to a detectable size in the laboratory chamber and are counted visually to provide a measure of concentration.

The CCN, Aitken and ice nucleus filter measurements were all made from the sampling bags. A new bag was used for each cloud sample to avoid problems of contamination. Fill time for the bags was adjustable but a time of order 5 to 10 sec was typically used.

The NCAR continuous ice nucleus counter [10] was operated by Dr. Gerhard Langer, its inventor, who was under contract to MSFC through Universities Space Research Association (USRA). This counter was operated at -20°C with a net sample flow of 10 l min^{-1} drawn in a continuous manner from the aerosol manifold.

Determination of cloud pH was considered a key measurement, so a primary measurement technique and two secondary techniques were developed for this flight. The primary technique consisted of replacing the aluminum foil in the foil impactor, which is mounted beneath the starboard wing of the aircraft, with 2-mil mylar film with two bands of litmus paper attached side by side. Each band was 0.5 in. wide. One covered the range 0 to 3 pH in half step increments, the other covered 0 to 9 pH, half step increments 0 to 2 pH and full step increments 2 to 9 pH. Secondary techniques consisted of the SUNY precipitation water sampler mounted atop the aircraft and use of a pH sensitive dye (p-Dimethylamino-azobenzene-o-carboxylic acid) in the formvar replicator.

The foil impactor consists of a foil transport unit that exposes the foil or, in this case, pH paper to the free air stream and a control and indicator unit. The mylar film with attached pH paper was brought forward from a supply spool containing 350 in. of film and passed around the front of a cylindrical drum located directly behind a shutter in the sampling aperture. For this flight the transport was operated in the auto mode, such that the shutter opened momentarily as the paper was transported across the sample area. Since the transport speed was 150 in min^{-1} and the unit was turned off between passes, more than sufficient paper was available for the first three cloud passes. A counter on the control box, which indicated the number of inches of pH paper used, was recorded after each cloud pass. The exposed paper was automatically rewound on a take up spool. Preflight laboratory experiments at MSFC demonstrated that when this pH paper was exposed to drops of 10^{-3} N to 1 N HCl acid it held its color quite well for several days if it was wound in a roll to minimize exposure to air and light.

The Formvar replicator [11] continuously collects cloud samples in a liquid plastic coating of polyvinyl formal resin (trade name Formvar) on a continuous mylar 16 mm film. On evaporation of the solvent, a permanent cast of the hydrometeor remains in the dried Formvar coating. These replicas can be quantitatively analyzed to obtain information about cloud particle type, size distribution, and particle concentration. Any solid material captured in the Formvar coating can be analyzed with an electron microscope or some other appropriate technique. The sampling volume at the airspeeds used (approximately 140 m s^{-1}) was about 1 l s^{-1}. Since the replicator was operated at 60 frames s^{-1}, the resolution

of each frame is about 0.02 sec (2.77 m of flight path). The threshold size for collection of liquid droplets was about 5 μm diameter. The sample slit width is 1 mm but at high airspeeds the larger drops deform or break up on impact so accurate sizing is difficult.

Two MSFC supplied electric field mills were mounted on the aircraft to measure the vertical component of the electric field. They were mounted near the electrocenter of the aircraft; one being mounted on top of the aircraft and the other on the belly almost directly below the upper one. The antenna wire which is normally attached from the tail of the aircraft to the forward fuselage was removed. There were no other nearby protruding electrical conductors.

A few days prior to the STS-3 launch a total of three NOAA aircraft test flights were conducted over the South Florida and KSC areas to insure proper instrument operation and to familiarize the pilots with the KSC area. These flights also provided valuable background counts of ice nuclei and CCN.

Early on the morning of the launch, March 22, 1982, the NOAA aircraft was deployed from Miami International Airport to Patrick Air Force Base (PAFB) adjacent to KSC. Approximately 30 min prior to the Shuttle launch, the NOAA aircraft departed PAFB for the assigned prelaunch staging area over the KSC Skid Strip about 15 km (10 miles) south of Pad 39A. This was just outside both the Impact Limit Line (ILL) and the designated STS-3 Aircraft Danger Airspace (Fig. IIc-6). A relatively thin layer of scattered strato-cumulus clouds was present in this area with bases at 550 m (1800 ft). The prelaunch counterclockwise holding pattern was conducted slightly below cloud base.

The Shuttle was launched on schedule at 16:00 Z (11:00 a.m. EST) through a small stato-cumulus cloud. Figure IIc-7, one of a series of photos taken from the two NASA T-38 chase aircraft, looks to the north from an altitude of 6700 m and shows the column cloud extending through the natural cloud. The color difference between the natural cloud and the column cloud is pronounced. Note the diameter of the column cloud as a function of distance behind the Shuttle and the length of flame extending behind the Shuttle. Also note the nearly cloud-free region over the ocean to the right. The exhaust ground cloud moved into this cloud-free area.

Following the launch of the Shuttle, the NOAA aircraft was given approval by Range Safety at L plus 2 min to cross the ILL and begin cloud penetrations. The first cloud penetration was made at 16:03:55 Z (11:03:55 a.m. EST) at an altitude of 700 m and a heading of 10 deg. A complete list of cloud penetrations and duration times is given in Table IIc-3. Plots of the aircraft track from launch to L plus 2.75 hr are given in Figures IIc-8 through IIc-12. GMT times are given every 5 min along the aircraft track. Since the first three cloud passes were the most interesting from a cloud microphysical standpoint, they will be emphasized. Plots of radar altitude versus time for the time span of the first three passes are presented as Figures IIc-13 and IIc-14. Figures IIc-15 and IIc-16 are plots of dew point temperature for this same time frame. Figures IIc-17 through IIc-24 show important cloud parameters for the first cloud pass. These include the vertical wind, Figure IIc-17; temperature, Figure IIc-18; Johnson-Williams (JW) cloud water, Figure IIc-19; and nimbiometer measured cloud water, Figure IIc-20, as well as hydrometeor pH, Figure IIc-21, and hydrometeor spectra. The primary hydrometeor spectra information was obtained with the PMS [12,13] 2-D Cloud and 2-D Precipitation probes. Figure IIc-22, taken from the first cloud pass, is an example of the 2-D cloud probe images obtained. Precipitation probe images are similar but much smaller. The hydrometeor spectra from the two respective probes on the first cloud pass are plotted in Figures IIc-23 (cloud probe) and IIc-24 (precipitation probe). Figures IIc-25 through IIc-36 are plots for cloud passes two and three of the same parameters, with the exclusion of hydrometeor pH, already described for the first cloud pass. Since the exhaust cloud was not observable with either the 5 cm PPI or 3 cm RHI onboard radars, radar images are not presented here.

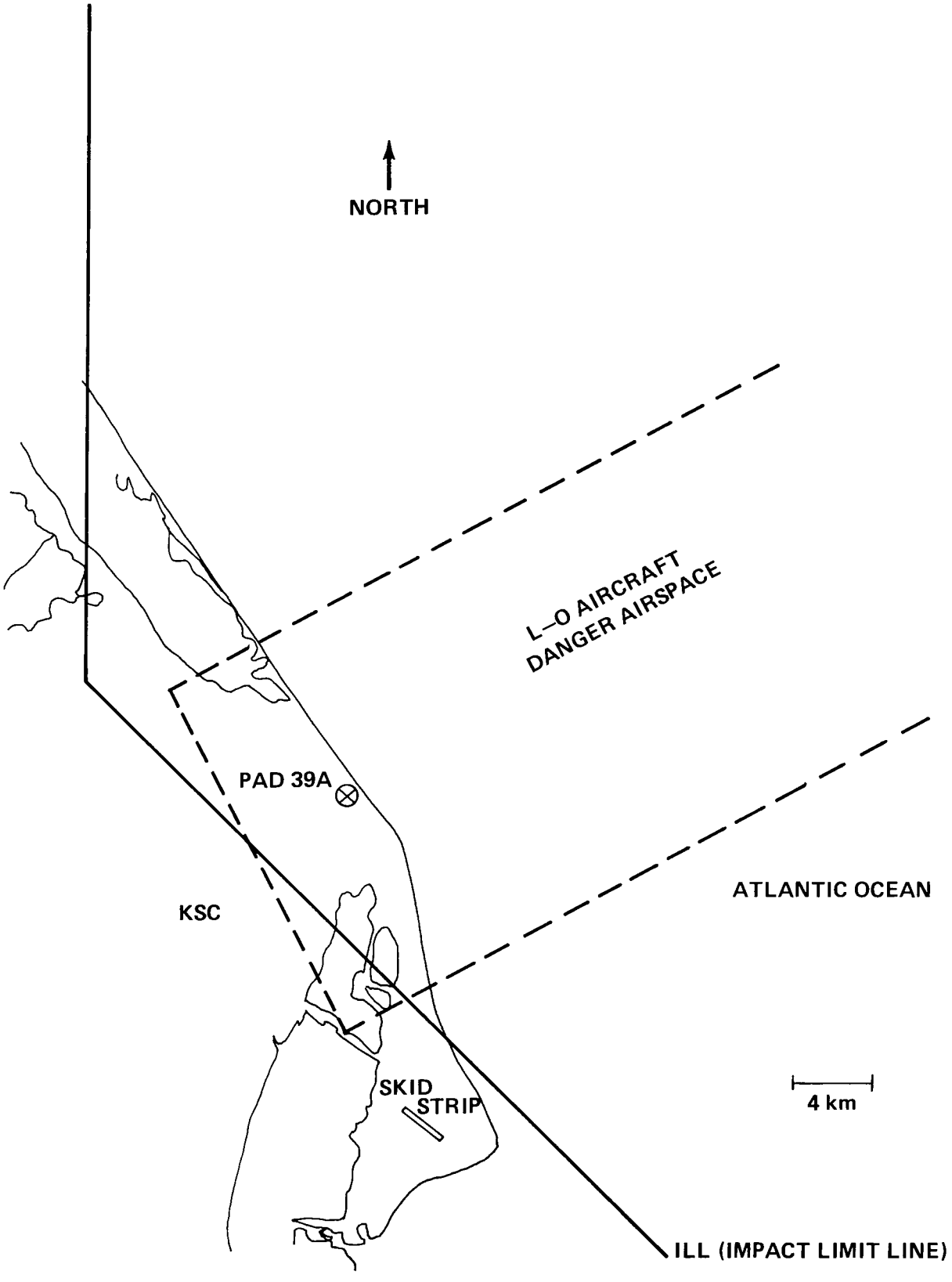

Figure IIc-6. Aircraft restricted areas during STS-3 launch.

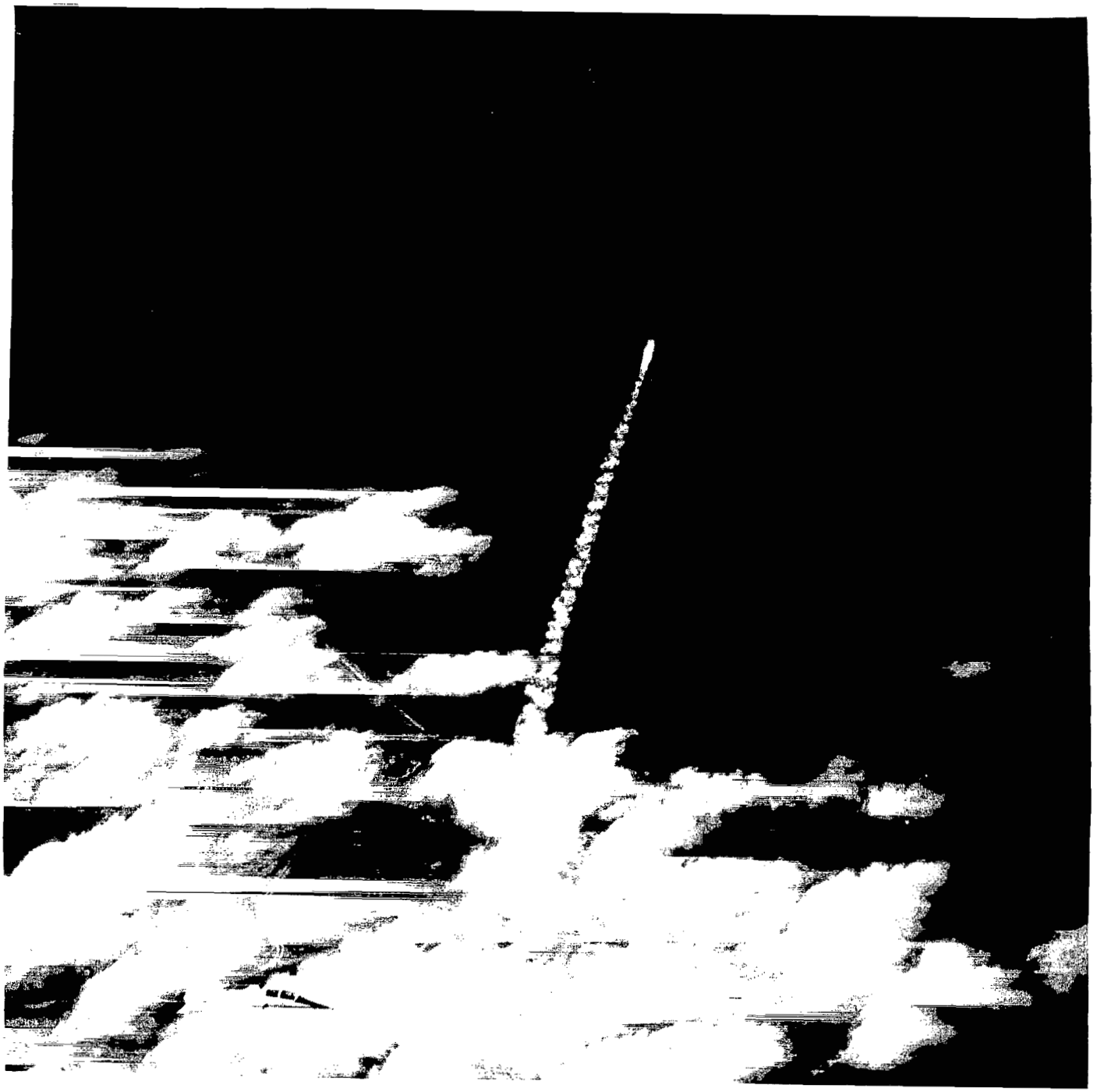

Figure IIc-7. STS-3 launch looking north from altitude of 6700 m.

TABLE IIc-3. CLOUD PENETRATION AND DURATION TIMES

Time of Cloud Penetration, EST	Duration of Cloud Penetration, sec	No. of Bag Samples	Time of Cloud Penetration, EST	Duration of Cloud Penetration, sec	No. of Bag Samples
Background Measurements		2			
11:04	13	1	13:11	195	
:07	10		:20	160	1
:09	36		:30	190	1
:12	22		:42	380	1
:14	49	1	:51	253	1
:18	67		Background Measurements		2
:22	52	1	14:29	190	
:24	52		:36	300	1
:29	60	1	:44	450	1
:33	47				
:36	107				
:39	127				
:42	91	1			
:45	66				
:49	48				
:51	110	1			
:55	80				
12:02	140	1			
:07	20	1			
:16	147	1			
Background Measurements		2			
:46	90	1			
:51	165				
:57	103	1			

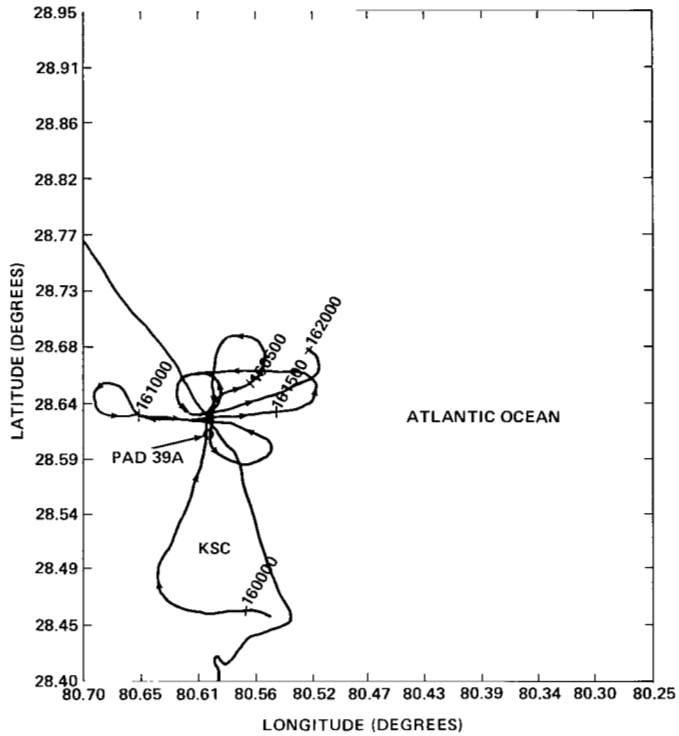

Figure IIc-8. Aircraft track for STS-3 from launch to L+20 min.

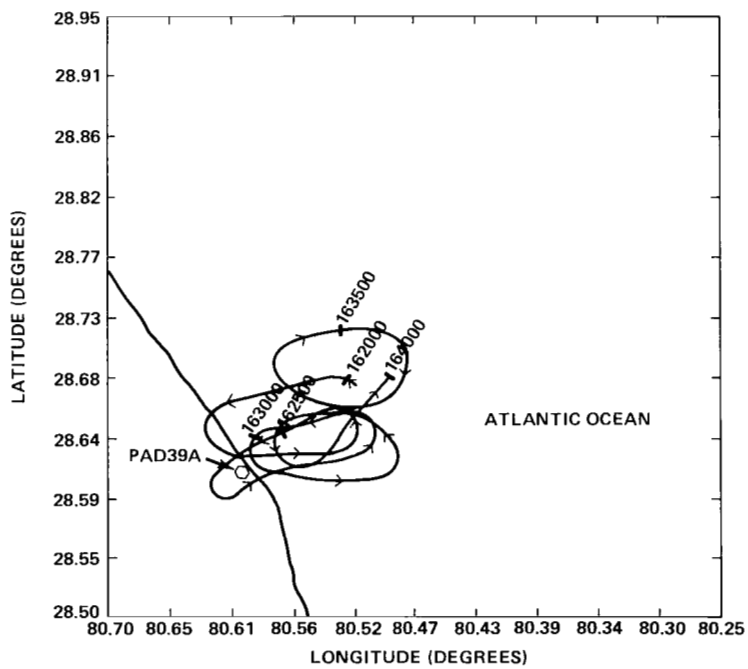

Figure IIc-9. Aircraft track for STS-3 from L+20 min to L+40 min.

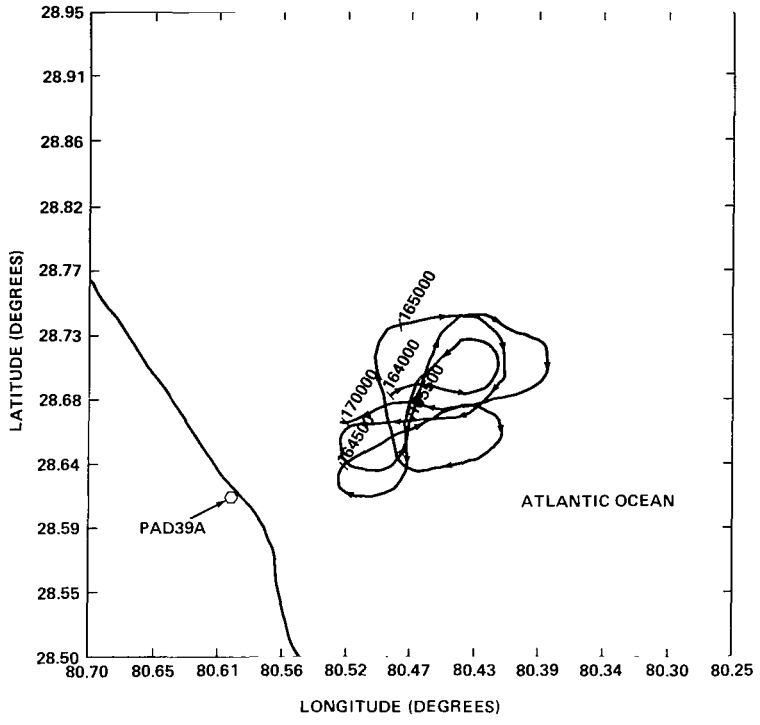

Figure IIc-10. Aircraft track for STS-3 from L+40 min to L+1 hr.

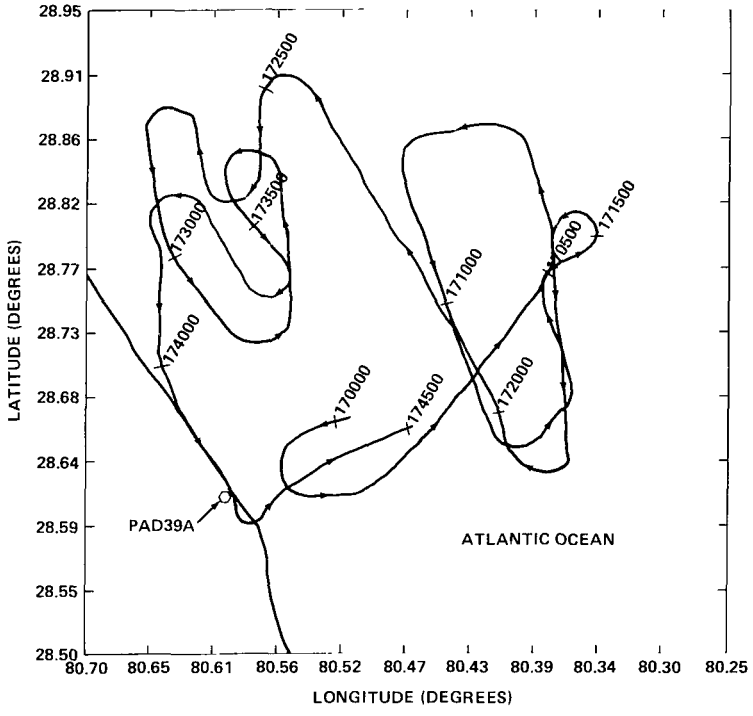

Figure IIc-11. Aircraft track for STS-3 from L+1 hr to L+1 hr 45 min.

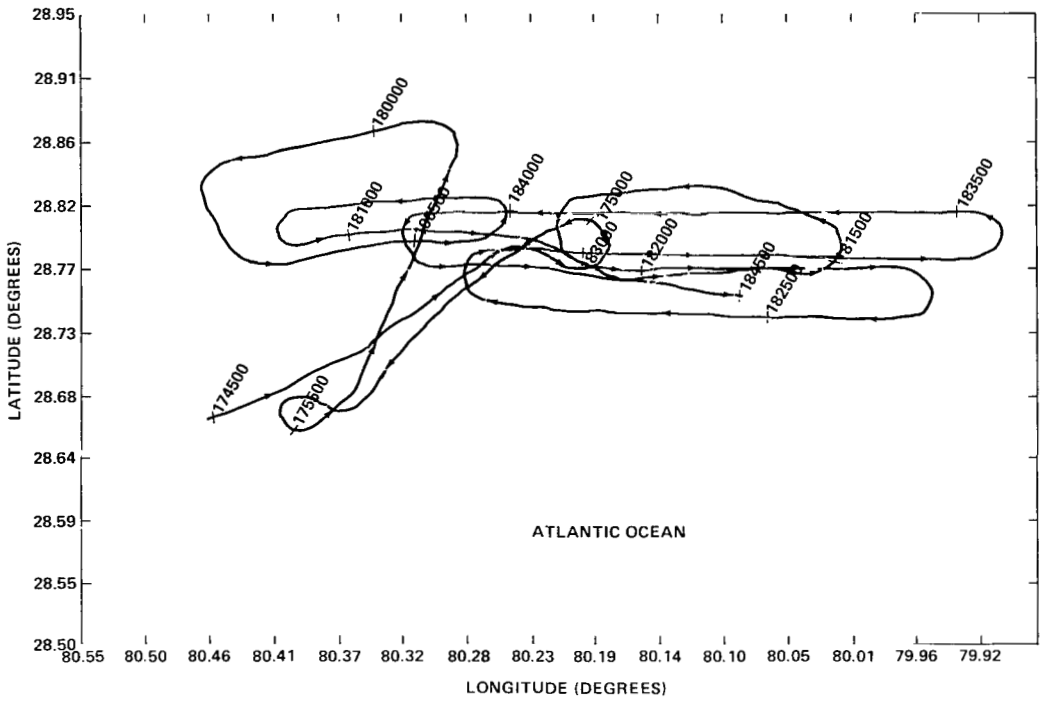

Figure IIc-12. Aircraft track for STS-3 from L+1 hr 45 min to L+2 hr 45 min.

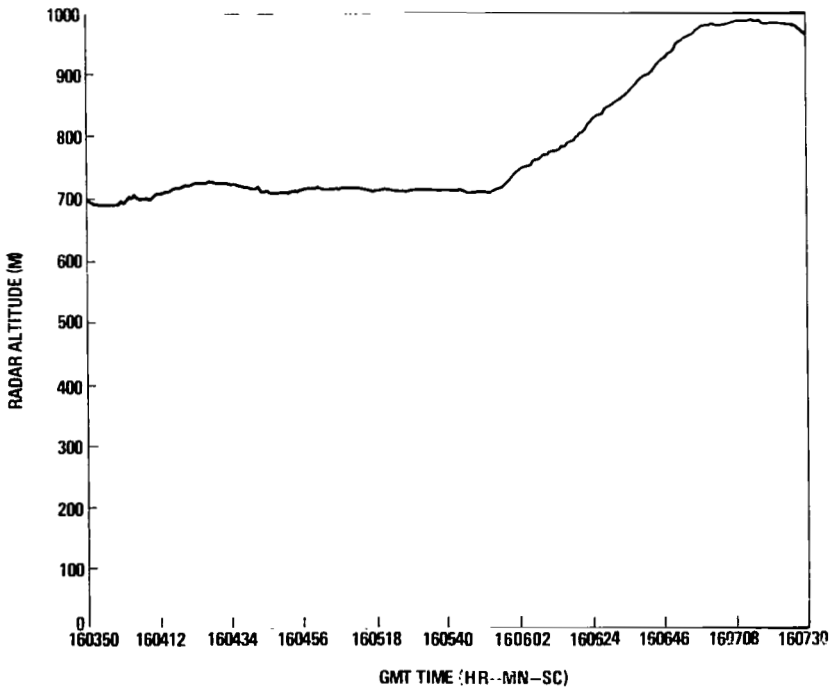

Figure IIc-13. Aircraft radar altitude versus time during cloud passes No. 1 and No. 2.

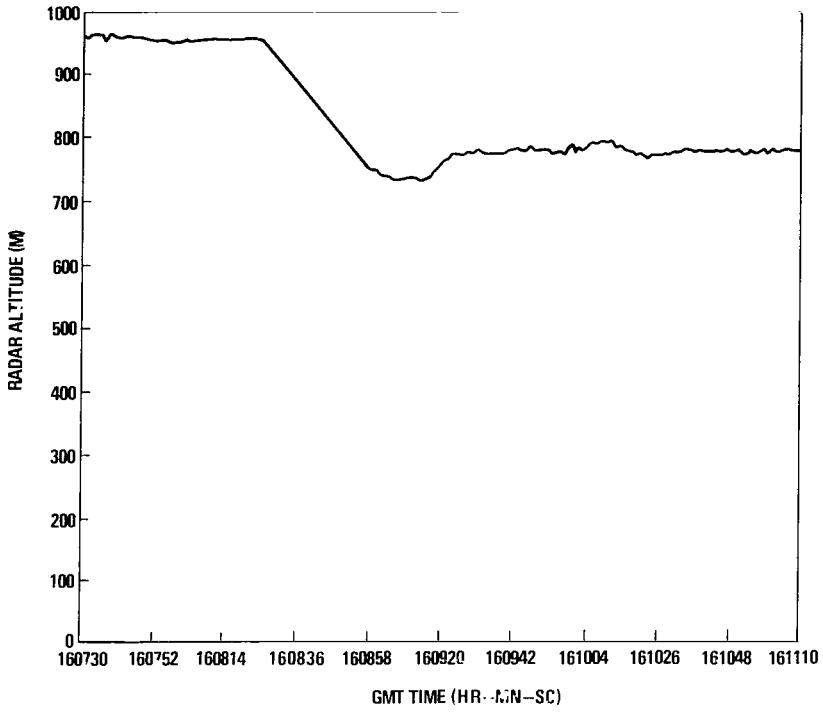

Figure IIc-14. Aircraft altitude versus time during cloud pass No. 3.

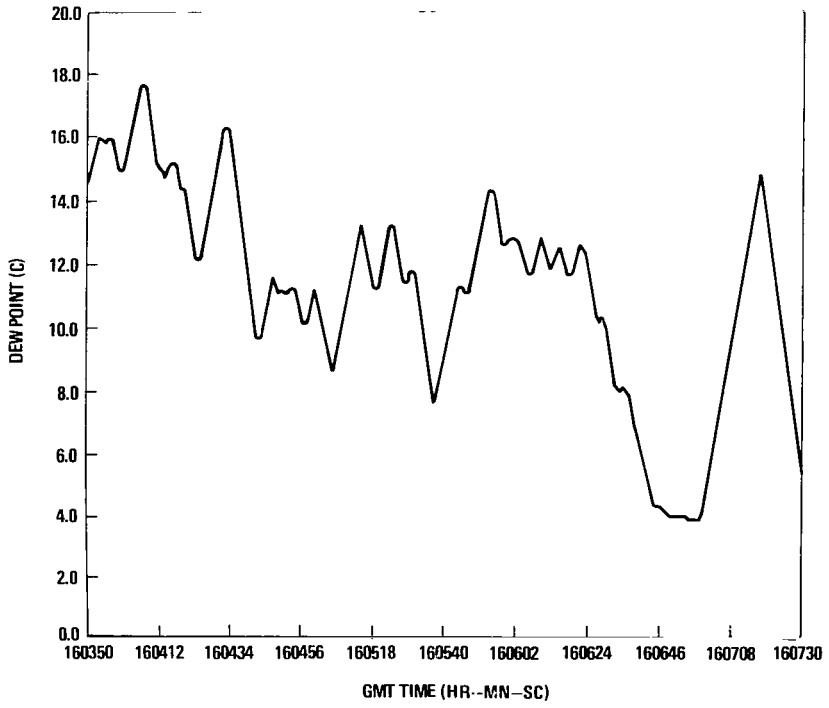

Figure IIc-15. Dew point temperature versus time during cloud passes No. 1 and No. 2.

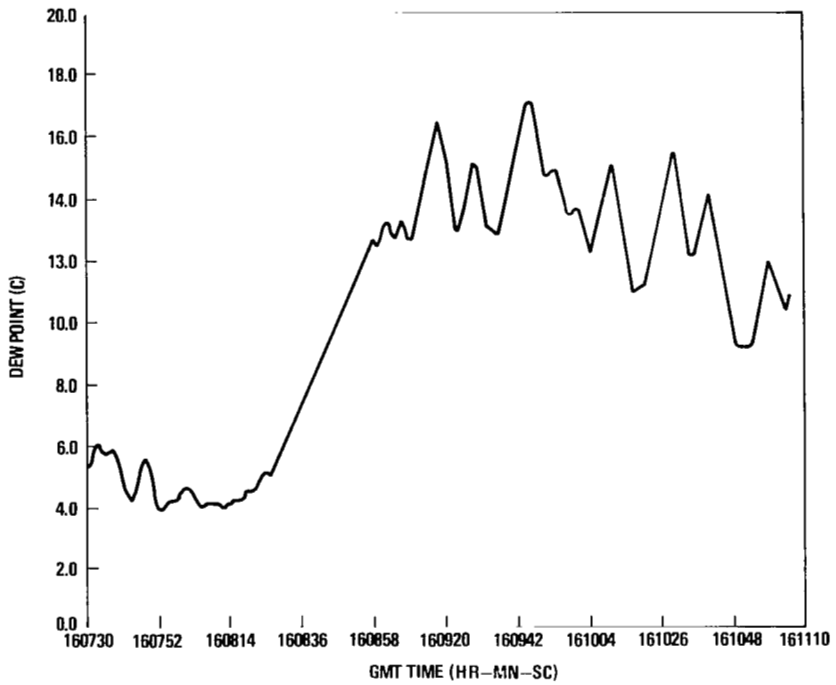

Figure IIc-16. Dew point temperature versus time during cloud pass No. 3.

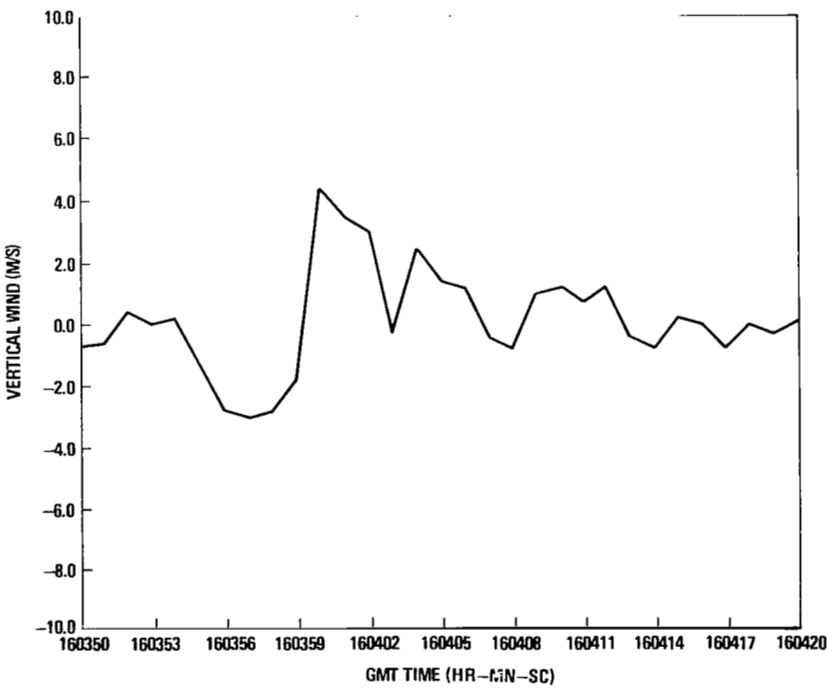

Figure IIc-17. Vertical wind versus time during cloud pass No. 1.

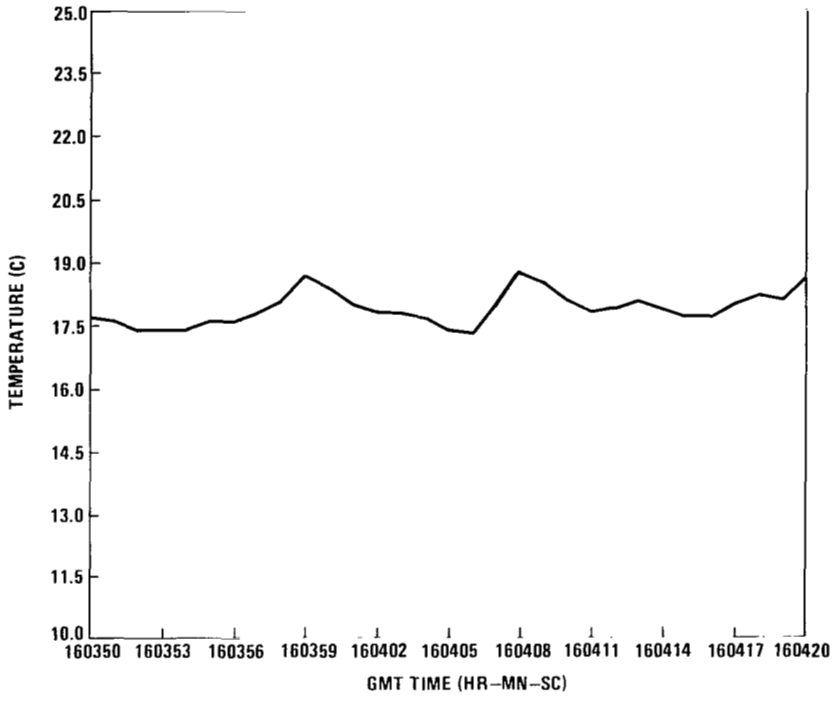

Figure IIc-18. Temperature versus time during cloud pass No. 1.

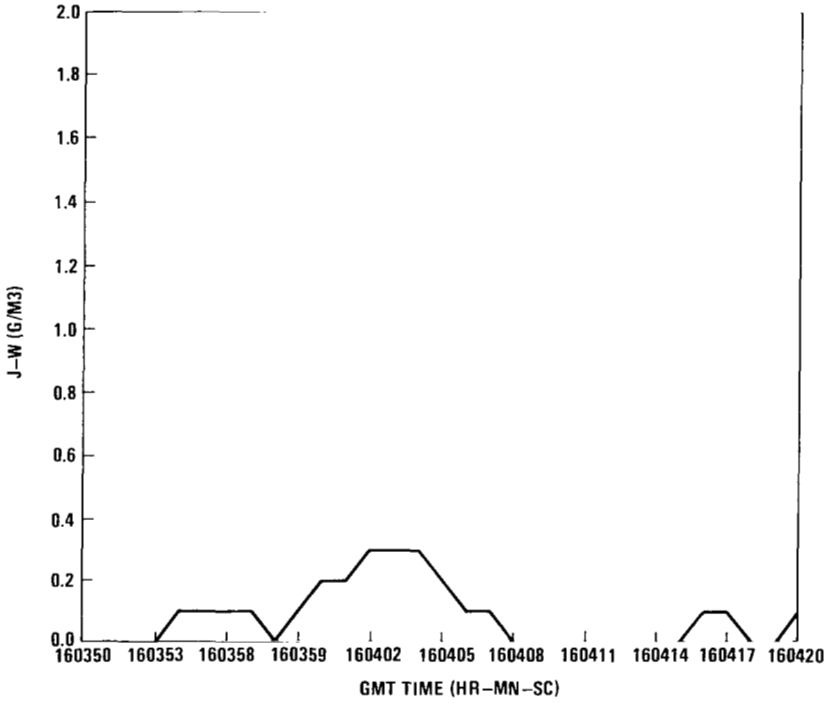

Figure IIc-19. Johnson-Williams (JW) cloud water versus time during cloud pass No. 1.

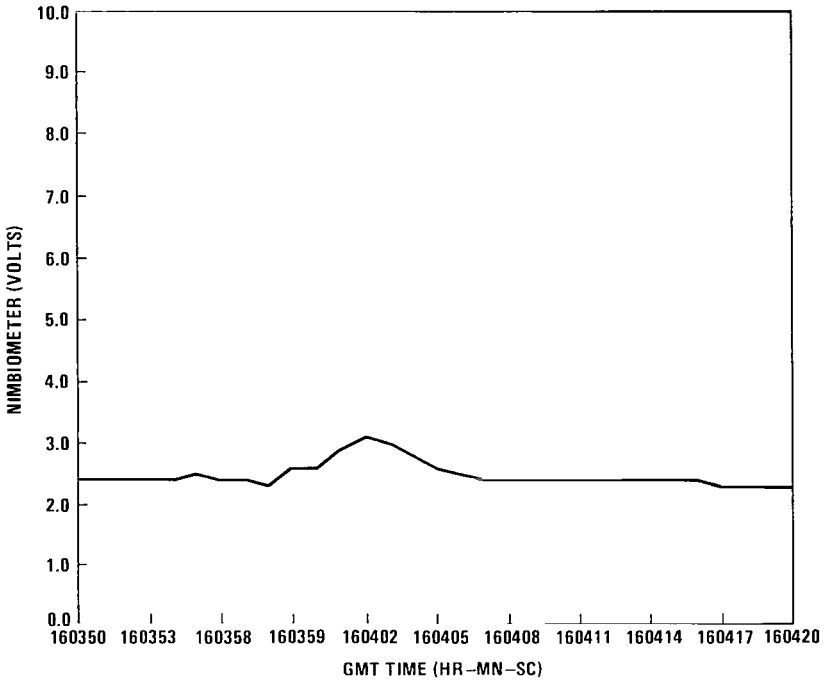

Figure IIc-20. Nimbiometer measured cloud water versus time during cloud pass No. 1.

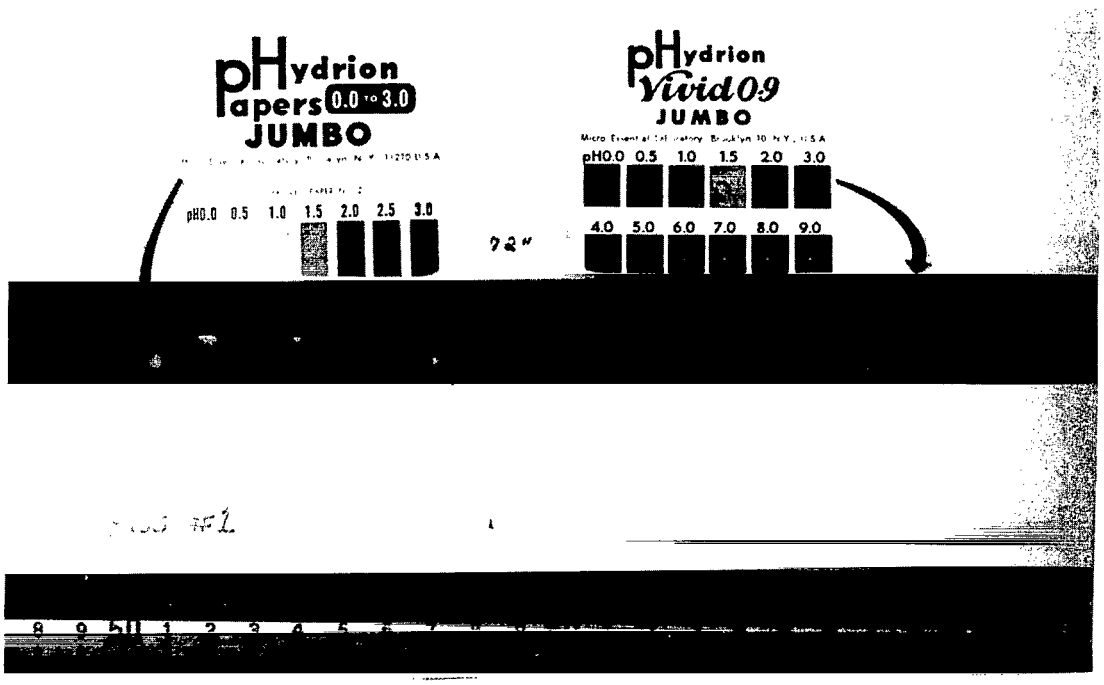

Figure IIc-21. Hydrometeor pH was less than 0.5, the lowest range on both pH papers. (Cloud pass No. 1, L+4 min, altitude 750 m.)

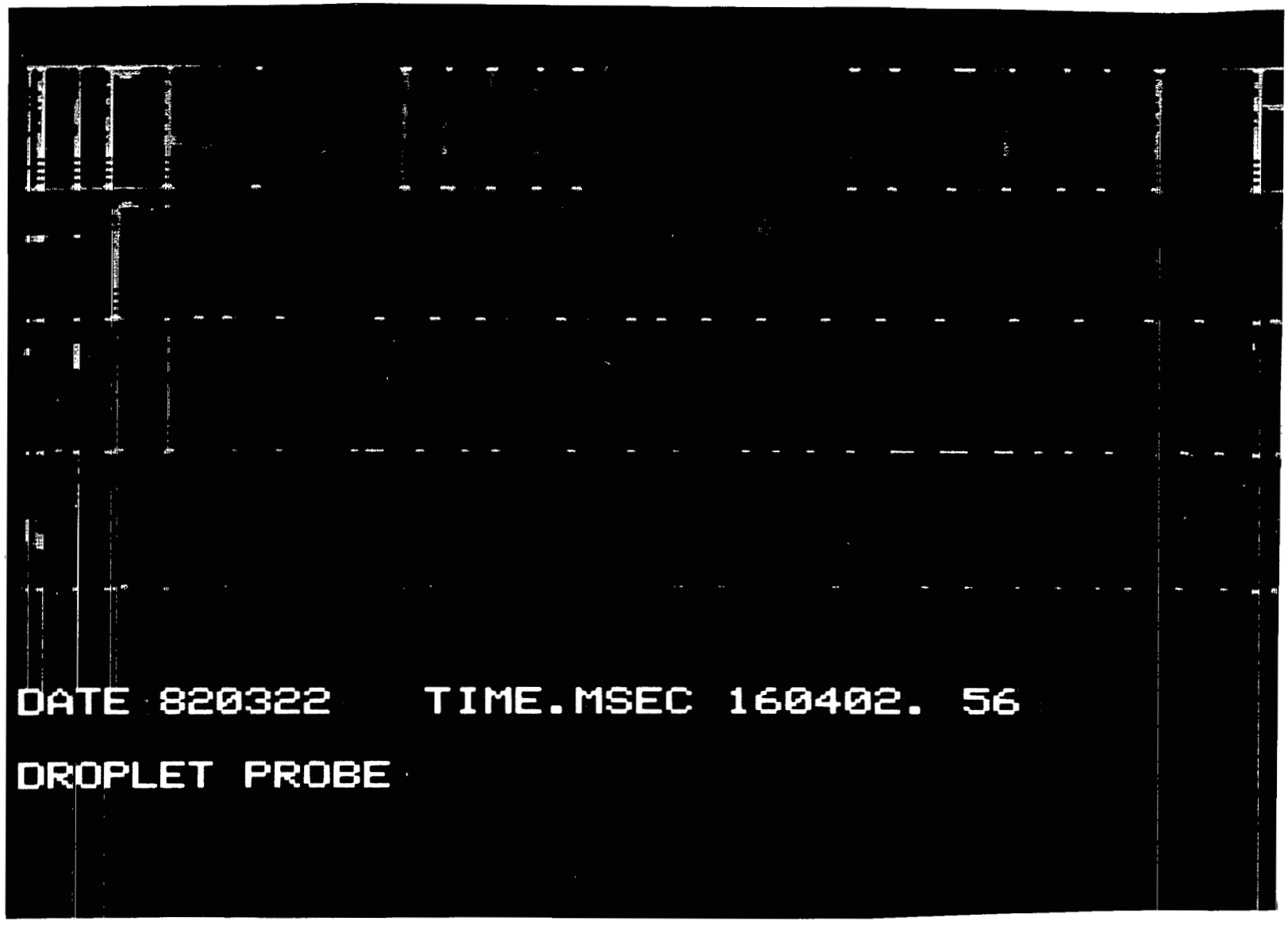

Figure IIc-22. PMS 2D cloud probe images from cloud pass No. 1.

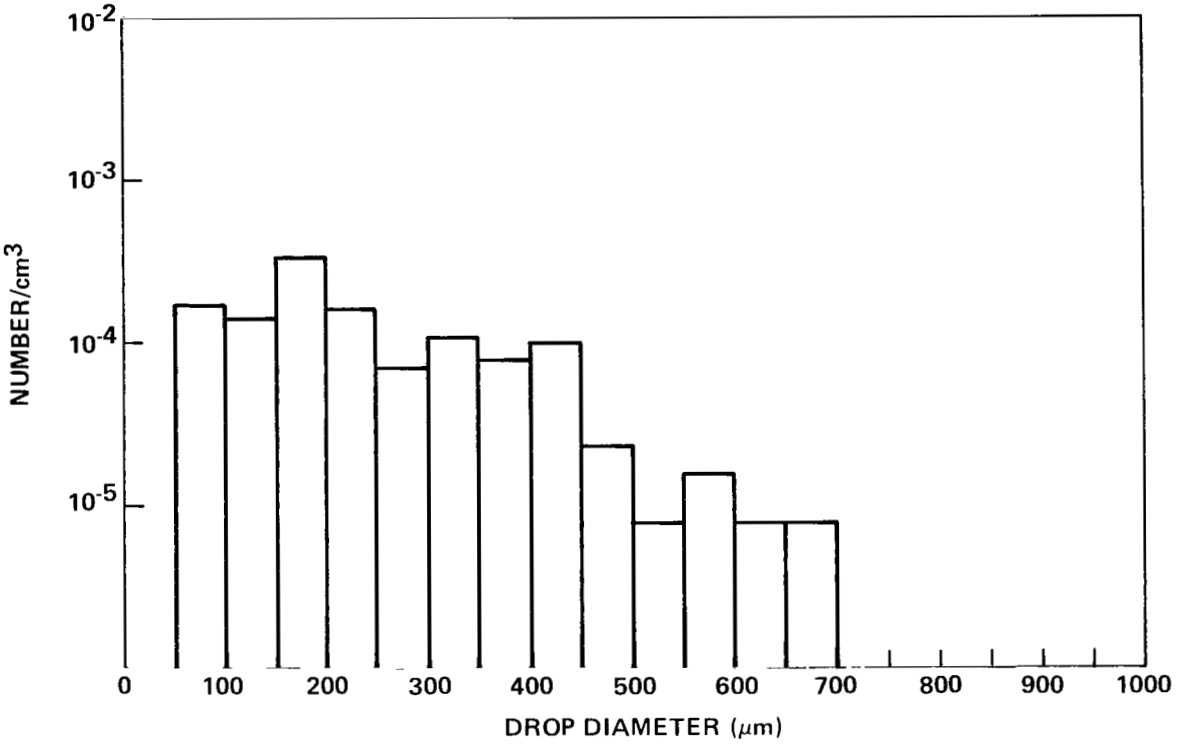

Figure IIc-23. Hydrometeor spectra from cloud probe, cloud pass No. 1.

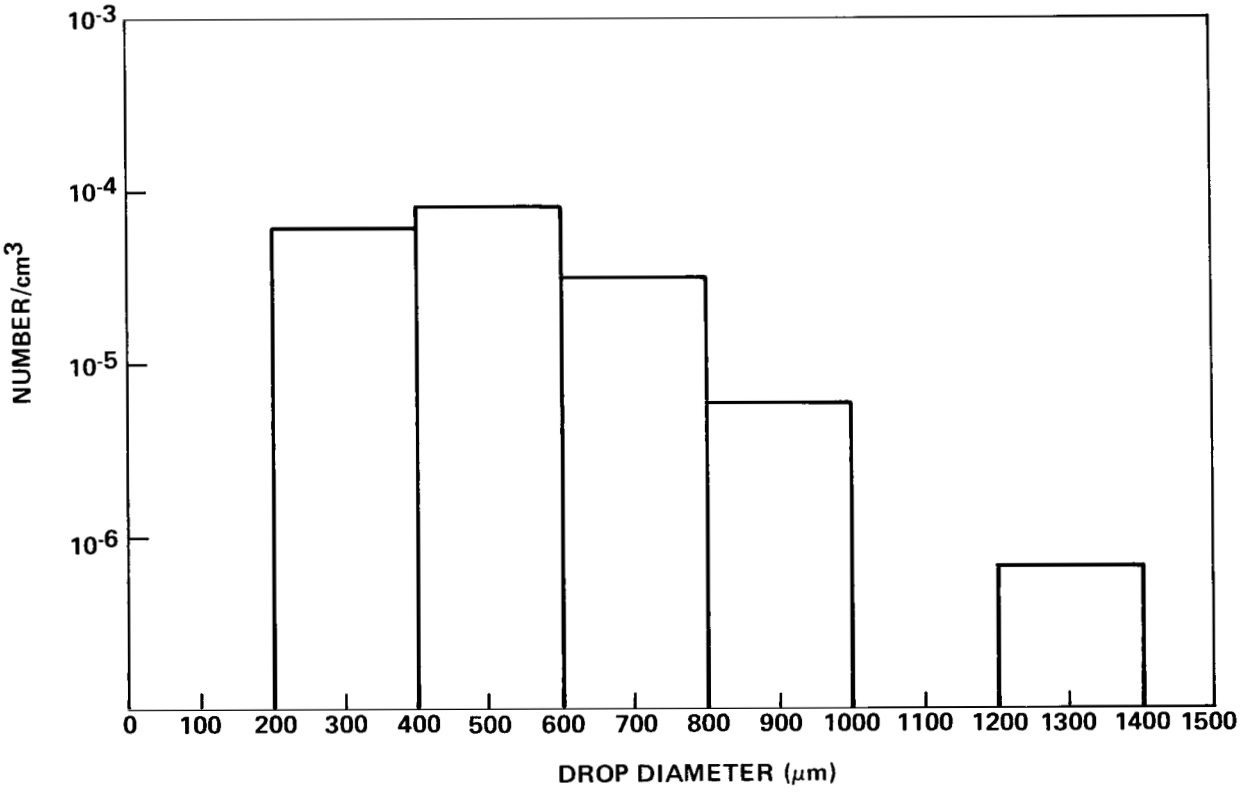

Figure IIc-24. Hydrometeor spectra from precipitation probe, cloud pass No. 1.

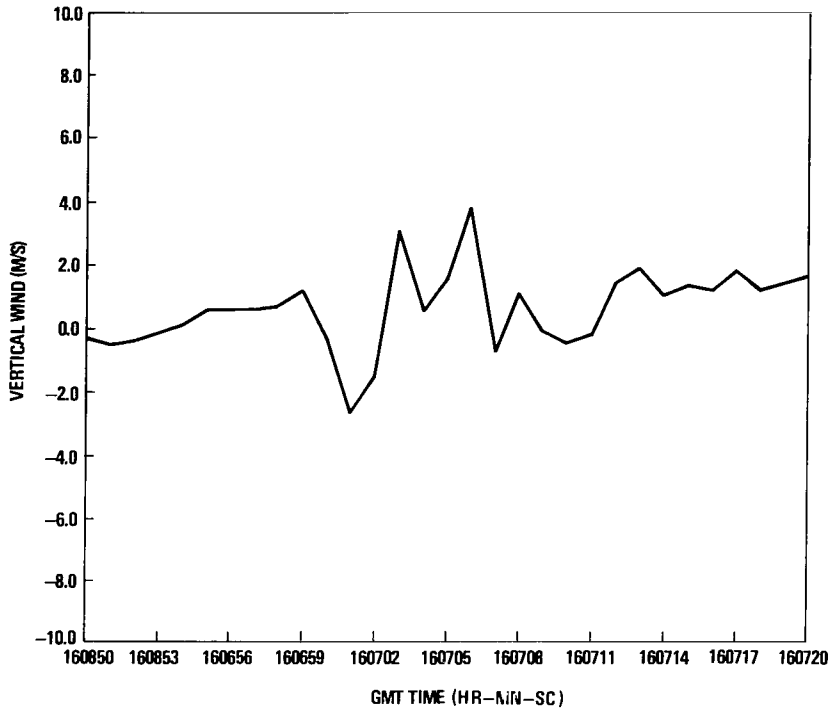

Figure IIc-25. Vertical wind versus time during cloud pass No. 2.

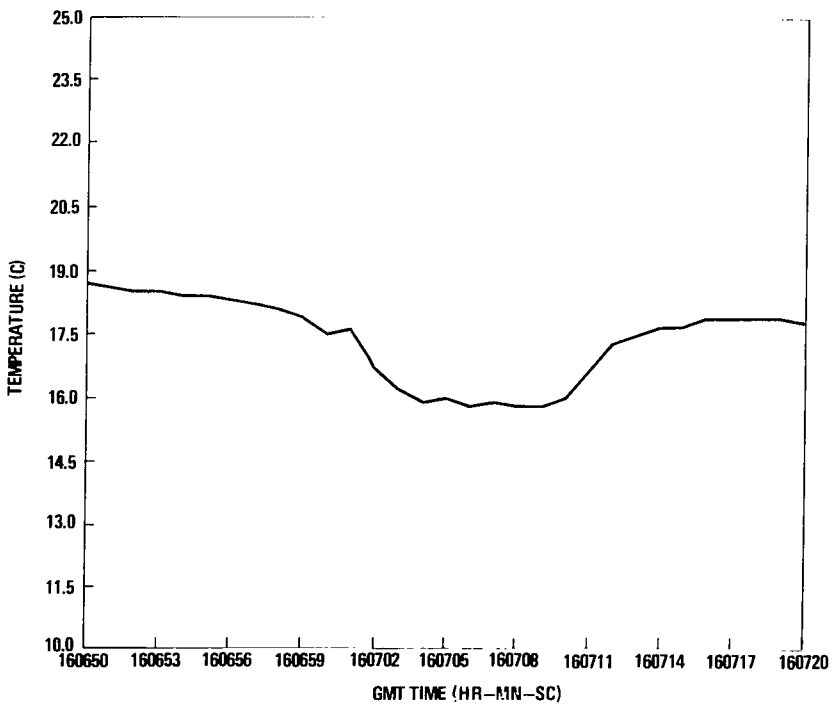

Figure IIc-26. Temperature versus time during cloud pass No. 2.

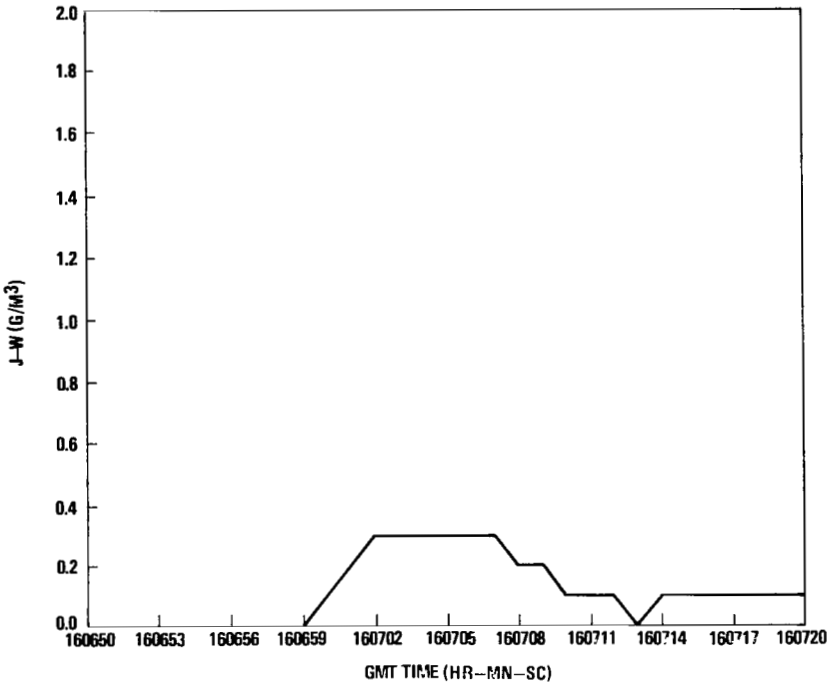

Figure IIc-27. Johnson-Williams (JW) cloud water versus time during cloud pass No. 2.

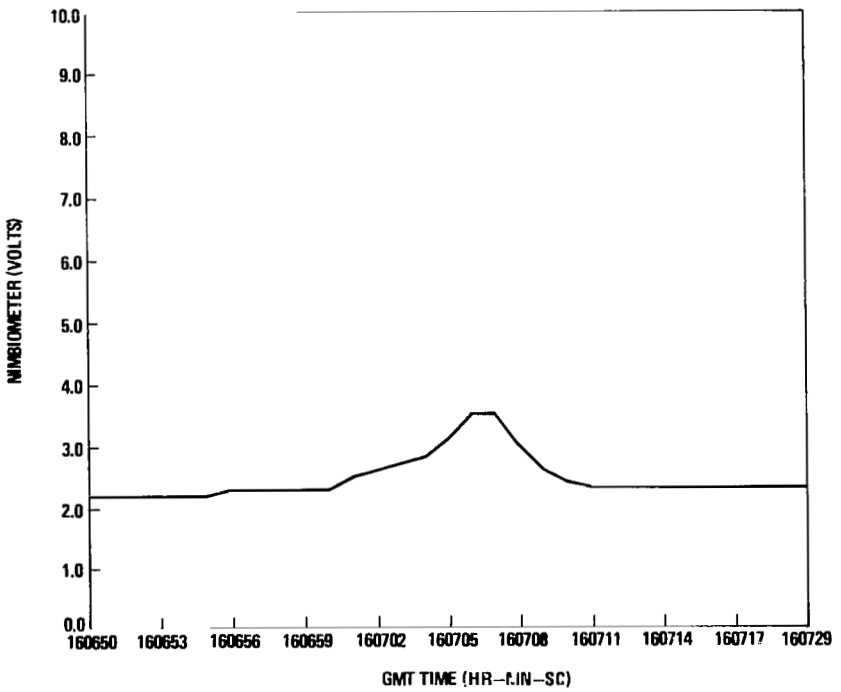

Figure IIc-28. Nimbiometer measured cloud water versus time during cloud pass No. 2.

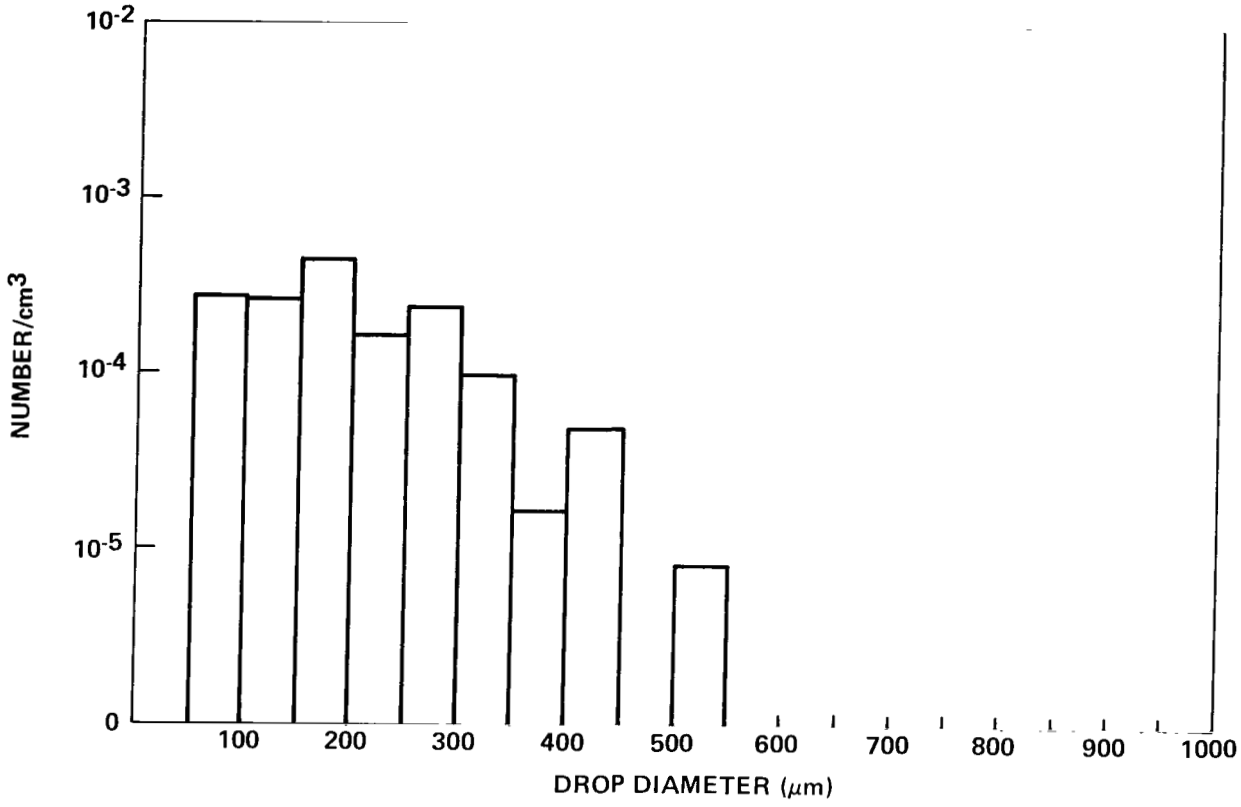

Figure IIc-29. Hydrometeor spectra from cloud probe, cloud pass No. 2.

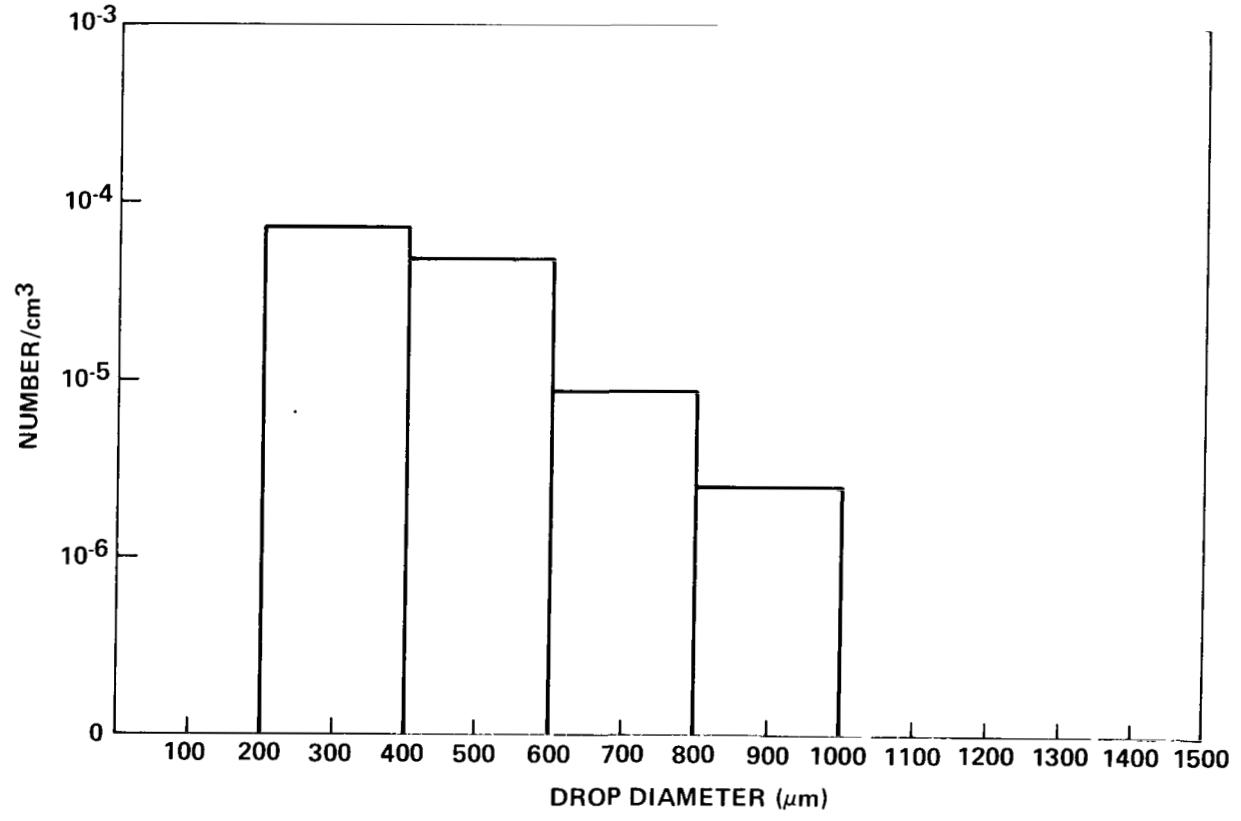

Figure IIc-30. Hydrometeor spectra from precipitation probe, cloud pass No. 2.

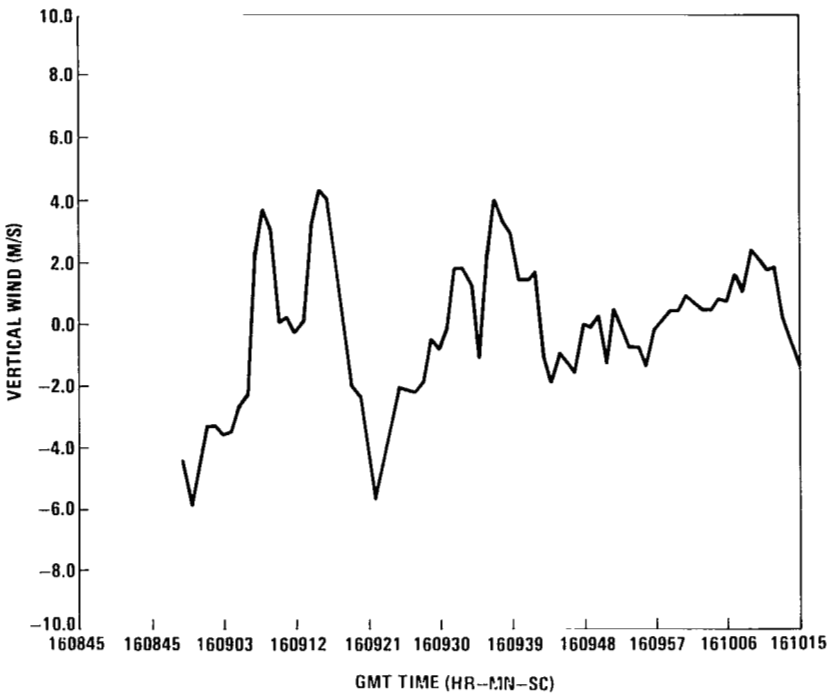

Figure IIc-31. Vertical wind versus time during cloud pass No. 3.

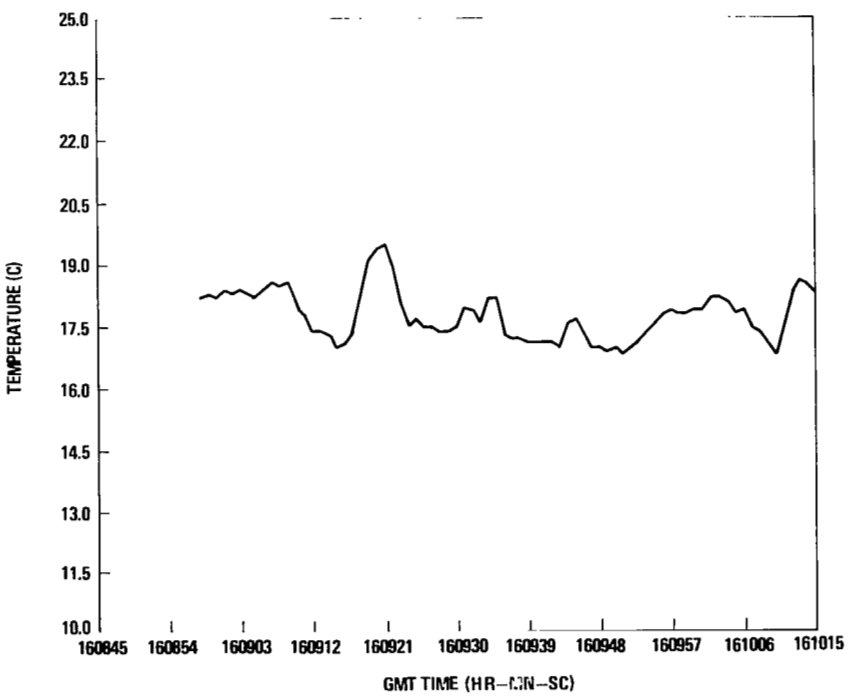

Figure IIc-32. Temperature versus time during cloud pass No. 3.

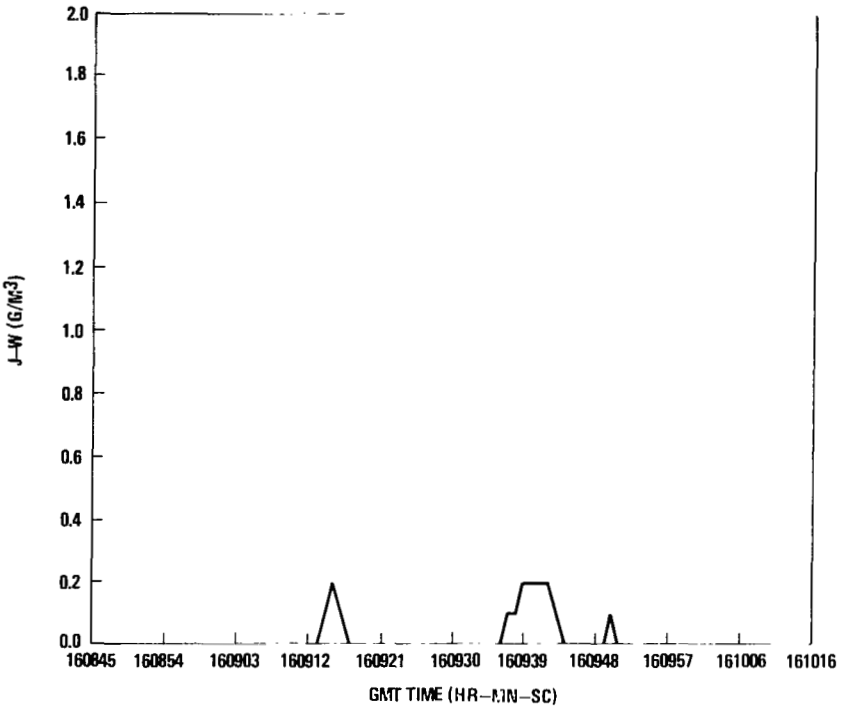

Figure IIc-33. Johnson-Williams (JW) cloud water versus time during cloud pass No. 3.

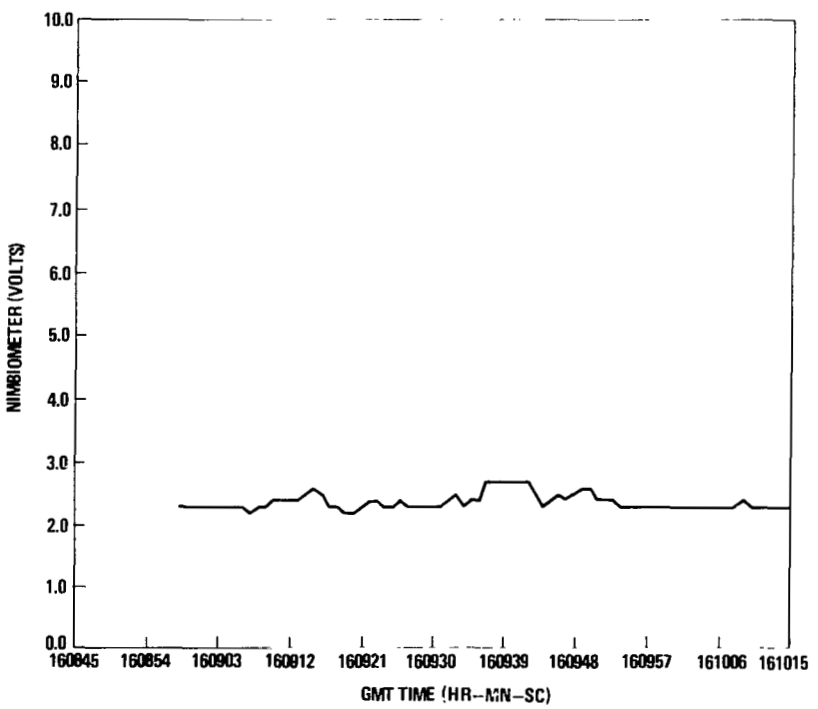

Figure IIc-34. Nimbiometer measured cloud water versus time during cloud pass No. 3.

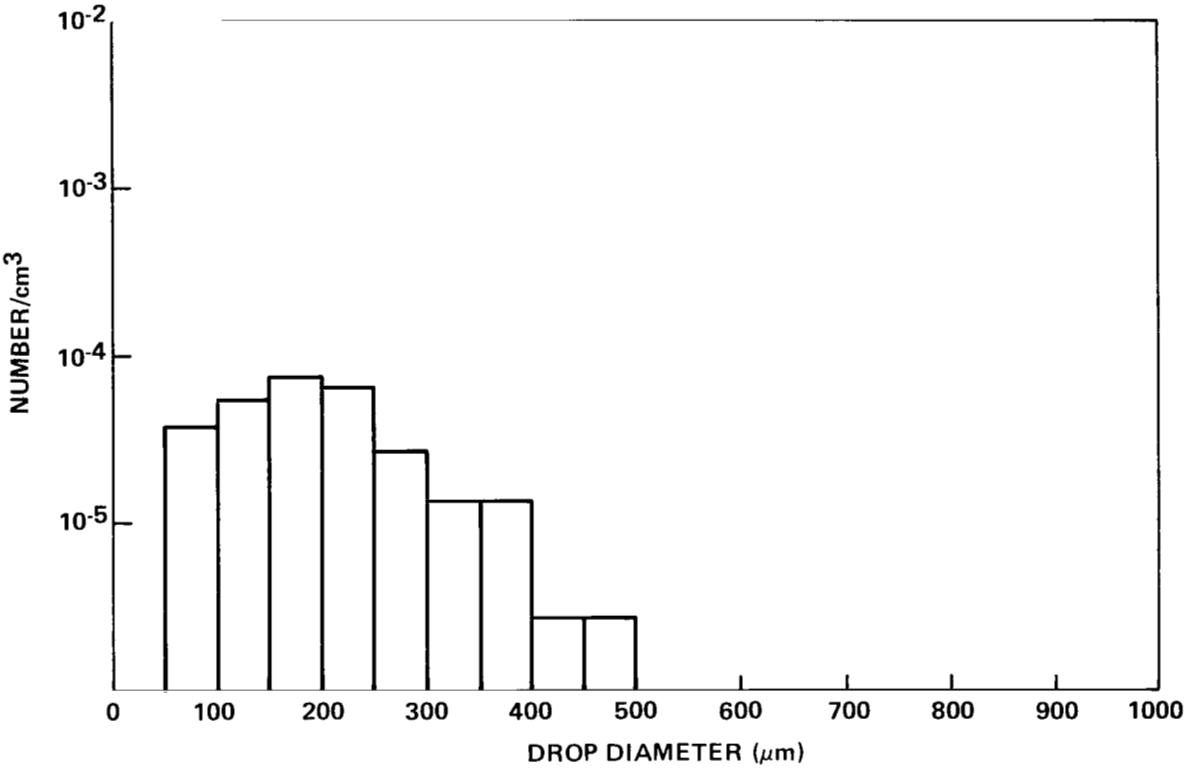

Figure IIc-35. Hydrometeor spectra from cloud probe, cloud pass No. 3.

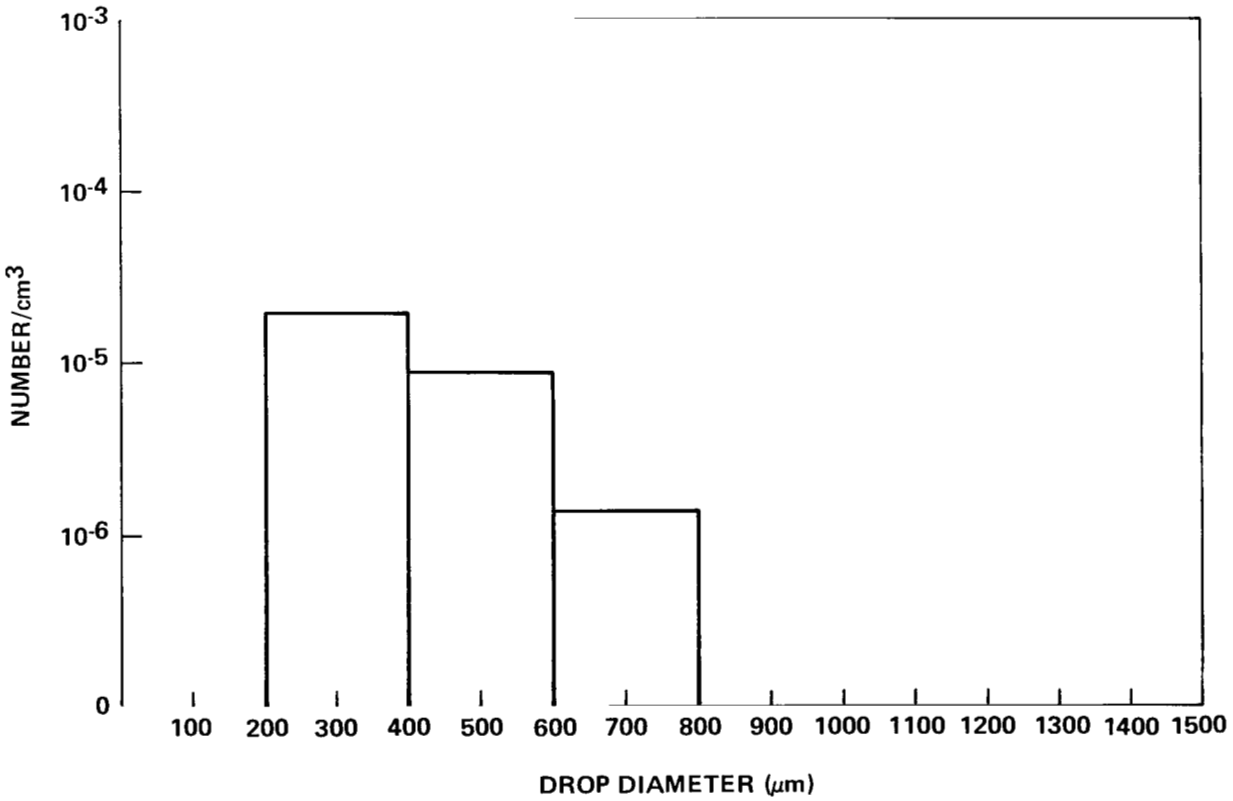

Figure IIc-36. Hydrometeor spectra from precipitation probe, cloud pass No. 3.

The aerosol was sampled from a total of 23 bags over a 5-hr period, providing 17 samples of the exhaust cloud along with six ambient samples for comparison. The concentration of cloud condensation nuclei (CCN) at 0.25 percent supersaturation and Aitken nuclei (CN) preceding the launch of the Shuttle to almost 4 hr after the launch are presented in Figure IIc-37 and Table IIc-4. Isolated data points are background values far removed from the exhaust cloud. The bag samples taken soon after the launch had a concentration decay much more rapid than expected. The total condensation nucleus counts decayed by a factor of 2 to 5 over a 3-min sampling period. This contrasts significantly from natural aerosol samples at the same concentration levels which typically decay to about 60 percent of their initial value in 15 min. The apparent explanation for this rapid decay is that the particles were relatively large and therefore sedimentation losses were substantial.

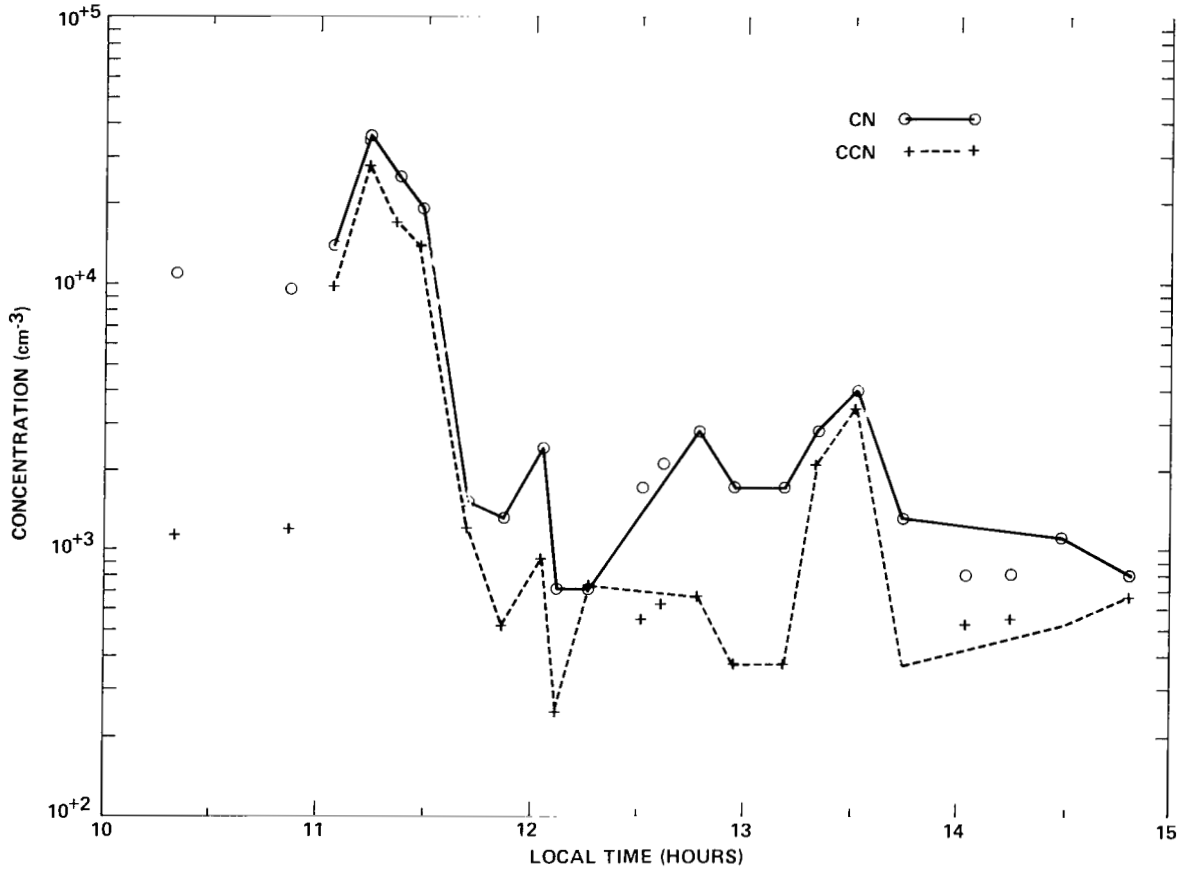

Figure IIc-37. Concentration of cloud condensation nuclei (CCN) at 0.25 percent and condensation nuclei in the Space Shuttle exhaust cloud. Isolated data points are background values.

TABLE IIc-4. AEROSOL MEASUREMENTS FROM THE SPACE SHUTTLE EXHAUST CLOUD

Time (1)	Cloud Pass (2)	Type (3)	CN (X1000) (cm^{-3}) (4)	CCN (X1000) (cm^{-3}) (5)						IN (ℓ^{-1}) (6)
			S	0.25%	0.25%	0.5%	0.5%	1.0%	1.0%	
10:44		Clear	31	1.14	0.97	1.11	1.39	1.39	1.67	1.85
10:52		Clear	9.5	1.19	1.17	1.49	1.87	1.60	1.78	1.3
11:04	1	Cloud	14 - 3.7	9.65	10.18	13.52	2.78	4.88	5.16	2.0
			S	0.25%	0.5%	1.0%	1.0%	0.5%	0.25%	
11:14	5	Cloud	36 - 2.8	27.74	19.39	13.09	9.72	10.92	15.85	1.2
11:22	7	Cloud	25 -12.5	16.73	7.86	7.48	6.19	6.09	4.55	3.05
11:29	9	Cloud	19 - 8	13.29	14.55	9.85	8.33	10.06	10.52	1.45
11:42	13	Cloud	1.5 - 0.8	1.18	0.64	0.69	0.57	0.35	0.32	2.35
11:52	16	Cloud	1.3 - 0.2	0.52	1.58	0.75	0.74	0.79	0.47	2.4
			S	0.25%	0.25%	0.50%	0.50%	1.0%	1.0%	
12:03	18	Cloud	2.4 - 1.7	0.91	0.62	0.73	0.86	0.97	0.93	
12:07	19	Cloud	0.7 - 0.45	0.24	0.57	0.63	0.46	0.41	0.41	1.15
12:16	20	Cloud	0.7 - 1.1	0.73	0.63	0.97	1.06	0.95	1.13	1.85
12:31		Clear	1.7 - 0.2	0.54	0.49	0.80	0.75	0.78	0.66	1.45
12:37		Clear	2.1 - 2.1	0.62	0.63	1.08	1.06	1.33	1.07	0.75
12:47	21	Cloud	2.8 - 1.1	0.66	0.47	0.72	1.11	1.18	1.24	1.6
12:57	23	Cloud	1.7 - 1.3	0.37	0.49	0.48	0.82	0.62	0.81	0.50

TABLE IIc-4. (Concluded)

Time (1)	Cloud Pass (2)	Type (3)	CN(X1000) (cm^{-3}) (4)	CCN(X1000) (cm^{-3}) (5)						IN (ℓ^{-1}) (6)
				S 0.25%	0.25%	0.50%	0.50%	1.0%	1.0%	
13:11	25	Cloud	4.5 - 4.5							
13:20	26	Cloud	2.8 - 3.5	2.11	2.02	2.36	2.59	2.79	3.96	
13:31	27	Cloud	4.0 - 4.8	3.40	3.11	4.37	5.81	5.06	5.82	0.65
13:44	28	Cloud	1.3 - 2.1	0.36	0.36	0.43	1.08	1.17	1.11	0.40
14:02		Clear	0.85- 0.85	0.52	0.62	0.93	0.84	0.90	0.96	0.75
14:15		Clear	0.85- 0.7	0.55	0.44	0.58	0.65	0.59	0.62	0.4
14:29		Clear	1.1 - 1.1	0.52	0.59	0.88	1.31	1.02	0.99	1.3
14:48			0.85- 0.7	0.66	0.48	0.46	0.54	0.77	0.52	

(1) Eastern Standard Time

(2) Number corresponds to flight director's notes

(3) Based on observer's comments

(4) Initial and final bag concentration

(5) Note changes in supersaturation sequence

(6) Concentrations at -20C, 100% relative humidity

The CCN instrument was configured for this study to provide two measurements each at supersaturations of 0.25, 0.5, and 1 percent with respect to water. All these measurements can be performed in a time period of less than 3 min. However, the rapid concentration decay made it impossible to obtain reliable CCN measurements at supersaturations other than the first value (0.25 percent). CCN values plotted are the initial values taken as soon as possible after filling the bag.

Ice nucleus data for the entire mission from takeoff at PAFB to landing at PAFB is given in Figures IIc-38 through IIc-40. Aircraft radar altitude in feet is plotted beneath the ice nucleus data. Exhaust cloud penetrations are indicated with time bars. Ice nucleus concentration as measured with membrane filters and processed by SUNY is given in Figure IIc-41. NCAR processed membrane filter results were essentially the same. Ice nucleus results are discussed in more detail later in section IIIc, Ice Nuclei.

It can be seen from these figures that there were areas in the cloud which had updraft velocities on the order of 4 m s^{-1} on each of the first three cloud passes. This is sufficient updraft to support millimeter size drops. The temperature of the cloud on these first passes was on the order of 1 to 2°C warmer than ambient. Compared to typical Florida natural clouds there was very little cloud water (maximum JW approximately 0.3 g m^{-3}) measured by the Johnson-Williams nimbiometer and the Formvar replicator. Unfortunately, the PMS Forward Scattering Spectrometer Probe (FSSP) which measures particles in the size range 3 to 45 μm was the one aircraft instrument which did not function. Presumably the small amount of cloud water, i.e., dearth of cloud drops in the size range of approximately 10 to 50 μm diameter, was the result of the high CCN concentrations which led to considerable competition for the available water vapor, thus preventing the drops from becoming very large by condensational growth. Millimeter or near millimeter size drops were recorded on each of the first three passes, i.e., to L plus 9 min, but none were recorded on later passes. Observation with a microscope of the large drops on the Formvar shows they each contained numerous aluminum oxide particles. Both pH papers indicated that the pH of the larger drops was less than 0.5. This means they were at least as acidic as 0.3 N HCl. The vertical component of the electric field was small. KSC ground based electric field measurements also showed only a small field.

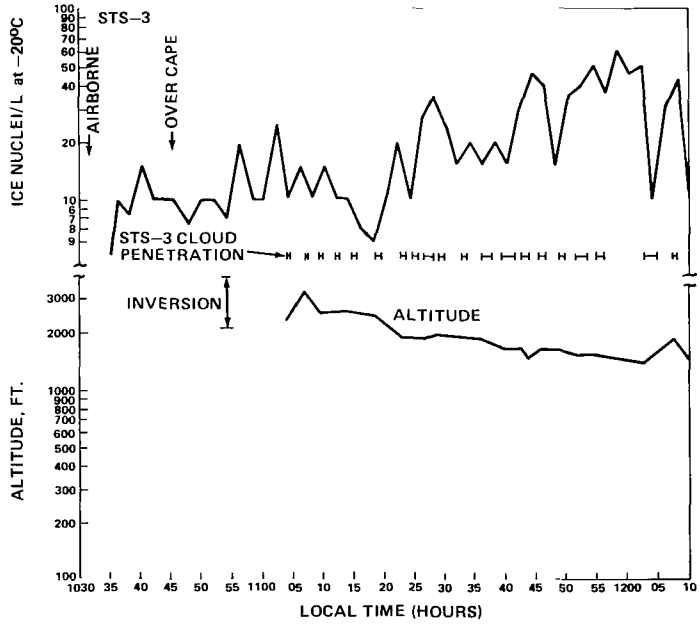

Figure IIc-38. Ice nucleus data from NCAR continuous counter aboard aircraft for STS-3 flight on March 22, 1982.

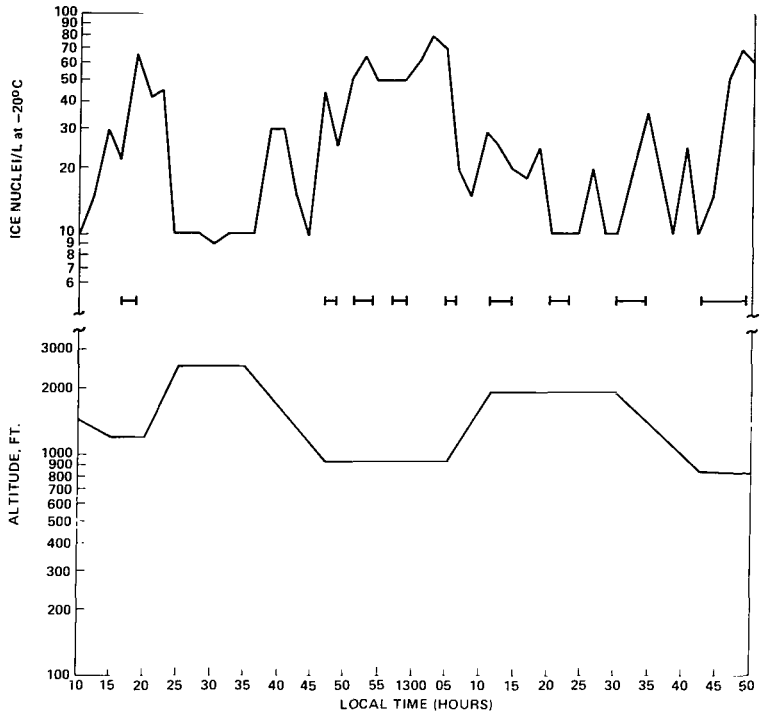

Figure IIc-39. STS-3 flight of March 22, 1982.

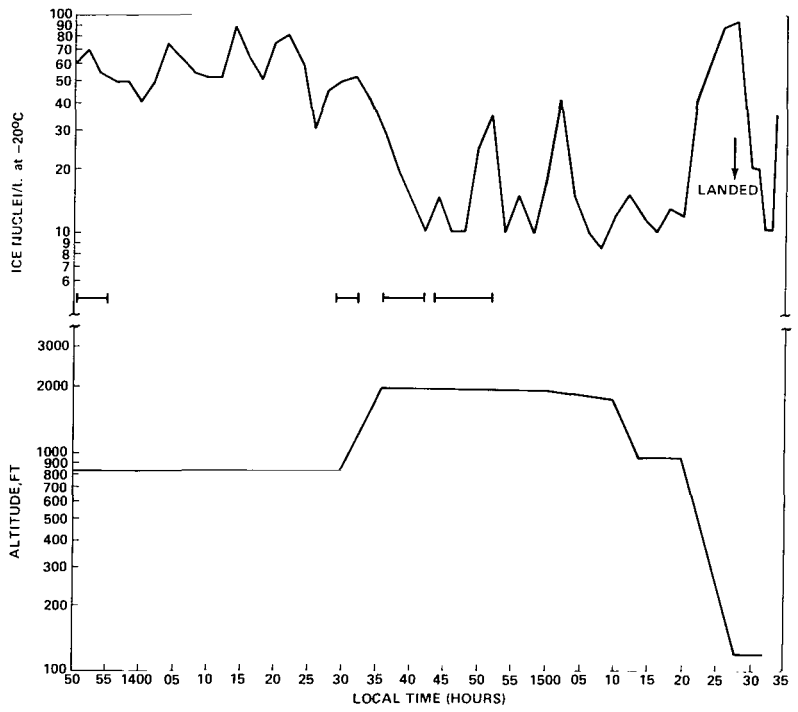

Figure IIc-40. STS-3 flight of March 22, 1982.

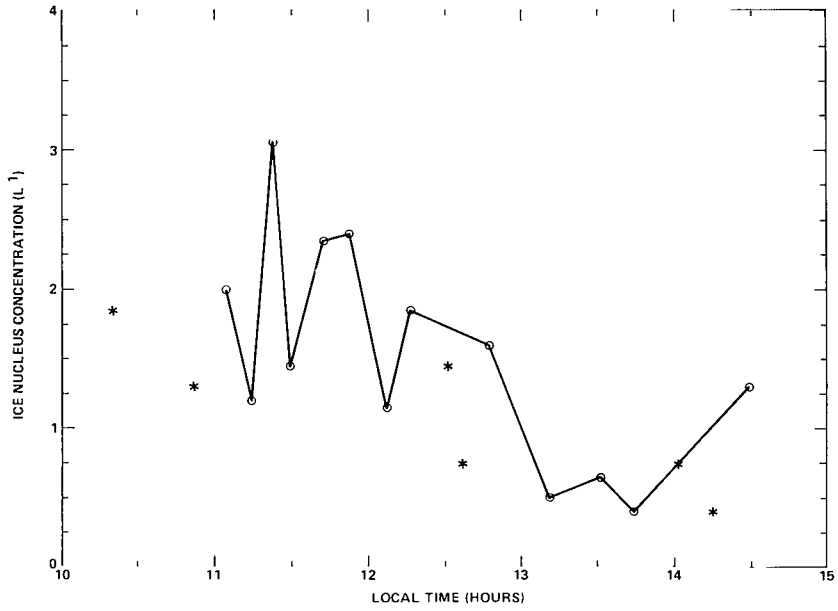

Figure IIc-41. Ice nucleus concentrations (-20°C, 100 percent relative humidity) measured with membrane filters in the Space Shuttle exhaust cloud. Isolated points are background values. Add 5 hours for GMT.

Concentrations of Aitken nuclei and CCN both increased to about 2 to 3 times the background value soon after the launch and then decayed to near background levels after the first hour. In contrast to natural clouds the CCN concentration was nearly equal to the total aerosol (Aitken) concentrations, demonstrating the hydrophilic nature of virtually all the aerosol. This close relationship between total aerosol concentration and CCN was maintained for the first 40 min after launch but became less definite as the cloud mixed with the environment. After the first hour, concentrations of both Aitken nuclei and CCN decayed toward background levels. Background levels late in the flight were significantly lower than those from before the launch, reflecting the difference between the natural aerosol over land and that over water some distance from land.

D. STS-4; June 27, 1982

There was no aircraft measurement program for the STS-4 launch so the only data is from the ground measurement program. This consisted of the deployment of copper plates along with the KSC pH papers, photography and other routine KSC environmental monitoring and meteorological measurements, and a repeat of the Air Force Geophysics Laboratory and MSFC effort to measure exhaust cloud properties at the "flame trench" site at the pad perimeter. The meteorological sounding is shown in a later section, Figure IIId-1.

The acid deposition pattern detected by the copper plates was very similar to that obtained from STS-3. The primary deposition was toward the ocean northeast of the pad and off-shore. Light traces were found on copper plates and pH papers located on the road to pad 39B, about 1.7 km west of

pad 39A. Traces of launch cloud debris, single or small clusters of Al_2O_3 spheres surrounded by small drops usually less than 200 μm diameter, also other unidentified materials, were found on copper plates up to 6 km NW of the pad. The wind record indicates that this might be expected and the sequence of still photos taken from UC-9, a site on the coast about 7 km NNW of the pad, clearly shows low level (<200 m) remnants of the exhaust moving inland. (The bearing from the camera site to the pad is 150 deg and the photos show additional westward movement.)

Several important bits of information were obtained from the instrumentation on the tower at the flame trench site even though there were several instrument failures. Perhaps most significant was a 7 ml sample of material collected in a 13.2 x 13.2 x 4 cm deep (square) dish. The dish had a blow-away cover to prevent dew collection and it contained 26 ml of mineral oil to suppress evaporation of water and HCl. The sample was composed of 30 percent solid material, by volume, and 70 percent liquid with a pH reading of 0.36. However, when titrated in the laboratory several months later the acid concentration was 2.36 N. Since the sample was kept in a sealed container evaporative loss of water cannot account for this discrepancy. The result indicates that the pH readings are not reliable this close to the end of the scale. A copper plate made to rotate at 2 rpm under a cover with a slit was completely coated with residue for 120 deg, implying that the heavy deposition all occurred in a period of about 40 sec at this site.

Two instruments were deployed to measure the air speed of the exhaust. The same NASA instrument used successfully on STS-3 was redeployed with the recording software reconfigured to record at a higher rate. This required use of a buffer memory for short term storage, with subsequent transfer of the data to tape. The information from this instrument was lost because the power failed before the data transfer was initiated. The second instrument was a Climatronics Corp., Wind-Mark I, three cup anemometer with a separate wind vane. The unit was provided by the Air Force Geophysics Laboratory. The data from this instrument (Fig. IId-1) is described in the following excerpt from the AFGL report.

> "Prior to ignition the winds were very light, less than 2 m/sec, and were generally from the south or east. This agrees well with the wind data taken at the 275 ft level. Just prior to ignition the wind speed at the 275 ft level was between 2 and 4 knots (1 to 2 m/sec) from the south.
>
> "Preliminary correlations of the wind vane as seen on our TV and the directions from the Climatronics equipment indicate that the first obscuration occurred about the time that the wind speed reached the top, heavy horizontal line (Fig. IId-1) at a wind speed of 20.1 m/sec. The small wiggles after the peak wind speed of 49.2 m/sec are taken as indications that one or more of the anemometer cups was lost about 2 sec after the cloud first reached the instruments. The decay of wind speed to the 5.6 m/sec point is consistent with the decrease of exhaust gases reaching the ground after 12 sec into the flight.
>
> "The turbulent nature of the cloud is exhibited by the large variations in wind direction during the first 2 sec. The tilting of the wind vane was such that it tended to indicate a south wind after it was bent from the vertical by the deluge. As mentioned above, one or more of the cups was lost about the time the maximum wind speed was recorded. If these events occurred at the same time, then the wind vane would no longer indicate the turbulence in the cloud, and the wind speed would tend to be underrecorded."

The TV mentioned in the AFGL excerpt is a black and white closed circuit system which was set up on the instrument tower looking past the wind vane toward the edge of the gantry. The video tape also revealed a 5.5 sec lapse from the first appearance of exhaust cloud at the gantry to the passage of the front edge of the exhaust cloud past the tower.

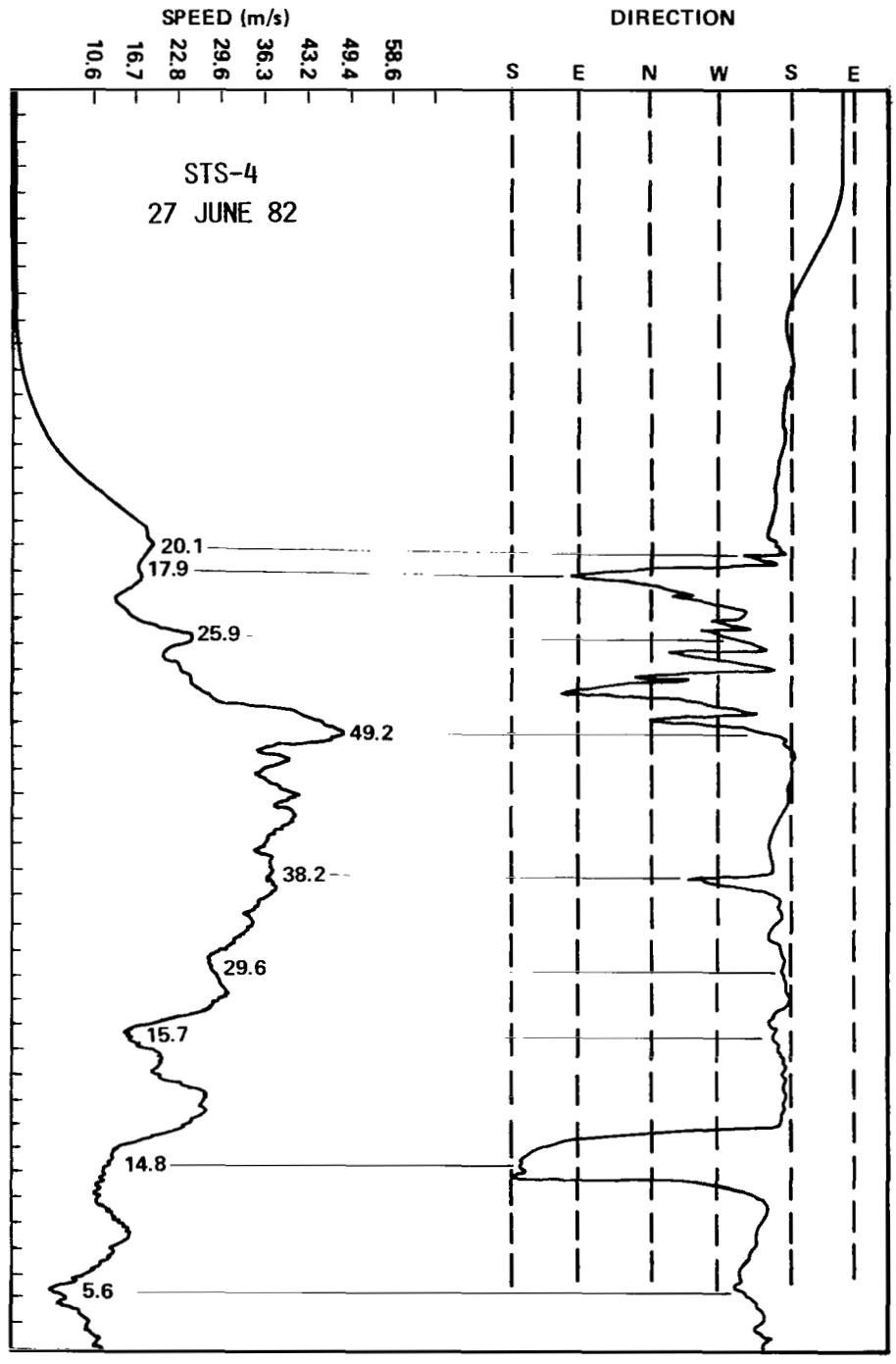

Figure IId-1. Anemometer data from the flame trench tower during the launch of STS-4. The tower is directly exposed to the SRB exhaust about 400 m from the pad. The wind speed is given on the left trace and the direction is on the right trace. Time increases downward and the paper advanced at 20 mm/sec which means that the horizontal lines are 0.25 sec apart.

The three PMS instruments set up to obtain particulate size and concentration information at the "flame trench" site again failed. This time a data tape was obtained but it contained no usable information. The instruments either fell victim to vibration damage due to the intense acoustic field, or their outputs were saturated by the high number density of the exhaust/water products.

E. 6.4 Percent Model Tests

In late May and early June 1982, the Marshall Center's Test Laboratory conducted a series of static firings of a "Tomahawk" solid rocket motor to test the initial overpressure suppression methods to be used on the western test range (Vandenberg A.F.B.). The tests utilized the Center's 6.4 percent Shuttle model facility. Initial overpressure (IOP) is the pressure wave generated by solid rocket motor ignition. Both the Kennedy Space Center and Vandenberg launch configuration can be modeled. The solid rocket motors use the same fuel as the Shuttle SRMs but their output is $(0.064)^2$ times less. Internal temperatures and pressures within the motors are comparable. Mass flow rates in the deluge/sound suppression water system are also scaled by this factor. Water flow velocities are scaled one to one, pressures are not scaled. Most linear dimensions of the launch mount are scaled down by 0.064.

Tests were conducted on May 17, 20, 24, and June 4. The May 17 test modeled the full deluge water flow rate planned for the WTR, subsequent tests used some fraction of that rate. For each test an array of copper plates and pH papers was deployed at 15 to 20 sites; the cloud development and dissipation were recorded by IR sensitive video (2 angles) and timed 35 mm still photography; and observations of temperature, relative humidity and winds were made. The observations from this test series are summarized in Table IIe-1.

TABLE IIe-1. 6.4 PERCENT MODEL TEST SUMMARY

Date (1982)	May 17	May 20	May 24	June 4
Time (CDT)	18:30	16:48	14:59	13:20
Temperature	24°C	23°C	27°C	25°C
Relative Humidity	70%	90%	64%	84%
Winds ($m\ s^{-1}$)	<1.5	2-4	<1	1-2
Deluge Water (percent of scaled baseline)				
Planned Flowrate	100%	50%	25%	50%
Actual Flowrate	95%	50%	26%	51%
Actual Total Water	45%	21%	18%	22%

Notes:
May 17: Cloud dissipated within 1 min, slight trace of smoke until 2 min. Acidic fallout covered 60 m radius circle centered about 100 m at 30 deg S of W from the pad. (Exhaust is ejected at roughly 20 deg above the horizontal so the cloud initially tends to develop at about 60 m at 35 deg S of W from the pad.

May 20: Cloud lasted less than 3 min. Acidic fallout spread in band about 100 m wide and over 300 m long. (Fallout could not be traced in forest beyond 300 m, questionable trace at 1700 m.)

May 24: Cloud rose rapidly, was very thin by 3.5 min, almost gone at 5 min. Acidic fallout in 80 m x 150 m oval centered at 110 m west of pad.

June 4: Cloud very thin at 2 1/2 min, trace visible to 5 min. Acidic fallout spread up to 150 m wide, range 550 m.

The most significant observation from this test series is the fact that acidic fallout essentially identical to that observed from the Shuttle launches occurred with each test, even though the exhaust clouds dissipated very rapidly. Figure IIe-1 shows residue from the deposition after the May 24 test. On May 17, for example, the ambient humidity was only 70 percent and the small cloud (the top only reached about 100 m) dissipated to a thin trace of smoke within 1 min. It was no longer visible after 2 min. Coagulation and other known "cloud microphysical" processes can not account for the production of the fallout particles in such a small, short-lived, dissipating cloud. Thus, these tests point to the conclusion that the fallout drops are produced directly in the exhaust – deluge water – flame trench interaction.

F. Laboratory Investigation of Copper Plate Method
(with M. T. Reischel)

The idea of using copper plates for detecting acidic drops was suggested by a report by Dawburn et al., 1980 [6]. Copper clad printed circuit board material, mechanically buffed and degreased with perchlorethylene, was tested in our laboratory prior to the launch of STS-2 for its reaction to drops of hydrochloric acid of various concentrations. The results of these tests can be summarized as follows:

1) pH = 5 (10^{-5} N HCl) – Faint brown spots. Spot diameter exceeds drop diameter slightly.

2) pH = 4 (10^{-4} N HCl) – Clear brown or violet spots, depending on viewing angle. Spots larger than 3 mm show a yellow cast.

3) pH = 3 (10^{-3} N HCl) – Spots less than 2 mm are yellow, larger ones show iridescent colors (rainbow pattern).

4) pH = 2 (10^{-2} N HCl) – Spots smaller than 2 mm show iridescent colors, larger spots are brown with white deposit on top.

5) pH = 1.0 (10^{-1} N HCl) – Brown spots with white deposits on top. Drops larger than 3 mm show traces of yellow or green.

6) pH = 0.1 (1 N HCl) – Spots are brown crystalline material with heavy green deposits around the circumference. Each drop is surrounded by brown or brown to violet iridescent pattern where vapor from drop has attacked the surface.

The tests also indicated that the spots were highly durable, but some changes in coloration do occur with age. It was concluded that the plates would be a useful indicator of both drop size and pH. Thus for each launch about a hundred plates, fifty for use and fifty for backup, were stamped with an identification number in the corner, buffed, degreased, and sealed in air tight plastic bags. The plates were taken to the Cape and deployed by the KSC environmental monitoring group to each of their field sites a few hours before the launch. Typically, the plates were clipped in a horizontal position on a light stand about a meter above the ground. Deployment sites, routes and times were the same as for the other KSC equipment.

During the STS-2 launch 16 plates were hit with acid drops. The plates were spotted from contact with acidic liquid as expected, but unlike the laboratory samples, the field samples showed large dark blue, purple, and black iridescent coloration around each liquid mark. This coloration was obviously caused by reaction of the surface with vapor released from the liquid. Subsequent laboratory testing revealed that the effect could be reproduced with HCl acid in concentrations of 0.1 N or greater by

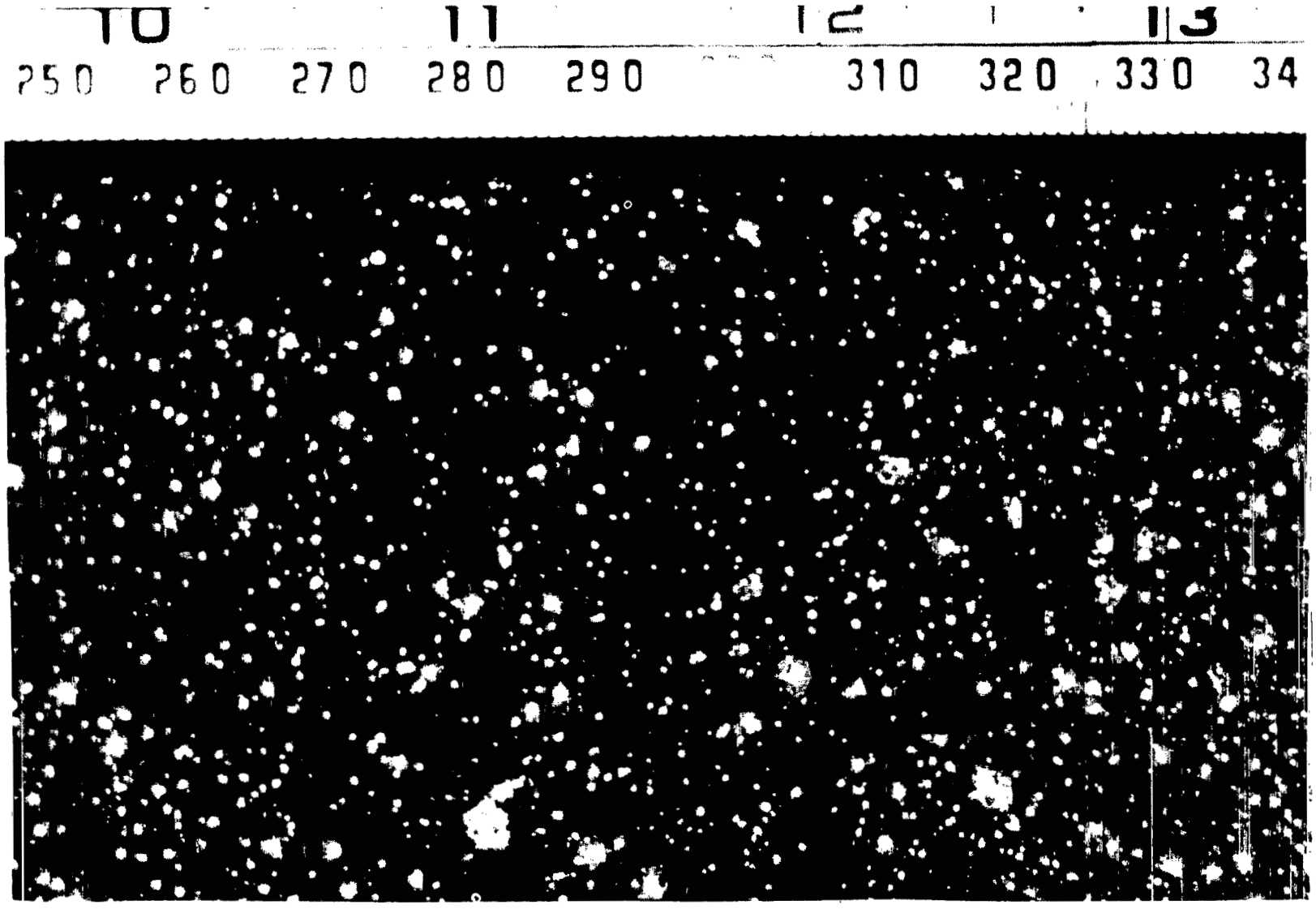

Figure IIe-1. Photograph of deposition residue on a rusted iron surface located approximately 90 m from the 6.4 Percent Model test stand. The scale is a centimeter rule; the test was conducted May 24, 1982.

placing the drops on the plates while they were exposed to strong sunlight. The intense coloration appeared as the last vestiges of the drop evaporated. These tests, as well as other experimentation with alternate surface treatments for the copper plates, made it obvious that the reaction pattern of the acid is a function of ambient temperature, wind speed, humidity, and the solar UV flux, in addition to drop size and acid concentration. Also, experience showed that the coloration on the field samples was not nearly as stable as for the laboratory samples – obvious changes occurred within 24 hr. Considering these complications, plus the problems of dealing with background salt spray and sulfur compounds in the KSC area, it was decided to not pursue a more detailed study of the relationship between drop composition and spot residue.

One of the major objectives of the copper plate deployment was to obtain an indication of the drop size distribution of the fallout by measuring the spot sizes on the plate. There are several factors which complicate the calibration; acid concentration which influences contact angle, impact angle and speed, for example. In the case of STS-2, the winds speeds were roughly equal in magnitude to the terminal velocities of the fallout drops, so the impact angles were on the order of 45 deg. As a result, the spots were elongated with length to width ratios from 3 to 6. Calculations using measured streak widths and corresponding lengths from several copper plates and assuming a reasonable uniform liquid thickness of 0.06 mm over the spot area (i.e., the solid deposits are often this high) yield a volume of liquid which corresponds to drop diameters nearly the same as the spot widths. Laboratory tests showed that when 1 N HCl drops having diameters 0.5 to 1.0 mm were dropped from small distances (about 10 cm) onto horizontal copper plates, which had air flowing laterally across them at speeds from 0.5 to 3 m s^{-1}, the resultant stain streaks had spot widths which were 1.0 to 0.6 times the drop diameter before impact. At terminal velocity (about 3 m s^{-1}) in still air, drops of this diameter impacting a horizontal surface at rest leave spot widths several times greater than the drop diameter, but it is doubtful that this occurred in the STS-2 case because of the high impact angles. More likely the spot width is somewhere between twice to 0.6 times the drop diameter; as a best estimate we assumed they were equal for STS-2.

In order to obtain a better estimate of drop to spot size ratio for use in cases where the winds were low and impact was near normal, as on STS-3 and -4, 400 and 700 micron diameter drops of various HCl concentrations in the range 0.2 to 1.0 N were dropped from 2.16 m and 11 m high, respectively, onto copper plates, and the resulting spot sizes measured. The drops were generated by using a syringe pump to feed a stream of acid through a polyethylene capillary, the end of which was vibrated by a driver attached to a speaker cone. The drop size was computed from the generation frequency and flow rate. The fall distance was adequate to allow the drops to reach terminal velocity. It was found that the relationship of spot to drop diameter ratios is best expressed by the equation

$$s = C + Bd^3 \qquad \text{(II.1)}$$

where s is the diameter of the spot on the plate in millimeters, d is the deposition drop diameter, C = 0.084634 mm, and B = 8.72976 mm^{-2}. The dependence on HCl concentration was weak so the data for all normalities were lumped together.

III. ANALYSIS

In the following sections several analyses of various processes which occur in the exhaust cloud are presented. The first two sections relate to the formation mechanism of the deposition. One discusses the possibility of formation by condensation and coagulation within the cloud, and the other discusses the HCl and water balances within the system. After that, there are three sections related to predicting the properties and effects of the cloud; ice nuclei, numerical model analysis of the cloud dynamics, and model development for prediction of deposition trajectories.

A. Condensation and Coagulation

Consider, to begin with, the formation of millimeter sized drops on a cold drink glass on a humid day. Note that the supersaturation, the driving force for condensation, is on the order of 300 percent and yet a few minutes are required to form large drops. It is not difficult to see that in the open atmosphere where supersaturations do not exceed 3 percent except for brief periods in the most vigorous thunderstorms, a few hundreds of minutes would be required to form the millimeter sized drops typical of precipitation. The theory of condensation shows that the growth rate, dr/dt, is inversely proportional to the radius. Thus, very small drops grow very quickly, easily forming visible clouds of typically 10 micron drops, but additional growth becomes progressively slower by condensation. Even where times of 10 to 20 min are available, as in natural clouds, other mechanisms must provide growth into the hundred micron size range.

In the Shuttle exhaust cloud the development of the large drops responsible for the acidic deposition is exceedingly rapid. Within 4 min after launch there are already particles throughout the range from 50 to 1000 microns in significant quantities, as the data from the aircraft penetrations of the STS-3 cloud illustrate. Deposition particles also form in the 6.4 percent model tests where the entire cloud lifetime is only 1 to 3.5 min. There is also considerable indirect evidence that not more than a few tens of seconds elapse before the deposition has developed. Thus, a simple condensation process, which would require about 1000 sec to yield a 100 micron drop, given a steady 1 percent supersaturation, is clearly not an adequate explanation. It should be pointed out that a rapid quenching process occurs as the hot exhaust mixes with the ambient air. This may produce a very high transient supersaturation but it will yield large quantities of small drops rather than a few large ones because of the inverse relationship between growth rate and radius. This has been verified in numerous experimental situations, supersonic nozzles for example, and it is especially true here because of the large numbers of aluminum oxide particles which are good nuclei for condensation.

The question next arises, having excluded condensation alone as a possible controlling mechanism, could condensation followed by coagulation of the many small drops be a sufficiently rapid production mechanism to explain the deposition from the exhaust cloud. This mechanism is responsible for the production of natural precipitation from some types of maritime clouds. Again the answer seems to be negative, although in this case the argument is not so simple or clear cut because difficulties arise from shortcomings in both the data set for the exhaust clouds and the state of the art of theoretical development. There exists, for example, a variety of data sets which exhibit considerable variation in form for the size distribution of the aluminum oxide aerosol and, as far as we know, no data for the distribution of wet particles in the 0.3 to 30 micron range. The theoretical coagulation problem is non-linear, even in the simplest formulation, necessitating the use of numerical modeling techniques for all but the most elementary calculations. Thus, the analysis must be based on simple upper-limit type calculations for the present study.

As was the case with the condensation alone, the central question is one of the efficiency of the condensation-coagulation process; can the large particles be formed quickly enough? First, a very simple estimate based on a size independent theory applicable to the mutual coagulation of small particles shows that the time required to halve the aerosol concentration (each particle collects one other) is about 1 hr [14] for the Al_2O_3 concentration expected at 8 sec after launch, 7.5 to 4.7 x 10^5 cm^{-3}. Since the minimum number of small particles which must coagulate to form a single deposition particle is 1000, and 25,000 or more is probable, this type of coagulation is obviously not fast enough. A much more efficient coagulation process occurs between drop pairs of different size when one drop is large enough to sweep through the population of smaller ones, but the numerical example given above illustrates the first difficulty in explaining the development of precipitation from the Shuttle exhaust by this mechanism, the process is too slow getting started unless it begins with a population of relatively large particles (40 microns) already established in the cloud. Since the theoretical maximum diameter for Al_2O_3 from the SRBs is 21 microns, it is not clear where this initial population would come from, although a variety of sources can be postulated (and the electron micrographs of the deposition do show a few Al_2O_3 particles as large as 50 microns).

Now consider the case of size dependent coagulation, the collection of large numbers of small drops (less than 20 microns diameter) by a few big drops (in excess of 40 microns) which pass through the small particle population because of their greater fall speed and slower response to the turbulent air flow. This process is definitely occurring in the Shuttle exhaust, as Figure IIb-5 illustrates. Each drop of acidic fallout leaves a residue of tan colored dust composed principally of Al_2O_3 spheres. The example shown in the Figure was collected on a copper plate at the launch pad perimeter. It contains an estimated 25,000 Al_2O_3 spheres, the triangular crystals are copper chloride from the reaction of the liquid hydrochloric acid with the copper substrate. This sample not only provides an indication of the composition of the fallout, it gives a verification of the rapidity of the process because of the location where it was found, within 400 m of the vehicle. Therefore, the question is whether coagulation is efficient enough to control formation of the acidic precipitation, or is it only a side process influencing the properties of the product.

When a large drop passes through a population of small particles the number of particles collected can be expressed as the product of the area of intersection, an efficiency factor, the path length, and the number concentration of small particles. The efficiency factor, E_i, accounts for the influence of hydrodynamic forces which tend to carry the small particles around the large one, wake interactions, and other effects. The numerical value is illustrated by Figure IIIa-1. Note the low efficiency for coagulation of particles less than 5 microns radius. For an upper limit calculation it is assumed that the efficiency is given by $B_i/10$ where B_i is the small drop radius expressed in microns. It is also assumed that the collector drop moves with respect to the small drop field with a velocity $V_i = K \times A$, where A is the drop radius. With K = 0.83 cm $(\mu m\ s)^{-1}$, V_i just exceeds terminal velocity. With these simplifications, the following expression for the minimum time required to grow a drop from A_o to A_f can be obtained:

$$T = \frac{3}{\pi k \sum_i N_i E_i B_i^3} \left[\ln \left\{ \frac{A_f + B}{A_o + B} \right\} + \frac{B}{A_f + B} - \frac{B}{A_o + B} \right] \qquad \text{(IIIa-1)}$$

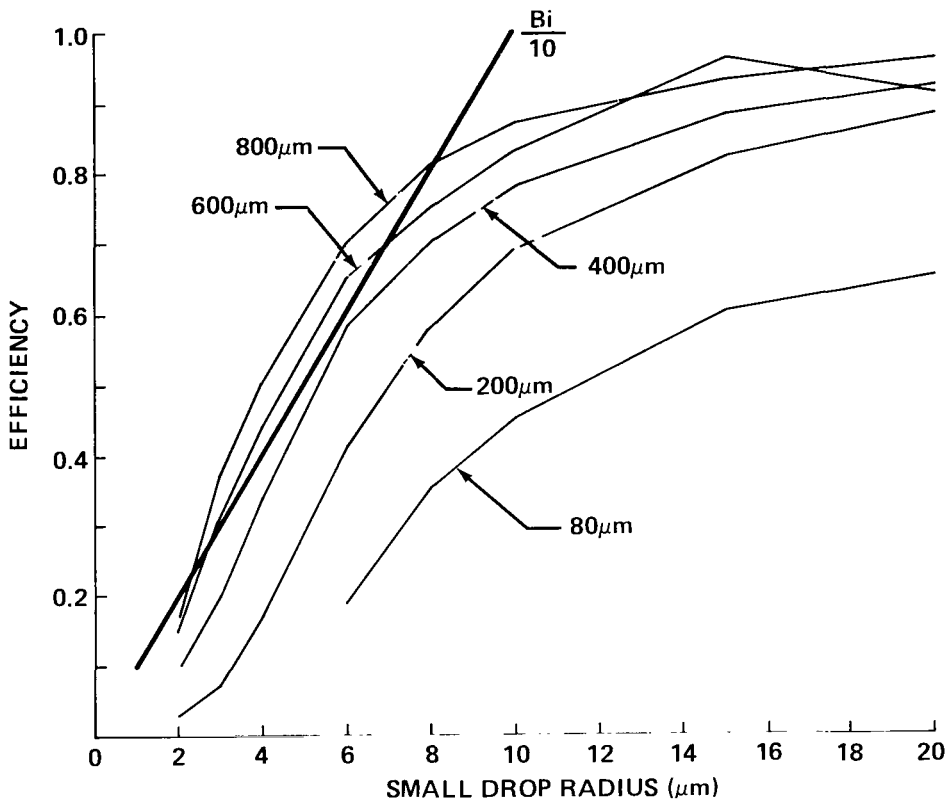

Figure IIIa-1. Linearized over-estimate of collection efficiency, $B_i/10$, plotted over theoretical values of collision efficiency from Referemce 17, p. 580. Curves are for various diameters of the collecting (large) drop. Collection efficiency equals the product of the collision efficiency and the coalescence efficiency, a number believed to be close to unity or perhaps slightly less.

Here we have assumed that the cross section of the volume swept out by the collector drop is $\pi \times (A+B)^2$ where B is a large "typical" value of B_i chosen to provide an upper limit of the collection rate. This expression is easily evaluated if the drop size distribution and the number concentration N_i for each wet particle radius, B_i, is known. Unfortunately, this is not the case for the Shuttle exhaust cloud. The attempts at making this measurement during the program fell victim to the extremely hostile environment near the vehicle at lift-off and no data has been found in earlier studies on the wet particle sizes in the first 2 min of the cloud's life. Therefore, we must resort to a construct for evaluating the minimum coagulation time.

To obtain an estimate of the small particle concentration we begin [15] with the fact that the two SRBs exhaust about 2.3×10^7 gm of Al_2O_3 in the first 8 sec. Photograph analysis shows that the SRB portion of the cloud occupies at least 1.4×10^6 m^3 at L+8 sec so the concentration of Al_2O_3 must be about 17 g m^{-3}. Beginning with this fact, two construct distributions were formed by using dry particle (Al_2O_3) distributions from References 6 and 16 and assuming additional growth by condensation so as to maintain the observed 3:7 solid to liquid ratio in the final product. The distributions are exhibited in Table IIIa-1 along with the resulting values for the minimum time to grow drops of 200 micron

diameter (the mode value from the STS-3 aircraft measurements) and 300 microns (the mass mean). Even though the distributions differ considerably they both yield minimum times of order one or 2 min to form large drops. The maximum time available, estimated from observations, is also about 1 min. Since these estimates have so little over-lap it appears unlikely that coagulation is the controlling mechanism in the production of the acidic fallout. It appears, rather, that the large drops are being produced by another mechanism – directly by atomization of the deluge water spray – and then modified by rapid scavenging of small drops of water and HCl condensed on Al_2O_3. The majority of the mass must come from the initial large drop. Visualized in this way, equation (IIIa-1) shows that the acidic fallout can collect the large number of Al_2O_3 particles observed in the deposition in a few seconds.

TABLE IIIa-1. CONSTRUCT PARTICLE DISTRIBUTIONS

CASE 1: (Ref. 16)

Index	Dry Radius	Wet Radius	Number cm^{-3}
1	3.15 μm	7.2 μm	3,170
2	4.70	7.6	1,910
3	5.90	8.2	966
4	6.95	9.0	591
5	8.15	9.9	366
6	9.70	11.3	109

Total Particle Concentration: 7,120 cm^{-3}
B: 10 μm
Initial Large Drop Radius: 20 μm
Minimum Time to Reach Mode Diameter (200 μm): 45 sec
Minimum Time to Reach Mass Mean Diameter (300 μm): 57 sec

CASE 2: (Ref. 6, p. 124, with changes)

Index	Dry Radius	Wet Radius	Number cm^{-3}
1	1.13 μm	3.3 μm	62,100
2	3.00	4.3	10,800
3	5.00	5.9	1,460
4	7.00	7.7	483
5	9.00	9.6	201
6	10.88	11.4	89

Total Particle Concentration: 75,100 cm^{-3}
B: 10 μm
Initial Large Drop Radius: 20 μm
Minimum Time to Reach Mode Diameter (200 μm): 70 sec
Minimum Time to Reach Mass Mean Diameter (300 μm): 95 sec

B. Water and HCl Sources

This section addresses the water, HCl, and energy sources present during a Shuttle launch or model firing. There are three separate cases to be evaluated, the Eastern Test Range (ETR – the Kennedy Space Center), the Western Test Range (WTR – Vandenberg), and the 6.4 Percent Scale Model of the WTR facility at MSFC. The water flows and facility designs are considerably different at each, so significant differences may be expected from one to the other. The relevant data are presented in summary form in Table IIIb-1. As can be seen from the following discussion which details how each entry in the table was evaluated, the values presented should be looked upon as "current best estimates" or "limiting values" as appropriate. The uncertainties in the data base for these calculations is always at least several percent, in some cases it may exceed 20 percent. In spite of these limitations they provide a useful basis for acid generation computations.

TABLE IIIb-1. WATER, HCl AND ENERGY SOURCES

	6.4 Percent Model (1 Tomahawk; 9.0 sec Burn)	ETR (1 SRB, 7.5 sec Burn)	WTR (1 SRB, 7.5 sec Burn)
a) Total Exhaust Mass Flowrate	19.5 kg s^{-1} (43 lb mass/sec)	5400 kg s^{-1} (11,900 lb mass/sec)	5400 kg s^{-1} (11,900 lb mass/sec)
b) Total Water Produced by SRB with Afterburning	50 l (13.3 gal)	11,590 l (3061 gal)	11,590 l (3061 gal)
c) Total HCl	35.6 kg (78.6 lb)	8508 kg	8508 kg
d) Heat Released (1200 cal/gm)	2.1 x 10^8 cal	4.9 x 10^{10} cal	4.9 x 10^{10} cal
e) Maximum Water Evaporated	360 l (95 gal)	8.3 x 10^4 l (22,000 gal)	8.3 x 10^4 l (22,000 gal)
f) Total Deluge Water	1090 l (288 gal)	2.82 x 10^5 l (74,500 gal)	5.6 x 10^5 l (148,000 gal)

a) Total Exhaust Mass Flowrate

The Shuttle SRB mass flux number was obtained from a computer reconstruction of the STS-3 launch using a modified Hercules Grain Design and Internal Ballistics program (Charles Martin of MSFC, private communication). It can be applied with high confidence to the initial Shuttle launches but it underestimates by several percent the output of the higher performance motors planned for later launches. The 5400 kg s^{-1} represents the average output over the initial 18 sec of burn time. The mass flux peaks approximately 18 sec after ignition and then decays. Thus, this figure is fairly consistent with the 9400 kg s^{-1} for two SRBs reported in Reference 15, a value which, apparently, represents the mass flux averaged over the entire burn. The mass flux shown for the Tomahawk (6.4 Percent Model) is the average value for the entire 9 sec burn since the entire time is spent on the pad. The number was derived from the total propellant mass, 175.6 kg, given in the manufacturer's data sheet.

b) Total Water Produced by SRB with Afterburning

The figures shown are estimates for the total amount of water produced in 7.5 sec by each SRB (9 sec for the Model) obtained from the product of the time, the total mass flux and the fraction of mass

flux which is water (afterburning with the chemical addition of air included). The time, 7.5 sec, is an estimate of the time the exhaust mixes strongly with the deluge water spray on the pad. It is about the time required for the vehicle to clear the tower. Including afterburning, the fraction of water in the total mass flux is 0.286 according to Reference 15. This fraction yields a figure of 11,590 l for the output of a single SRB. For comparison, the three SSME engines combined produce about 13,500 l (3600 gal) of water in the same time, with afterburning. Although the primary source of the water fraction given in Reference 15 does not appear to be correctly referenced it is consistent with a fraction of 0.093 at the nozzle exit plane. This latter figure is given by several computer models of the exhaust plume. Since these models contain a number of inherent uncertainties in the chemical reaction rate kinetics and do not consider interactions with the deluge water spray, the water fraction must be considered approximate.

c) Total HCl

The total amount of gaseous hydrogen chloride produced by each SRB was computed in the same manner as the total water produced, only in this case 0.21 was used as the fraction of HCl in the total mass flux. This value for the HCl fraction matches to within a fraction of a percent the exit plane figures from both Reference 15 and the one-dimensional equilibrium computer model of the exhaust plume used at MSFC. The impact of afterburning is unclear for HCl. Reference 15 indicates the fraction should be down to 0.189 with afterburning, but Reference 18, supposedly the original source for Reference 15, indicates an increasing fraction. In any case, the impact of mixing with the deluge water spray has not been modeled so the uncertainty in the figure is at least on the order of several percent. The mass fraction used for the Tomahawk, 0.203, was derived from the manufacturer's data and is very similar to that used for the Shuttle.

d) Heat Released

The heat released is determined by the product of the total exhaust mass flowrate, the time, and the heat content per unit mass of material. Unfortunately this latter quantity is poorly known. The thermodynamics of the rocket motor and exhaust plume is very complex and dependent upon a number of poorly known parameters (chemical reaction rates and eddy diffusion coefficients, for example). A variety of computer codes have been developed which treat the problem. They yield estimates of 1062, 1117, 1140, and 1198 cal s^{-1} for the sensible enthalpy. Other energies which must be added for some applications are the kinetic energy which evolves to turbulence and to heat, and heat released by afterburning when the plume mixes with air. The kinetic energy is of order 700 cal s^{-1} of propellant; no estimate of the afterburning energy has been found in the available sources. For estimates of the buoyancy of the cloud the heat removed due to vaporization of the deluge water must be considered. In the current study we wish to obtain an estimate of the maximum amount of deluge water evaporated in the flame trench. For this application the kinetic energy should not be included and we are forced to neglect the afterburning because no estimates are available. Thus, we assume about 1198 cal s^{-1} are released by the SRB fuel (the largest of the enthalpies calculated by the models).

e) Maximum Water Evaporated

The maximum water which can be evaporated in the initial 7.5 sec (9.0 sec for the 6.4 percent model) was calculated from the total heat available, assuming 100 percent efficiency and 5.863×10^5 cal kg^{-1} for the heat of vaporization. After launches at KSC the grass directly in line with the SRB flame trench shows damage due to acid but not heat (i.e., dead but little or no charring). Likewise the temperature rise at the tower 400 m from the vehicle and in line with the SRB flame trench is only on the

order of 30°C (Table IIc-1). This is consistent with the assumption of a high efficiency evaporative cooling process in the flame trench area. It should be noted that some of the heat of vaporization is later released as the water condenses to form the ground cloud.

f) Total Deluge Water

These figures represent the total quantity of water per SRB dumped into the flame trench area from the start of flow until L + 7.5 sec. The figure for the 6.4 percent model represents the planned flow, measured values vary about this figure by a few percent. The figures for ETR were derived from engineering data for the STS-2, -4, and -5 launches provided by the KSC Ground Systems Directorate, Mechanical and Pneumatic Systems Branch. The figure represents half the water dumped into the SRB side (amount per SRB) plus half the total "rainbird" flow on top of the mobile launch platform (0.5 x 24,000 gal). WTR data were derived from design data provided by Martin Marietta Corp., Vandenberg Operations, Special Studies and Analysis Office. Here the water is all dumped into the SRB holes, there is no equivalent to the ETR "Rainbirds."

There are two major sinks for the material listed in Table IIIb-1, the exhaust cloud and the ground in the vicinity of the launch pad. The exhaust cloud is a very dynamic system which must pass through three principle stages. In the first stage, it is produced as a combination of hot exhaust gases, water vapor from the deluge water and exhaust, Al_2O_3 particles, large water drops produced by the mechanical shears of the exhaust-deluge water interaction, and air. The next stage occurs as the cloud cools due to expansion, lifting, and mixing with more ambient air; it is marked by the growth of large numbers of small cloud drops as the temperature falls below the saturation point of the cloud. The final stage is dissipation; mixing with ambient air dries the cloud. The transition from the first to the second stage appears to require only a few tens of seconds, the transition from second to third takes longer, the time varying with atmospheric conditions.

Material too large to be carried into the cloud is deposited on the ground in the "near field." Observations at ETR indicate the near field deposition extends to about 1 km from the pad; on the 6.4 percent model it usually reaches to about 70 m which fits well with the scale factor, 1 km x 0.064 = 64 m. Photographs taken from the NOAA aircraft the day before the STS-3 launch (Fig. IIIb-1) and just 4 hr after the launch (Fig. IIIb-2) show the area around Pad 39A most heavily impacted by the exhaust cloud fallout. At WTR the SRB exhausts are split into two separate trenches, one to the north and one to the south. Thus, a double near field deposition pattern is to be expected, about 1 km out in each direction. Of course, moderate to strong winds are capable of moving these patterns around considerably.

In the cloud the material exists in several states; vapor, small particles less than 40 micrometers diameter, and large particles 40 micrometers to a few millimeters in size. Interchange between these states is very dynamic. For the portion of the cloud formed from the SRB exhaust, the primary source of water vapor in the initial seconds is the deluge water vaporized by the exhaust heat, about 2 x 83,000 l = 166,000 kg H_2O in 7.5 sec. Next most important is vapor from the ambient atmosphere, of order 0.02 kg m^{-3} x 10^6 m^3 = 20,000 kg at L+8 sec. However, this quantity will increase an order of magnitude by L+24 sec because of the rapid expansion of the cloud. The output from the SRBs including afterburning is about 23,200 kg H_2O in 7.5 sec. Vapor is also added because the subsaturated ambient atmosphere will cause some of the deluge water to evaporate, but this effect is difficult to evaluate. The cloud must also contain a considerable quantity of liquid water atomized from the excess deluge water (deluge water dumped in the initial seconds but not vaporized, about 199,000 l up to L+7.5 sec at ETR). However, the atomized deluge water is expected to contribute primarily to the large drop population which falls quickly into the near field. The relative importance of surface energy compared

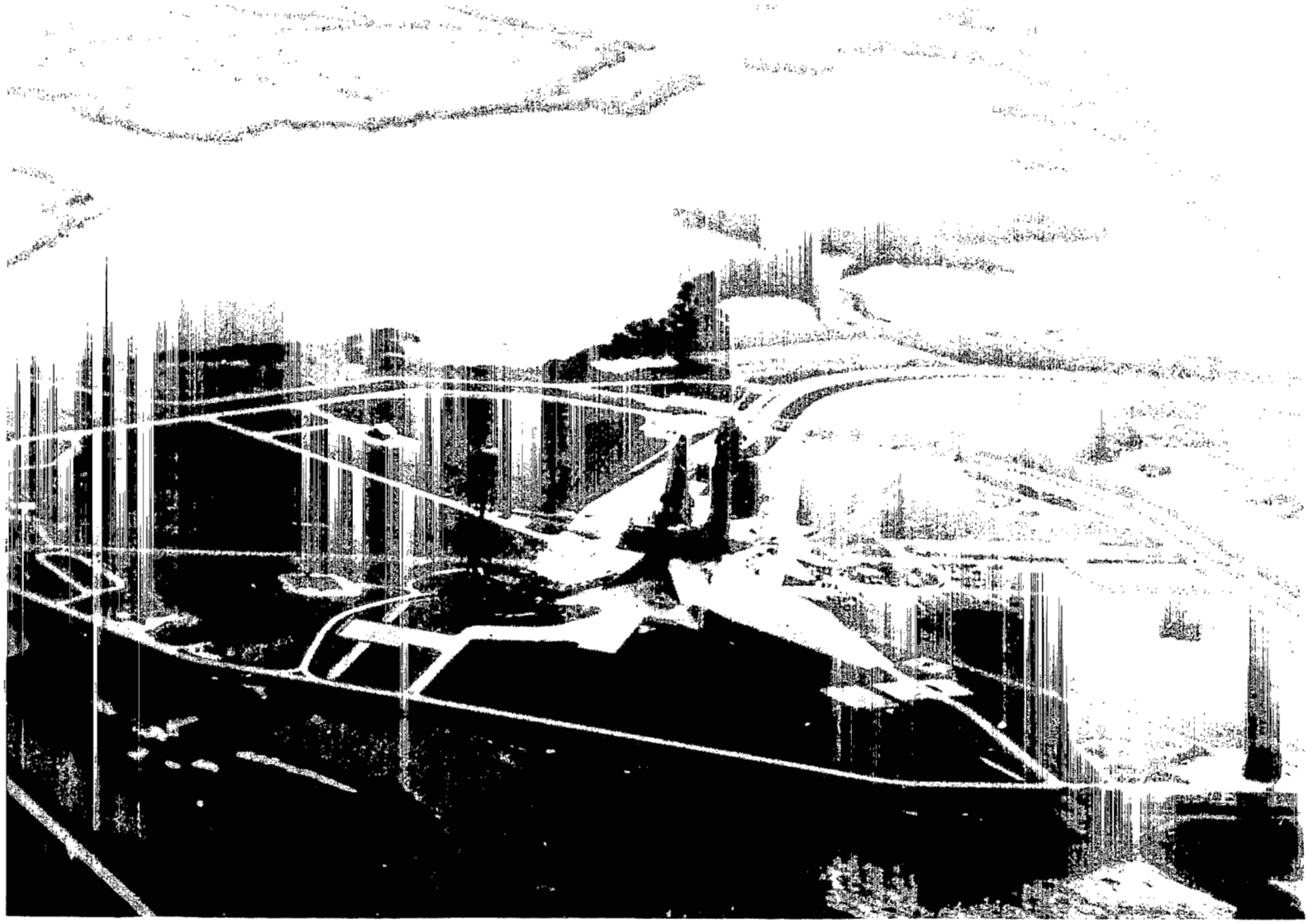

Figure IIIb-1. KSC Pad 39A one day before STS-3.

Figure IIIb-2. KSC Pad 39A 4 hr after STS-3. The deposition pattern, which is marked by a clear transition from green to brown on the original color photograph, is bounded by the dashed lines. Note the color change on the road surface.

to kinetic energy in the atomization mechanism tends to work against formation of small particles which can remain in the cloud. Currently there is insufficient data to adequately address the complex problem of the division between cloud water and vapor and the more significant question – the division of the atomized water into near field and cloud entrained water. The matter is under study.

C. Ice Nuclei

(With G. Langer and G. Lala)

Aluminum oxide is known to act as a moderately efficient ice nucleating material under some circumstances [17]. This fact, coupled with the large quantities produced and dispersed by the Shuttle exhaust cloud, has made the possibility of inadvertent weather modification via an ice phase process – ice nuclei from the exhaust cloud seeding natural clouds – a matter of concern for some time [2]. Therefore, ice nucleus counts were obtained by two methods during the STS-3 cloud penetrations (Section IIc, Aircraft Observation) and the results can be compared to background data obtained on the test flights from the days preceding the launch.

Figure IIIc-1 from the first test flight on March 18, which was limited to a 1.5 hr instrument check-out from Miami International Airport over the south Florida peninsula, shows an increase in count to 10 IN l^{-1} as altitude was gained. On climbing further the counts dropped, presumably because the aircraft rose into and above the inversion level. Upon entering an area of convective activity, an increase in count was seen. Air with a higher aerosol concentration was apparently convected from below cloud base by the cloud updrafts. Generally, micron sized soil particles are the source of IN rather than sub-micron air pollutants, except from some metal processing operations. The high counts at -23°C shows the importance of not allowing any temperature excursions in the cloud chamber.

The second flight (Fig. IIIc-2) on March 19 exhibited some of the above trends but they were more pronounced. Again, there was the pattern of a definite increase in activity with increased altitude up to the height of the inversion layer. Upon descent the IN count dropped an order of magnitude. This flight featured penetrations of small cumulus clouds resulting in rapid increases in IN count that averaged nearly 40 IN l^{-1} at -20°C.

The flight on March 21 (Fig. IIIc-3), which was staged from Patrick Air Force Base over the Cape Canaveral area, was a rehearsal of the flight pattern for STS-3. From takeoff until 13:25 EST the pre-launch stand-off pattern was practiced 15 to 20 km south of Pad 39A. The counts were again lowest on or near the ground. The IN concentration assumed a fairly consistent level of 40 to 70 IN l^{-1} at 800 m (2600 ft) in the haze layer above the Cape. It is speculated that the enhanced IN activity at this level may be due to the increase in relative humidity. No cloud penetrations were included in the stand-off pattern portion of the flight. During a climb to 1800 m (6000 ft) through clear air to find clouds, the counts decreased an order of magnitude. They increased again upon entering convective cells. After leaving this cloud system, the counts dropped until the previously mentioned haze layer was encountered again. On the final descent to PAFB the counts diminished two orders of magnitude.

These background IN counts were somewhat higher than previous data collected with NCAR ice nucleus counters in the Florida area. In March 1978 two flights [19] were made in the Cape Canaveral area with counts varying from 1 to 5 IN l^{-1} at -20°C. The air mass investigated originated from the northern part of the continent and was aged, polluted air. In 1975 extensive IN measurements were made during the summer in Southern Florida [20]. The aircraft flew mostly at cloud base [approximately 550 m (1800 ft)]. The counts increased by a factor of 2 to 3 during afternoon convective activity. It was surmised that the nuclei came from surface dust due to wind erosion by the storms. Maritime air masses were prevalent in this study. At -20°C the IN counts ranged from 2 to 30 IN l^{-1}.

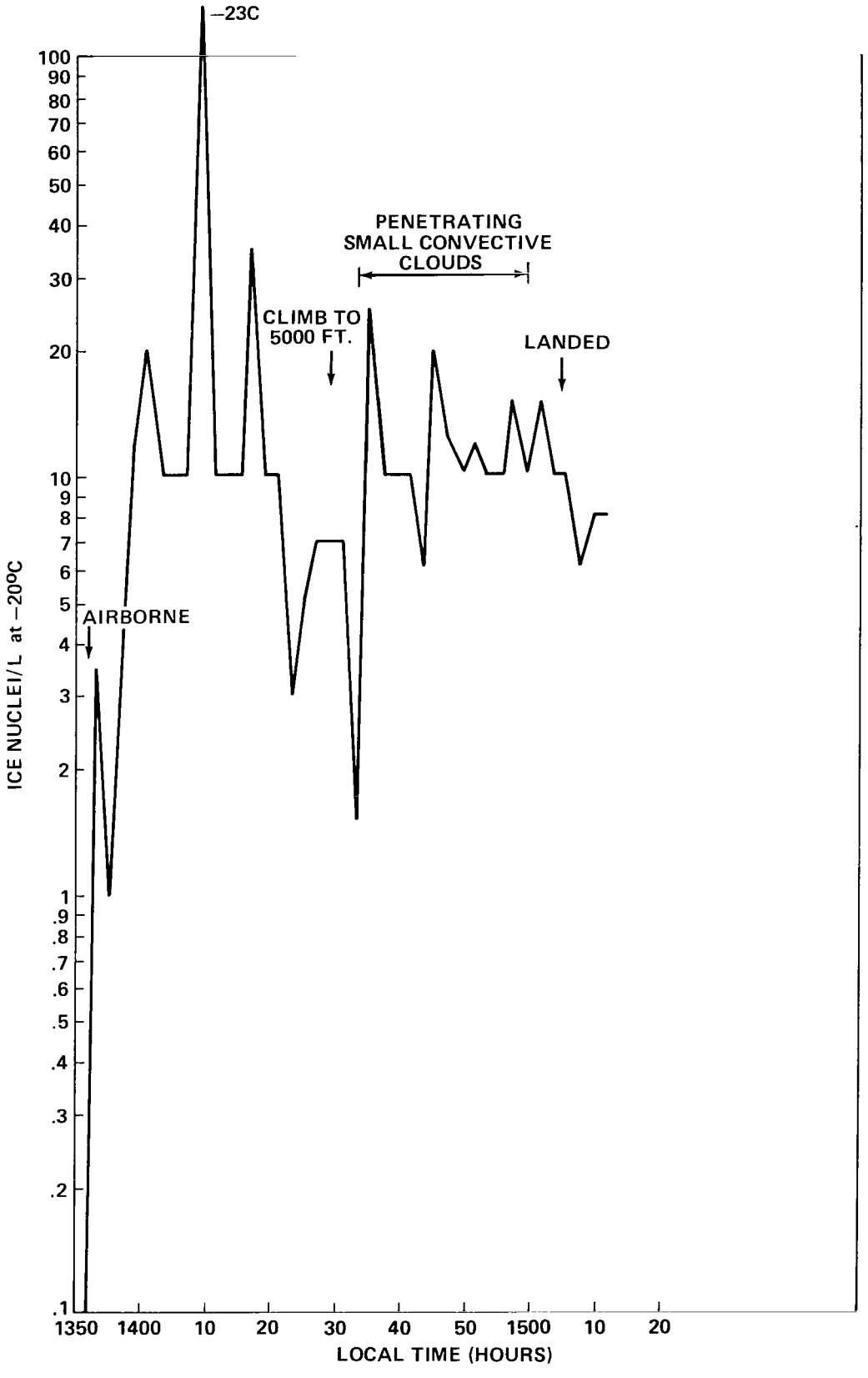

Figure IIIc-1. Flight of March 18, 1982.

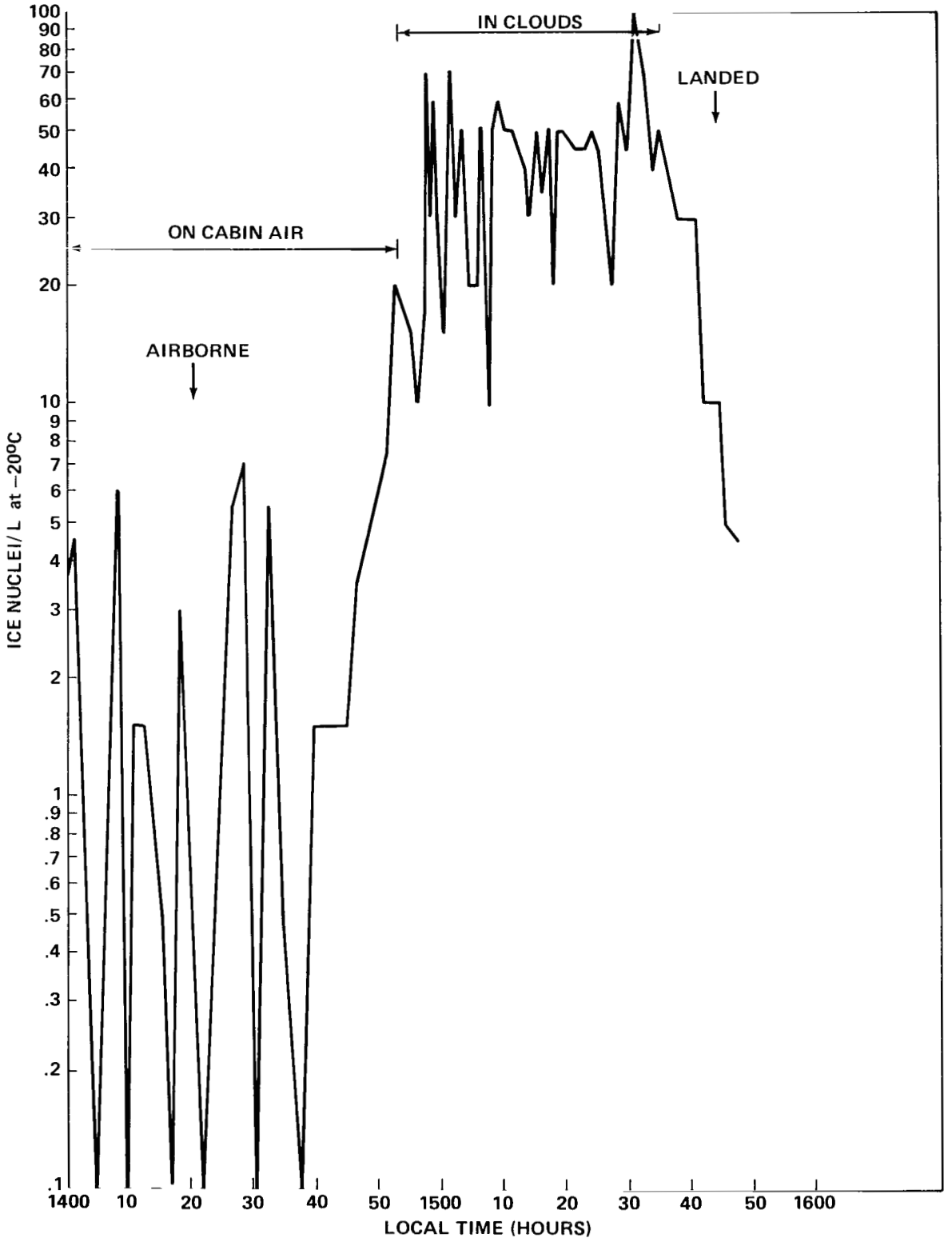

Figure IIIc-2. Flight of March 19, 1982.

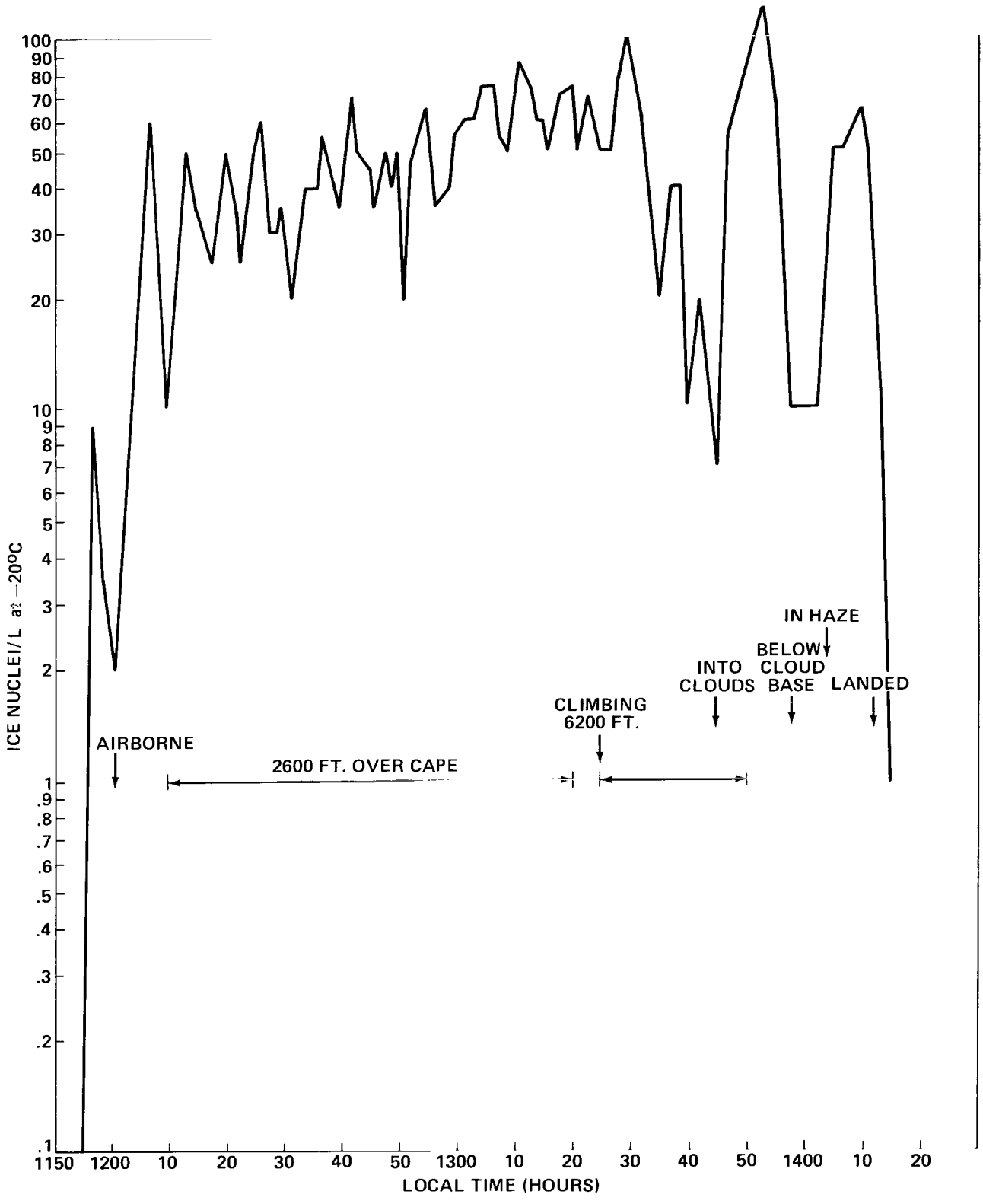

Figure IIIc-3. Flight of March 21, 1982.

Evidently, the IN counts over Florida are subject to considerable variations, indicating local sources of nuclei. There is also an indication from these studies that the IN may accumulate at the inversion level or become more active there. This has similarly been observed in the Denver area where high counts of nuclei were found at the top of the smog layer [21].

The IN data for the STS-3 launch, a sea breeze regime day with an inversion between 1900 to 3000 ft, showed no sudden change in counts following cloud penetration, but there seemed to be a gradual increase in counts by a factor of four during the first 30 min after launch of the Shuttle. However, it should be noted that during this same time the aircraft was gradually descending. This relation was studied in more detail. When a five unit running mean of the IN counts was chosen to smooth out small scale fluctuations, the inverse relationship between the IN and altitude was quantitatively confirmed with a linear correlation coefficient of -0.8. This negates the first impression that the IN counts are increasing gradually after cloud penetrations began. Analysis of all NCAR continuous ice nucleus counter results show no evident IN concentration changes due to the exhaust cloud.

Ice nucleus concentration values obtained during the flight with membrane filters were, as expected because of the differences in principle of measurement, lower than those determined with the NCAR counter. The data are presented in Figure IIc-41. They varied from 0.3 to 3 IN l^{-1}. Ice nucleus counts obtained with the filters during the flight were similar to natural concentrations measured under the same conditions, i.e., same altitude and whether or not over land or water.

A question might arise regarding the NCAR counter's ability to respond to sudden short-term changes in IN counts as expected when the aircraft penetrates the cloud at approximately 140 m s^{-1}. For example, the first two penetrations lasted only 13 and 10 sec, respectively, (Table IIc-3). After that, the penetrations were mostly over a minute with the longest one, 7.5 min, occurring 3.5 hr after launch. During the first 1.5 hr after launch the plane spent over 28.5 min in the cloud while making 20 penetrations with 2 min intervals between most penetrations in the first hour. Following this time block, 27 min were spent in clear air collecting background data. The question is, if there had been pulses of high counts, would the NCAR counter have resolved them?

Airborne NCAR counters have been used successfully for more than a decade to delineate silver iodide plumes (e.g., Reference 22) but at slower speeds than a P-3. The counter response to sharp changes in nuclei concentrations was reviewed by Heimbach [23]. Probably the most pertinent tests were done in the laboratory using a syringe to inject 5 sec pulses of 3000 IN into the sample intake [24]. The counter responded within 15 to 20 sec and decay to background counts took 5 min. The rise in count was rapid and was followed by an exponential decay. For most of the STS-3 penetrations the leading edge of the cloud should have given a distinct count (if enough IN were present), since enough time had elapsed before the cloud was entered again to allow the IN counts to drop to at least half the in-cloud value. With this in mind, an estimate can be made of the minimum significant IN concentration change between in and out-of-cloud. The average count during the first 1.5 hr of cloud penetrations was 25 ± 16 IN l^{-1}. At a 95 percent confidence limit a count of near 60 (average plus two standard deviations) would mean a different population of IN was encountered. No change in count of this order occurred during the flight in any of the 2 min count intervals (Fig. IIc-40). The fact that individual in-cloud counts were comparable to the out-of-cloud counts is quantified below.

A statistical test was made of the relationship between in-cloud and out-of-cloud IN counts with the earlier mentioned altitude effect removed. The individual IN counts in and out-of-cloud were averaged and were respectively 31 ± 20 and 26 ± 16 IN l^{-1}. The variability of the two averages is such that there is no statistically significant difference between them, i.e., the in-cloud counts were not above 60.

These results were contrary to expectation of several hundred IN l^{-1} based on past laboratory work and on flight samples taken during the launch of smaller rockets using similar solid rocket motors, e.g., Titan III [25-26]. To clarify these discrepancies, laboratory tests were made with small pieces of SRB propellant. The tests showed a time delay in nucleation, and scanning electron X-ray microprobe analysis indicated that the active particles, 1 μm or so in diameter, showed only traces of aluminum. This indicates that in laboratory tests where the propellant is burned at low pressure the properties of the resultant aerosol are much different than actual SRM exhaust. Further testing is being conducted.

D. Numerical Analyses

(With R. Sarma and G. Emmitt)

There are a series of questions that arise regarding the microphysical evolution of the Shuttle cloud and its interaction with various environments. For instance:

> How is the coalescence process affected by the input of unnatural amounts of liquid water and CCN? Is it theoretically possible to grow large precipitable drops in the cloud over its short lifetime?
>
> What happens if the cloud is initiated in a very unstable atmosphere and a self-sustaining cell is generated?
>
> What happens if the Shuttle is launched into an already existing cloud?

The infinite number of environmental conditions and cloud development scenarios necessitates using a numerical model to put some bounds on this type of problem. It was with the purpose of bracketing the acid precipitation events that a cloud model was employed. The initial set of questions being asked was most efficiently addressed with the 2-D time dependent model developed at the Institute for Atmospheric Sciences, South Dakota School of Mines and Technology. The model execution and evolution was done with the cooperation of University Space Research Association.

1. Description of the 2-D Model

The two-dimensional, time-dependent cloud model has been developed at the Institute of Atmospheric Sciences, South Dakota School of Mines and Technology, under the sponsorship of the National Science Foundation and the Bureau of Reclamation. The model is the result of approximately 14 years of research and developmental work [28-33]. It has been used with success in simulating convective situations ranging from small cumulus clouds to hail-bearing severe storms. The model has as its domain an area of 20 km by 20 km in the XZ-plane with a grid spacing of 200 m in the vertical and the horizontal. Atmospheric wind, potential temperature, water vapor, cloud liquid, rain, cloud ice, snow, and hail are the primary dependent variables. The initial conditions to the model are given in the form of a sounding – a vertical profile of temperature, dew point, and wind speeds. Natural clouds are initialized in the model by providing small perturbations in temperature and/or water vapor fields near the surface. It is also possible to enhance or inhibit convection by imposing a convergence or divergence field near the surface. Results from various cases show that rainfall amounts and rain rates predicted by the model are in reasonable agreement with the observations and exhibit proper trends [31]. Realistic airflows and water content fields are also predicted by the model.

2. HCl Modification of Two-Dimensional Model

One reason for selecting the IAS cloud model was its previous use in addressing the question of SO_2 scavenging in the formation of acid rain near the power plants. For the Shuttle case, modifications have been developed to simulate the distributions of heat, water vapor, and hydrogen chloride introduced in the atmosphere along the flight path and the distributions of liquid water and vapor introduced by the deluge water at the launch pad. The cloud model was modified to include equations that calculate the scavenging of the hydrogen chloride gas by cloud droplets and raindrops. The transfer of hydrogen chloride from one liquid water field to another, release of hydrogen chloride during droplet evaporation, and its transport by advection and turbulent mixing were parameterized. In the design of the equations determining the perturbations introduced by the launch, the initial momentum imparted to the ground cloud was not considered.

The hydrogen chloride gas that is produced by the solid rocket motors is assumed to diffuse into the atmosphere along the flightpath. It is then transported by the advective and turbulent mixing processes of the cloud model. At the same time, part of the gas is also scavenged by cloud droplets and raindrops. Here it is assumed that hydrogen chloride gas comes into equilibrium with the hydrogen chloride in solution in a very short time relative to the model time step. This assumption is reasonable as we are dealing with cloud droplets and small raindrops, and the model time steps are usually greater than 10 sec.

In this study, the evaporation of liquid water is assumed to be unaffected by the dissolved HCl. As the drops and droplets evaporate, the equilibrium calculation will release the excess HCl back into the atmosphere. Simulation of the interaction of HCl and the ice phase microphysics is not attempted in this study.

3. Conclusions from the Two-Dimensional Study

The selection of cases for model simulation was based upon the overall objective of examining the plausible range of acid precipitation events. Therefore, extreme situations were favored with the questions of frequency of occurrence being deferred to a climatological study.

Seven cases were chosen for the initial analysis:

1. STS-4 launch on 27 June 1982.
2. KSC morning fog conditions.
3. Vandenberg stable sounding.
4. Vandenberg unstable dry.
5. Vandenberg unstable moist
6. Highly unstable sounding known to produce thunderstorms.
7. Launch into an existing cumulus cloud.

A brief summary of cases 1, 2, 5, 6, and 7 is presented.

a) STS-4 Launch

The rawinsonde sounding at L+10 is shown in Figure IIId-1. The dry layer beginning at 600 mb (approximately 4500 m) inhibited cloud development to any higher levels. Use of "natural" perturbations in the model for this sounding produced only shallow clouds with tops at 1500 m. Figures IIId-2 to IIId-4 show the model results for a Shuttle launch temperature and moisture perturbation. The cloud in the lower half of the figures is the ground cloud, and the one in the upper half is the remnant of the column cloud. Some of the cloud characteristics are listed in Table IIId-1. The contribution to the rainwater field by the breakup of the deluge water is introduced as follows:

$$\Delta(\text{Rain @ } (x,z)) = A_R \exp\left(- \frac{(x-x_o)^2}{\ell^2} - 0.001\ z \right)$$

where

A_R = amplitude of rain perturbation = 2×10^{-5} g/g, and ℓ = 200 m.

This would correspond to approximately 2500 l (660 gal) of total liquid water introduced into the cloud by this process.

Note that the pH of cloud water ranges from -0.67 to 1.0 (Table IIId-1). The whole cloud stays considerably acidic through the 24 min of simulation. The upwind side (in this case, the left-hand side) of the cloud was, in general, more acidic (lower pH values) than the downwind side. This is due to cloud droplets being evaporated by the mixing of sub-saturated air on the upwind side. As the droplets evaporate they release water faster than the HCl which was in solution. In the model, this process occurs faster than the dilution due to the mixing of any more fresh air. Hence, it raises the concentration of HCl in the gas phase in that region. This process is evident in Figures IIId-3 and IIId-4 where local maxima of HCl concentration are found along the left edge of the ground cloud. Even though there was rainwater present in the model domain, very little reached the ground. It is also clear from the figures that the ground cloud helps keep the HCl in a small region at relatively high concentrations, whereas the HCl column immediately above the ground cloud dissipates rapidly.

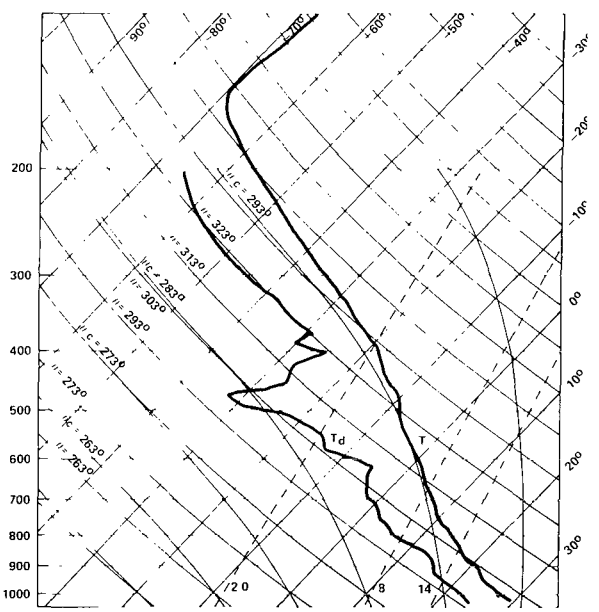

Figure IIId-1b. Meteorological sounding for STS-4 launch (1510Z, 27 June 1982).

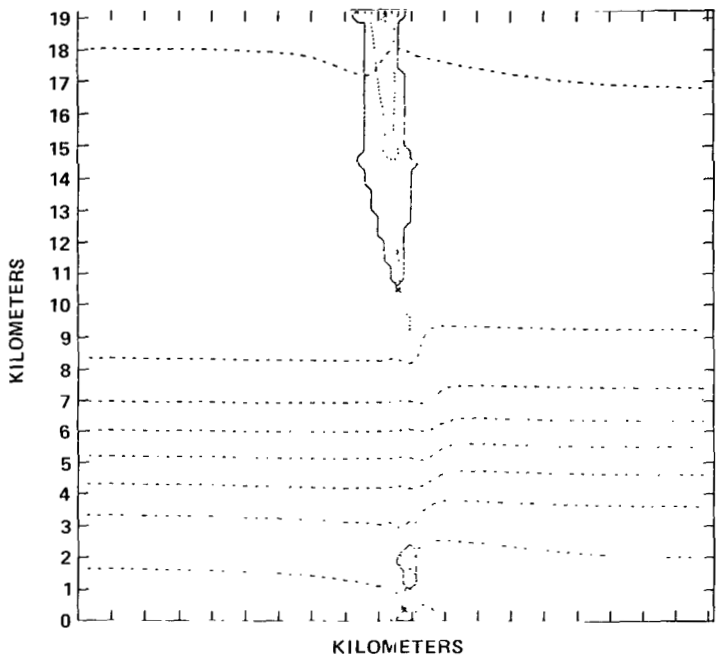

Figure IIId-2. Cloud outline (solid lines), streamlines (dashed lines), and HCl contours (dotted lines) for the STS-4 case at 3 min after launch. The HCl contours start at 50 ppm and are in intervals of 50 ppm; x denotes a local maximum of HCl concentration. Each large mark along the axis represents 1 km.

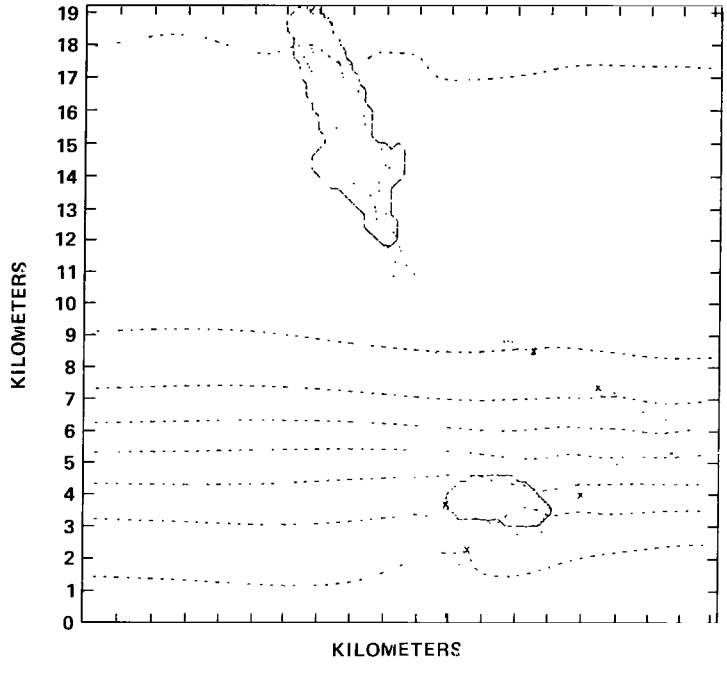

Figure IIId-3. Same as Figure IIId-2 except at 15 min after launch.

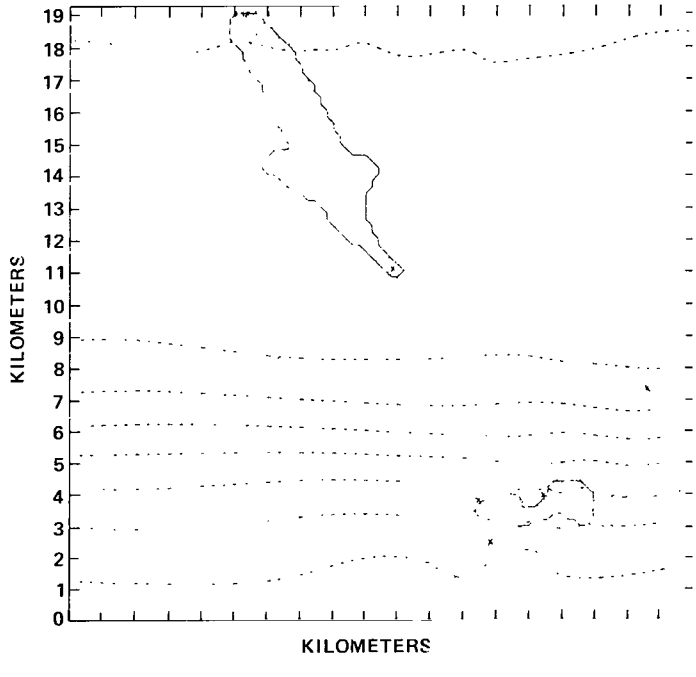

Figure IIId-4. Same as Figure IIId-2 except at 21 min after launch.

TABLE IIId-1. SOME CLOUD CHARACTERISTICS OF STS-4 CASE WITH $A_R = 2 \times 10^{-5}$ g/g

Time After Launch in Minutes	Max. Cloud Water Content g/g	Max. Rain Water Content g/g	pH Range		Max. Updraft m/sec	Cloud Top Height km
			Cloud Water	Rain Water		
3	2×10^{-4}	5×10^{-6}	-0.67 to -0.65	-0.67 to -0.4	11.7	2.4
6	3.2×10^{-3}	3.4×10^{-6}	-0.65 to 0.17	-0.67 to -0.5	11.3	3.6
9	4.5×10^{-3}	2.7×10^{-5}	-0.60 to 0.20	-0.67 to 0.2	12.4	4.2
12	4.3×10^{-3}	1.4×10^{-4}	-0.63 to 0.30	-0.63 to 0.7	6.2	4.6
15	4.0×10^{-3}	3.9×10^{-4}	-0.67 to 0.30	-0.67 to 0.3	4.0	4.6
18	4.8×10^{-3}	5.1×10^{-4}	-0.63 to 0.40	-0.63 to 0.4	4.4	4.4
21	5.2×10^{-3}	4.9×10^{-4}	-0.65 to 1.0	-0.65 to 1.0	3.8	4.4
24	4.7×10^{-3}	4.0×10^{-4}	-0.65 to 0.40	-0.65 to 2.0	3.1	4.4

b) Ground Fog

The STS-4 launch sounding was modified to produce a fog layer 800 m thick near the ground. Figures IIId-5 and IIId-6 display the cloud outlines, streamlines, and HCl contours for this case at 3 and 21 min after launch. Soon after launch, due to the mixing of hot exhaust gases, the fog in the immediate vicinity of the launch pad dissipates. The fog layer continues to dissipate downwind of the ground cloud because the airflow downwind is changed by the cloud. The inversion near the ground keeps the ground cloud trapped below 3 km. Most of the HCl is either absorbed by the ground cloud or carried up due to the buoyancy generated by the hot exhaust gases in the first few minutes after launch. Thus, the fog layer remains unaffected as far as acidity is concerned, even though the trapped ground cloud displays high acidity.

c) Vandenberg Low Level Inversion

A sounding obtained at VAFB on 10 November 1973 (Fig. IIId-7) was used for a simulated HCl-free Shuttle launch. As seen in Figure IIId-8, the resulting cloud looked like a column cloud, extending throughout the model domain in the vertical. Strong shear in the vertical probably prevented the cloud from becoming organized in an otherwise unstable atmosphere.

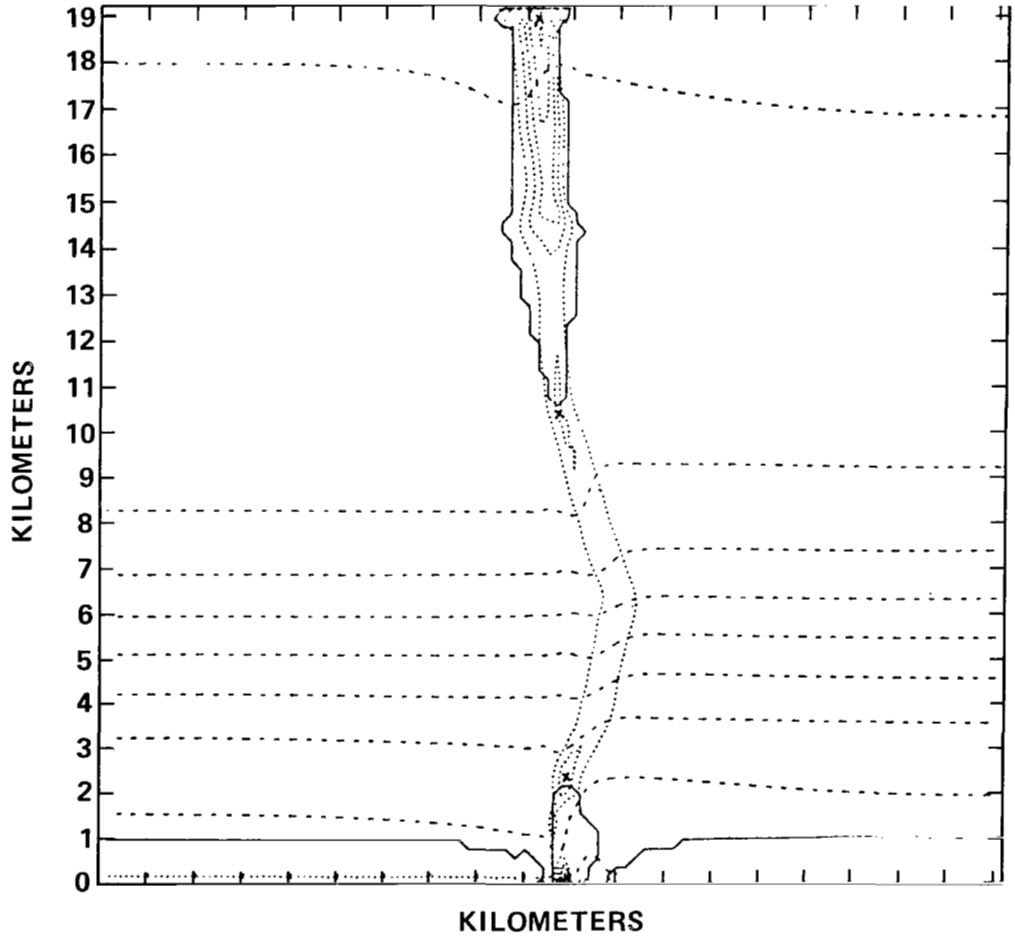

Figure IIId-5. Cloud outline (solid lines), streamlines (dashed lines), and HCl contours (dotted lines) for the KSC-Fog case at 3 min after launch. The HCl contours start at 25 ppm and are in intervals of 25 ppm; x's denote local maxima of HCl concentration.

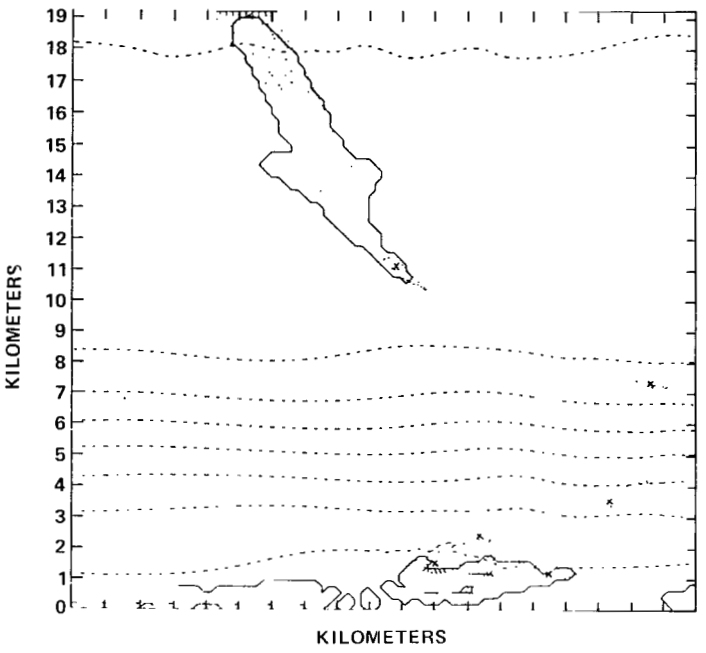

Figure IIId-6. Same as Figure IIId-5 but at 21 min after launch.

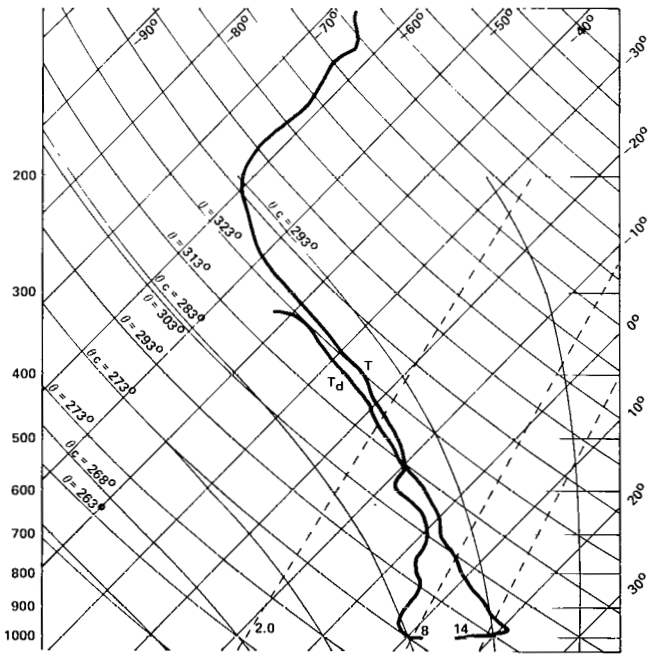

Figure IIId-7. Sounding VAFB (1109Z, 10 November 1973).

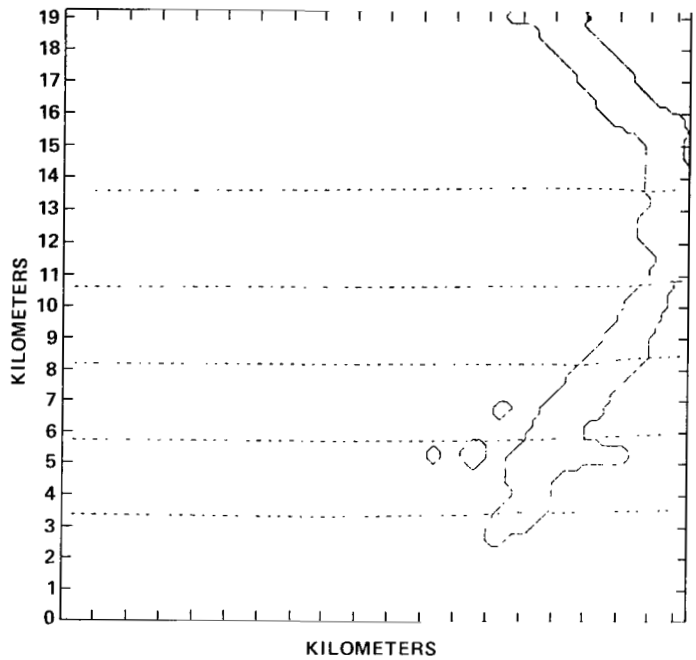

Figure IIId-8. 10 November 1973 VAFB cloud outlines at 6 min after simulated launch.

d) Very Unstable Sounding

For this case the launch perturbations were used with an unstable sounding (Fig. IIId-9). Figures IIId-10 and IIId-11 show the cloud outline, streamlines, and HCl contours for this case at 3 and 15 min after launch. An interesting difference between this case and the STS-4 case is the high levels of HCl near the ground soon after launch. The local maximum near the ground at 3 min after launch (Fig. IIId-10) was 176 ppm (by mass). This dissipates very rapidly to less than 25 ppm in 6 min. In the STS-4 case, most of the low level HCl was dissolved in the ground cloud to be released later as the cloud evaporates, whereas in the unstable case, cloud base was much higher leaving the low level HCl to be dissipated by atmospheric turbulent diffusion.

The same sounding has been tried with perturbations simulating natural convection in some earlier studies (unpublished). In those cases, the cloud formed 21 min after model initiation, the cloud bases were lower, and the clouds grew to severe storm proportions. The unstable case ground cloud, on the other hand, loses its convective nature after about 24 min. The reason for this difference between the ground cloud and the natural cloud seems to be the following: In the natural case, the cloud base was lower than the Shuttle case. Also, convection was fairly slow in the earlier stages of the cloud growth. This helped set up a low level inflow pattern which helped to augment convection. In the Shuttle case, the ground cloud fails to set up such an inflow which could bring more moisture to the updraft region. Instead, inflow is situated at a higher level, thus bringing in relatively drier air (lower water vapor mixing ratios) which helps to evaporate the cloud. Also, the launch perturbations have a smaller lateral extent than natural perturbations.

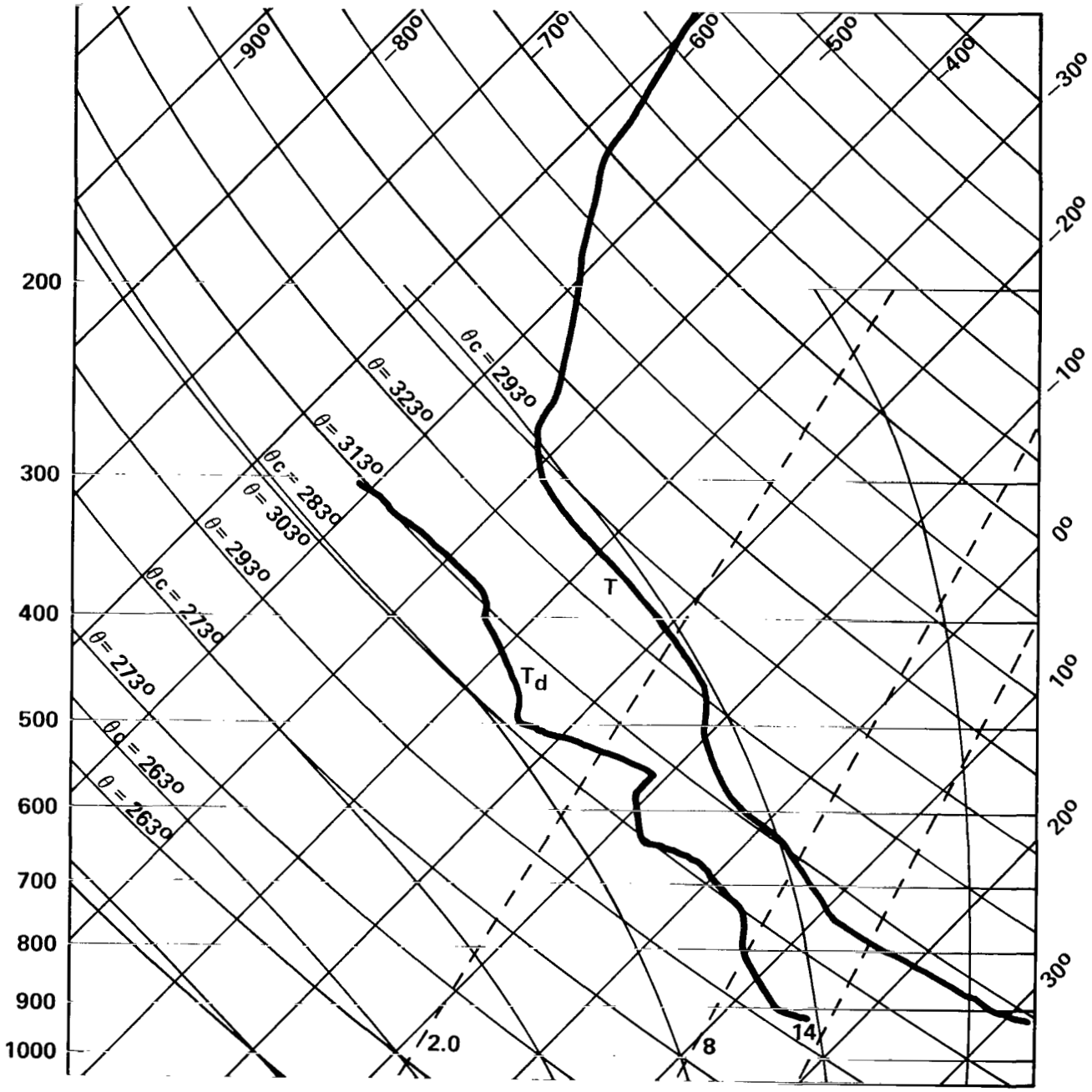

Figure IIId-9. Unstable sounding.

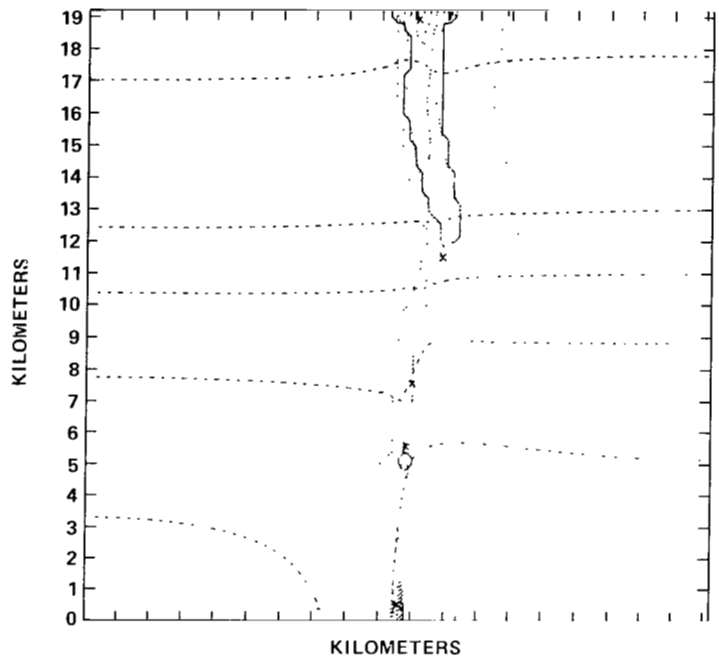

Figure IIId-10. Unstable case at 3 min after launch. The HCl contours start at 0 ppm.

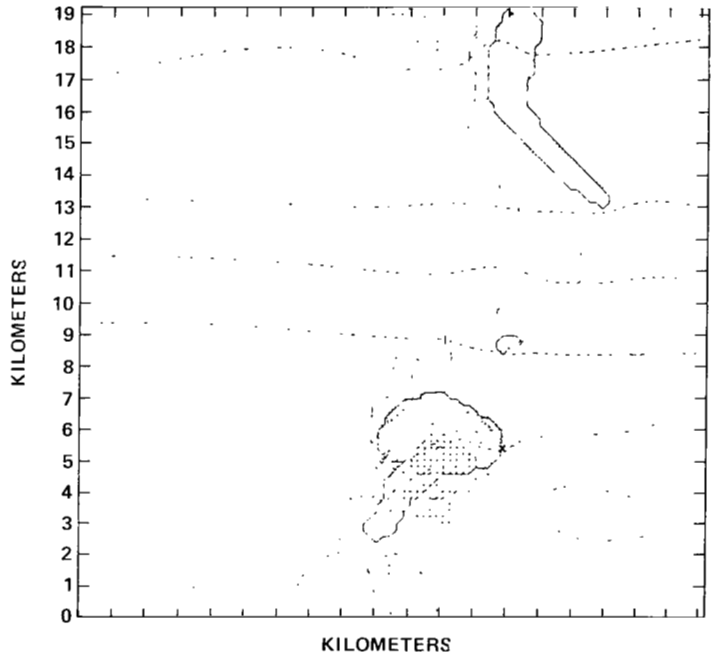

Figure IIId-11. Same as Figure IIId-10 but at 15 min after launch.

e) Launch Into a Cumulus Cloud

If the rocket was launched in an unstable environment in which there are small cumulus clouds, it is possible that the vehicle might go through one such cloud, possibly altering the dynamics of that cloud. To simulate this situation, the Very Unstable (Case 6) sounding was used to model natural convective clouds, and the launch perturbations were introduced 9 min after cloud formation in such a way that the flight path will intersect one of the clouds in the model domain. Another model run in which the launch perturbations were not introduced was used as a control. Figures IIId-12 and IIId-13 show the launch case clouds at 0 and 9 min after launch. Figure IIId-14 shows the control case cloud after the same amount of time. These figures show that the cloud into which the rocket was launched grew bigger and formed precipitation earlier than the control cloud. The launch case displayed updraft velocities that were 3 to 5 m/sec greater than the control case. It also displayed higher cloud tops.

The pH values in the launch case cloud ranged from -0.6 to 7.0, while the cloud immediately to the right of it remained "clean" until about 3 min after launch. Then the pH of its cloud water started dropping near the inflow region. Nine minutes after launch, cloud water in its inflow region displayed pH values in the range 2.3 to 3.0. This happened because the outflow from the first cloud contaminates the inflow of the second.

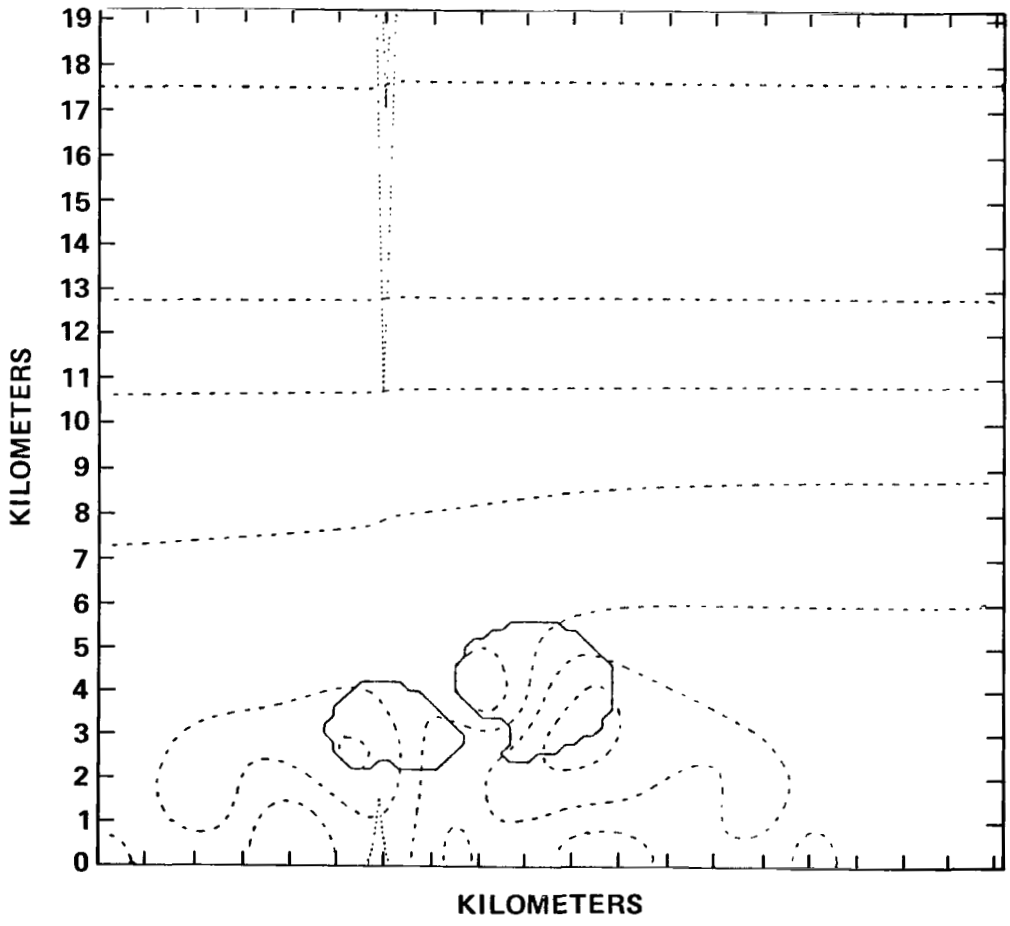

Figure IIId-12. Cloud outlines, streamlines, and HCl contouring for the "launch through a cloud" case. The HCl contours start at 100 ppm and are in intervals of 100 ppm.

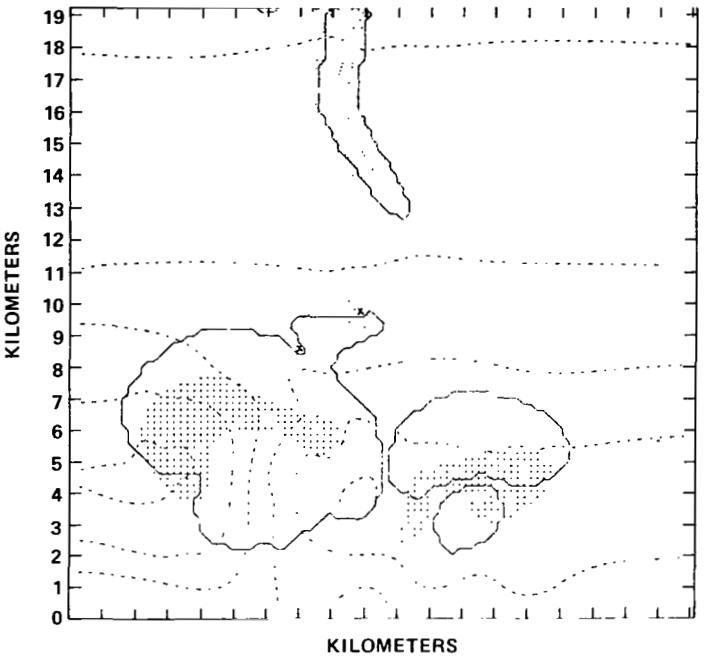

Figure IIId-13. Same as Figure IIId-12 at 9 min after launch.
The stippled areas represent regions having rainwater content greater than 1 g/kg.

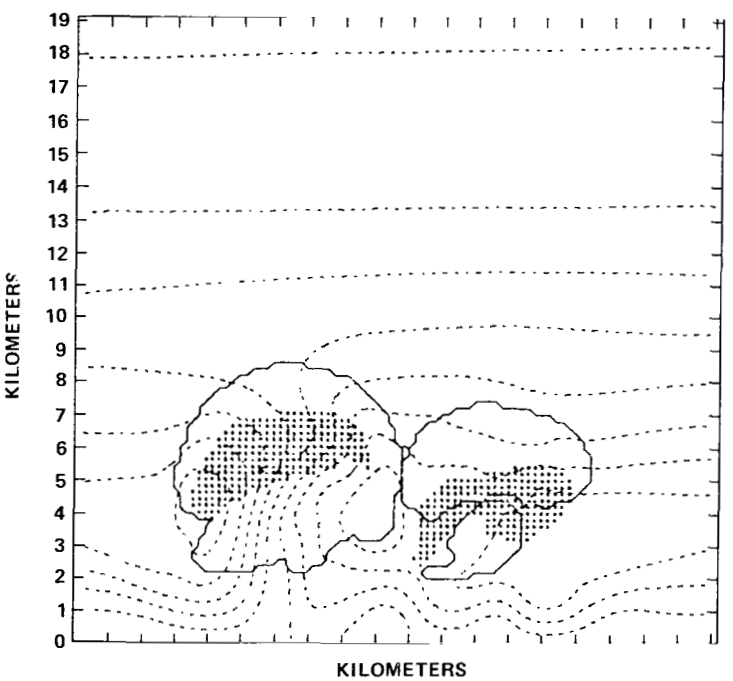

Figure IIId-14. Cloud outlines and streamlines for the control case corresponding to Figure IIId-13.

4. Summary of Two-Dimensional Studies

The exhaust cloud simulations made in this 2-D cloud model study indicate that the launch of a large rocket can produce ground clouds of varying size and convective potentials in different environmental situations. In a marginally stable environment the launch produced a ground cloud which persisted for 20 to 30 min, whereas a natural cloud (which was forced by a natural thermal bubble) did not survive for more than 10 min and was much smaller in size. In an unstable environment, the ground cloud displayed less convective growth than a natural cloud, though this cannot be generalized to all unstable situations. In the case tested, the ground cloud failed to set up an inflow pattern which would supply it with more water vapor for further growth.

The cloud water and rainwater associated with the ground cloud showed high acidity (minimum pH observed was -0.67) due to the scavenging of HCl. The upwind edges of the cloud had lower pH values than the cloud interior. Also, higher concentrations of HCl gas were found near the upwind edges. This HCl was released from cloud water when mixing of dry air near the cloud edges caused the cloud water to evaporate.

Introduction of liquid water due to the atomization of deluge water made formation of precipitation easier. As the rainwater displayed high acidity, increasing the liquid water contribution by deluge water breakup increased the possibility of acidic rain near and downwind of the launch pad.

It was found that launching of the rocket during fog resulted in the fog dissipating near the pad area. The fog itself did not seem to be contaminated by HCl. In the case simulated, the ground cloud was trapped near the ground by the inversion that contained the fog layer.

Launching into a natural cumulus cloud in an unstable atmosphere caused it to grow more vigorously than if left to natural evolution. The rocket penetrated cloud produced precipitation earlier than the corresponding control cloud.

E. Deposition Trajectory Model

1. Objective

The objective in developing a simple exhaust cloud-drop fallout trajectory model is to determine, given only the atmospheric sounding near launch time, the location of the acidic deposition footprint which results from each launch of the Space Shuttle. This capability provides a tool for real time prediction of exhaust cloud effects when used with predicted soundings a few hours prior to launch. For this application, the model should be able to perform two important functions: (1) indicate the most probable deposition pattern of exhaust products (liquid and gas), and (2) indicate in an "alarm" mode when the meteorological conditions are such that the assumptions upon which the model prediction is based are no longer valid so that other means of predicting exhaust effects may be employed.

2. Description

Since the acidic deposition is formed by the atomization of a portion of the deluge water followed by rapid scavenging of Al_2O_3 particles and HCl gas, it forms very quickly following SRB ignition and most of the large acidic drops are deposited in the immediate pad vicinity. Some of the acidic drops, however, are lifted in the updrafts of the buoyant exhaust cloud as it rises, stabilizes, and moves with the prevailing winds. These drops fall from the exhaust cloud when the updraft velocity in their

portion of the cloud decays below the terminal velocity for that particular drop size. Drop fallout begins at cloud initiation and continues (sometimes irregularly depending on the evolution of the updrafts) until the drop concentration is depleted. Since stabilization height of the exhaust cloud is a function of atmospheric stability and since drop evaporation rate is a function of humidity, the atomization – scavenging – transport process results in an acidic deposition footprint on the ground which varies in location from one launch to another depending on winds, humidity, and atmospheric stability.

In this section we discuss a modeling approach which addresses one portion of this problem, deposition pattern modeling under "normal" launch conditions. "Normal" in this context means that the exhaust cloud forms near the ground, rises until the cloud "stabilizes," i.e., stops rising, with its top 1 to 3 km high, and then slowly disperses. The model presented in this paper is very preliminary, designed only to indicate the methodology which may be employed to develop an operational model.

In general, both a cloud's internal dynamics (updraft structure in space and time) and the development of the liquid drop size spectra are very complex processes which are dependent upon the existing meteorological conditions. Numerical modeling of such a multiphase, time dependent, three dimensional system for general operational applications is beyond current modeling technology. However, in the case of the Shuttle exhaust cloud simplifying assumptions can be made. First, atomization of deluge water at the pad is the primary generating process for the deposition, so the total quantity of fallout is not expected to be highly dependent upon meteorology. Thus, for "normal" launches the total fallout is assumed to be constant from one launch to another and need not be modeled. Second, the location of the deposition is primarily determined by what happens after the material leaves the cloud because the residence time in the cloud is less than the free-fall time. Therefore, the exhaust ground cloud may be treated as a "black box" whose location is approximately known as a function of time and the fallout trajectories of representative size drops may be computed from the cloud's position with respect to the ground.

This approach was first utilized in an attempt to explain the deposition pattern detected by the copper plate array after the launch of STS 2. A very simple drop trajectory model was developed and coded in HP-Basic for use on a Hewlett-Packard Model 9845 B desktop computer. This model showed that for the high wind conditions prevalent for STS-2 the fallout could indeed be explained as having come from the exhaust ground cloud; thus, it was not necessary to assume that the fallout came from as high as the column cloud, as some had suggested.

Sometime later, Dr. Andrew Potter of the Space Environmental Office, JSC, requested that the model be enhanced to include deposition as the exhaust cloud rises to stabilization height and to also include drop evaporation. The model has been modified to include these suggestions, recoded in Fortran IV and operated on MSFC's Hewlett-Packard Model 1000 F series minicomputer. A copy of the program listing for the current model is presented in Appendix I. The assumptions on which it is based are summarized in Table IIIe-1. Tables IIIe-2 and IIIe-3 list the program inputs and outputs. When the computer program is run, the important output parameters are written on a computer disk file named by the operator in response to the prompt, ENTER FILE NAME, as well as output on the printer. Using a second program named VPLOT, the program listing for which is also given in Appendix I, multiple plots can be made without re-executing the main program. The plots give the exhaust cloud ground track and drop impact positions on an XY coordinate system marked off in 1 km units. Since the origin of the XY coordinate system can easily be moved to different positions on the plot paper by simply specifying its position as a decimal fraction pair of the unit X and Y lengths available, all runs can be plotted on 8½ by 11 in. paper oriented vertically with the Y axis (North) along the longer dimension.

TABLE IIIe-1. MODEL ASSUMPTIONS

1. Cloud base and cloud top are predetermined as a function of time:

   (a) Presently, by measurement on available STS exhaust cloud photographs.

   (b) In the future, possibly from a one-dimensional modified existing cloud model.

2. XYZ right hand coordinate system: plus X is east, plus Y is north. Origin at launch pad. For launch pad 39A: at T = 0 (L plus 0); exhaust cloud center is given by X = 0, Y = 500 m. (Both SRB exhausts are directed to the north at high velocity.)

3. Any number of sounding levels may be used. (The more the better, particularly below 500 m). All sounding levels from just above cloud base to just below cloud top are used to determine the average weighted wind which acts on the cloud as it rises.

4. Time step = time between successive cloud height observations. (Typically 30 sec).

5. New X, Y, Z position of cloud center computed each time step.

6. Not necessary to compute cloud position later than L plus 10 min. (Drops have already departed cloud.)

7. The deposition footprint for the entire cloud lies inside the deposition envelop of drops falling from cloud base and cloud top.

8. Drop fall velocity is recomputed at each sounding level using empirical equations developed for pure water.

9. Drop retains its size and has constant terminal velocity throughout a given layer.

10. Time spent in given layer equals distance between adjacent sounding levels divided by drop terminal velocity.

11. Average wind in layer acts on drop during time spent in that layer.

12. Relative humidity at each sounding level is computed using temperature and dew point temperature.

13. Amount drop evaporates is function of temperature, relative humidity, and time in the layer. Evaporation rate equation is that for pure water.

14. Drops initially consist of 30 percent particulates and 70 percent liquid by volume.

15. Drops cannot become smaller by evaporation than the dry particle diameter. If drops become less than 100 μm diameter their trajectory is no longer followed.

TABLE IIIe-2.

Variable Model Inputs	Name	Format	Type of Unit	Input
Number of cloud height observations	NCHO	Integer	None	Program (line 57)
Number of sounding levels	M	Integer	None	Program (line 58)
Number of drop sizes	NDS	Integer	None	Program (line 197)
Drop diameters	D (NDS)	Decimal	Micro-meter	Program (lines 199-208)
Time after launch	TT	Decimal	secs	Data statement
Height of cloud base	CLBS	Decimal	Meters	Data statement
Height of cloud top	CLTP	Decimal	Meters	Data statement
Sounding height	HT	Decimal	Ft	Data statement
Wind speed	U	Decimal	Ft/sec	Data statement
Wind direction	DIR	Decimal	Degrees	Data statement
Temperature	TC	Decimal	Degrees C	Data statement
Dew point temperature	TD	Decimal	Degrees C	Data statement

TABLE IIIe-3.

Model Outputs	Variable Name	Format	Units
Sounding data:			
Height	HT	F10.1	meters
Wind speed	U	F5.1	m/s
Wind direction	WD	F5.1	degrees cw from n
Temperature	TC	F6.1	degrees C
Dew point temperature	TD	F6.1	degrees C
Relative humidity	RH	F5.1	percent
Cloud position versus time:			
Time after launch	TM	F10.1	minutes
Cloud base	CLBS	F10.1	meters
Cloud top	CLTP	F10.1	meters
Cloud center	CLCTR	F10.1	meters
X-coordinate of cloud position	SCLP	F8.1	meters
Y-coordinate of cloud position	YCLP	F8.1	meters
Distance from launch pad	RCLP	F8.1	meters
Angle from launch pad	THETA	F5.1	degrees cw from n
Drops falling from cloud base/top:			
Time after launch	TM	F10.3	minutes
Drop diameter	DIA	F13.2	micrometers
Terminal velocity of drop	V	F11.2	m/s
Height of drop above ground	ZN	F10.1	meters
Distance from pad	R	F12.1	meters
Angle from pad	THET	F17.1	degrees cw from n
X-coordinate of drop position	X	F11.1	meters
Y-coordinate of drop position	Y	F11.1	meters
Summary of drop fallout:			
Time drop began falling	TDBF	F6.2	minutes
Time drop impacted ground	TOFI	F6.2	minutes
Initial drop diameter	DIAIN	F8.1	micrometers
Final drop diameter	FDIA	F8.1	micrometers
X-coordinate of drop impact	FXC	F8.1	meters
Y-coordinate of drop impact	FYC	F8.1	meters
Distance from pad	FDIST	F7.1	meters
Angle from pad	FANG	F5.1	degrees cw from n
Drop fell from cloud base/top	ORG	1A2	none
Drop "wet" or "dry" at impact	WOD	1A2	none
"Dry" particle diameter	PRAT	F8.1	micrometers

Figures IIIe-1 and IIIe-2 are examples of the model output for STS-1 and STS-2, respectively. Since the model does not presently predict cloud height as a function of time, it is necessary to input cloud height from photographic measurements after the launch or use data from previous launches. Photogrammetrically measured cloud base and cloud top heights versus time after launch which were used in the model run for STS-1 are given in Figure IIIe-3. Cloud heights for STS-2 were very similar. Cloud heights measured from STS-3 photographs are plotted in Figure IIIe-4. Average cloud top rise rate for the first 3 min after launch was about 8 m s^{-1} for both STS-1 and STS-2. For STS-3 it was about 4 m s^{-1}. Model runs were made for STS-4, STS-5, and STS-6 first using STS-1 cloud height observations and then using STS-3 cloud height data. In each case the sounding data used was that tabulated in NASA, MSFC Technical Memorandum for that particular launch such as from Johnson et al. [4] for STS-1 and Johnson and Brown [5] for STS-2. For the plotted output such as Figures IIIe-1 and IIIe-2, pen color (1), which is normally blue, is used to draw the X and Y axes, the exhaust cloud ground track (denoted with dots), and the fallout from the top of the cloud. Pen color (2), normally red, is used to draw the symbols which represent fallout from the cloud base. Fallout from both the cloud base and cloud top is denoted with a circle if the particles are "wet" when they impact the ground and a cross if they are "dry." The diameter of the circle and the circumscribed diameter of the cross have a scaled size of 1 km which is roughly representative of the exhaust cloud diameter. Predicted fallout is heaviest in the areas of overlapping circles but may occur anywhere within any of the area bounded by circles or crosses. It should be noted that some strongly acidic liquid will remain trapped in the spaces between adjacent aluminum oxide particles even after the particles become "dry."

3. Model/Observation Comparisons

Observations of Al_2O_3 deposition residue and spotting on vegetation were used by the KSC environmental effects study group to map the deposition footprint (Fig. IIa-1) resulting from STS-1. Comparison of the model output for STS-1 (Fig. IIIe-1) with observations shows reasonably good agreement in deposition location although some deposition was observed a few kilometers east of the boundary predicted by the model. Comparison of the model output for STS-2 (Fig. IIIe-2) with observations of the fallout pattern mapped with copper plates (Fig. IIb-2) also shows reasonably good agreement. The exhaust ground cloud track and deposition footprint from both the STS-3 and STS-4 model runs extend roughly northeastward from Pad 39A over the ocean in general agreement with observations. The STS-5 exhaust ground cloud moved westward across the JCS-6 camera site, where on-station KSC personnel observed deposition occurring, and over the Indian River. Again the model output agreed with these observations.

For STS-6 there was considerable wind shear with height below 5,000 ft, so the model output using STS-1 cloud height data is somewhat different from that obtained using STS-3 cloud height data. Although in both cases the ground cloud track extends north-northwest from Pad 39A and fallout from cloud base lies to the west of the cloud track, when using the STS-1 cloud height data the model output shows fallout from cloud tops impacting considerably farther north and east then when using the STS-3 cloud data. In both cases, however, all fallout occurs in the quadrant between West and North.

It is worthwhile emphasizing that the accuracy of a deposition footprint prediction for any launch is highly dependent on how well the model input winds, which may be required several hours before a launch, represent the real wind conditions in the vicinity of the exhaust cloud at launch time. This limiting factor should be considered when determining the level of sophistication to be incorporated into a final model. To display the wind variability and to make the deposition prediction more conservative, the model could be run consecutively with anticipated wind extremes. This is important since this model does not account for any type of diffusion.

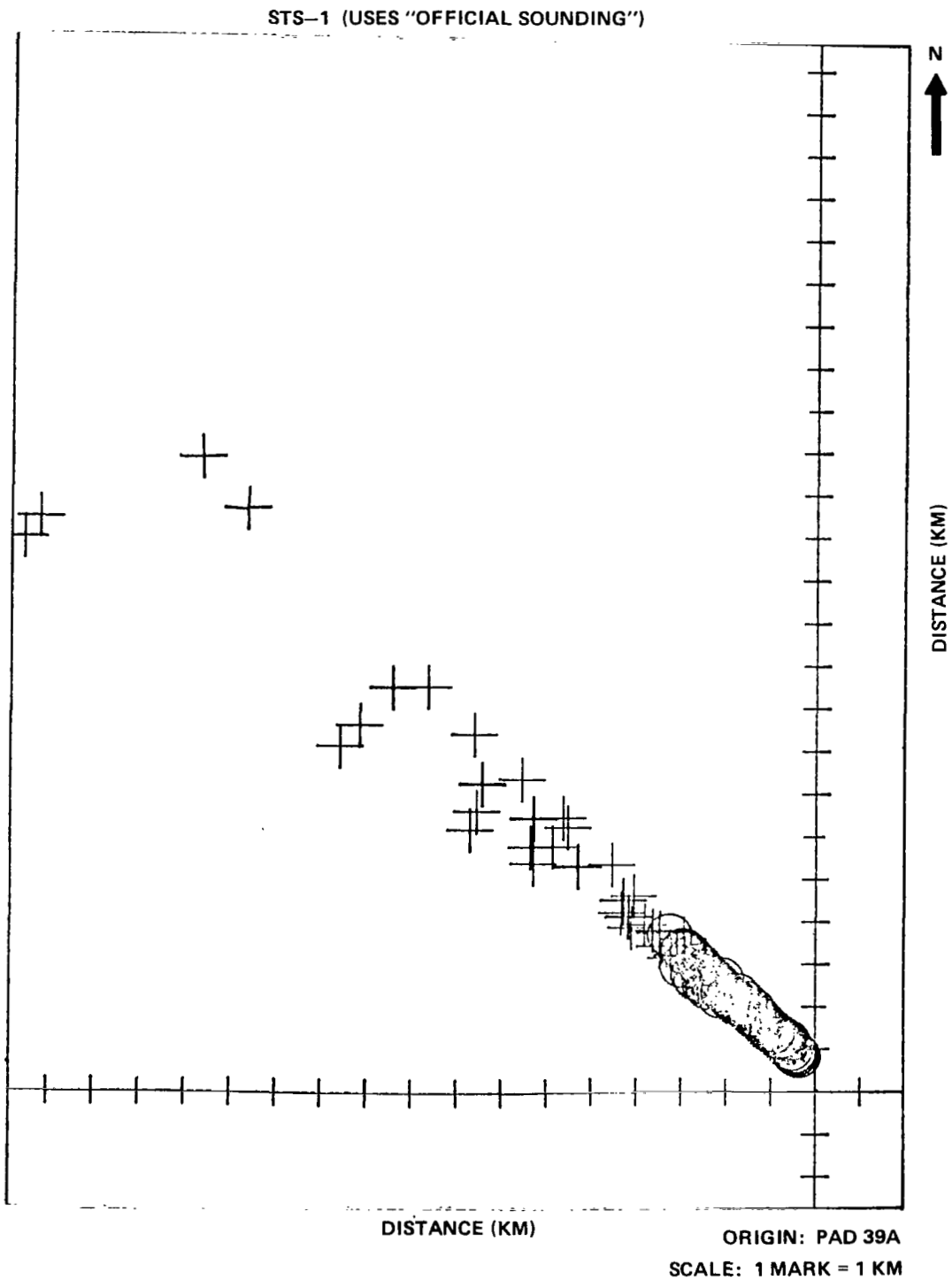

Figure IIIe-1. Deposition trajectory model output for STS-1. The exhaust cloud ground track is denoted by dots. "Wet" fallout is represented by circles and "dry" fallout by crosses. The origin is centered on launch pad 39A.

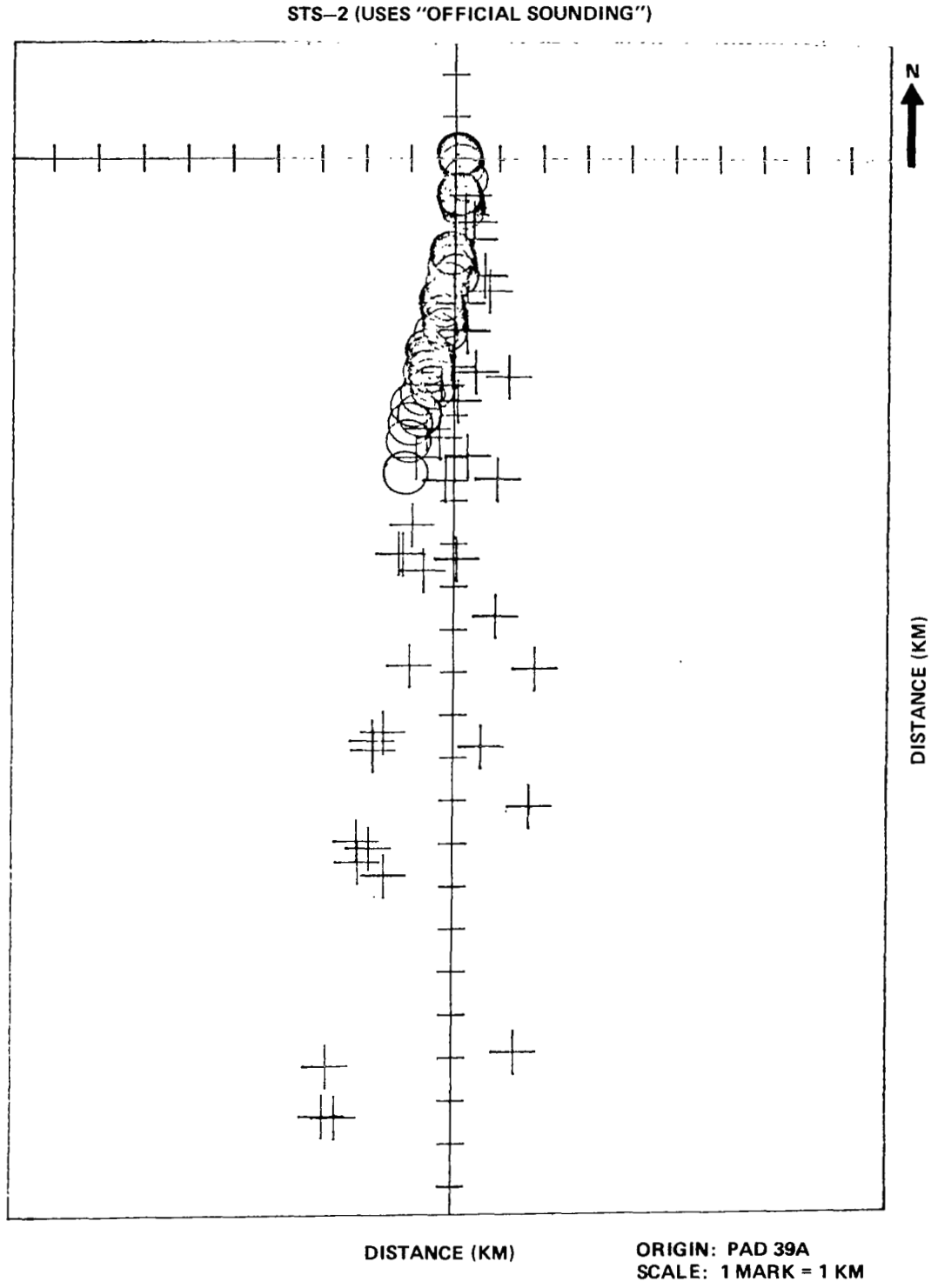

Figure IIIe-2. Deposition trajectory model output for STS-2. The exhaust cloud ground track is denoted with dots. "Wet" fallout is represented by circles and "dry" fallout by crosses. The origin is centered on launch pad 39A.

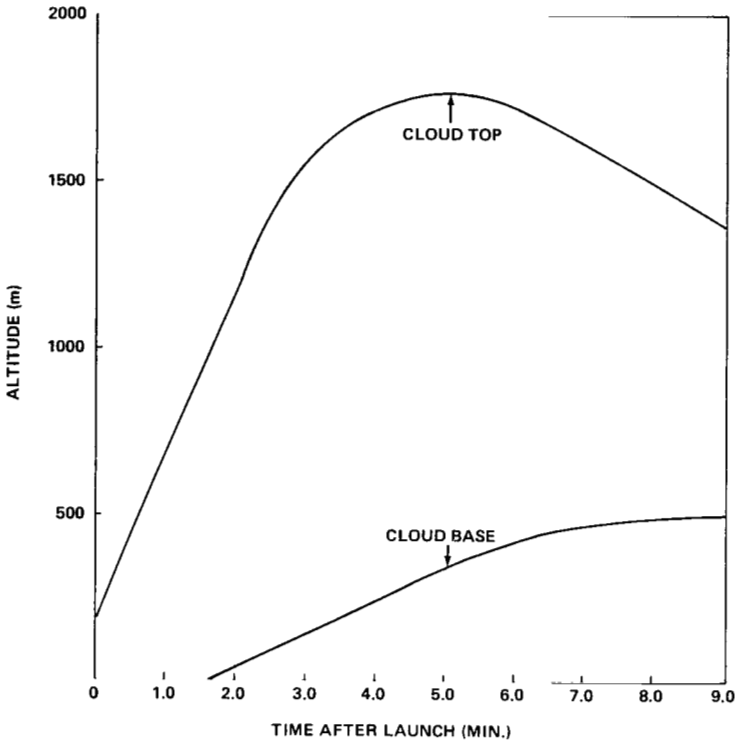

Figure IIIe-3. Height of exhaust cloud base and cloud top as functions of time after the STS-1 launch. The curves are based on analysis of KSC photographs taken at 30 sec intervals.

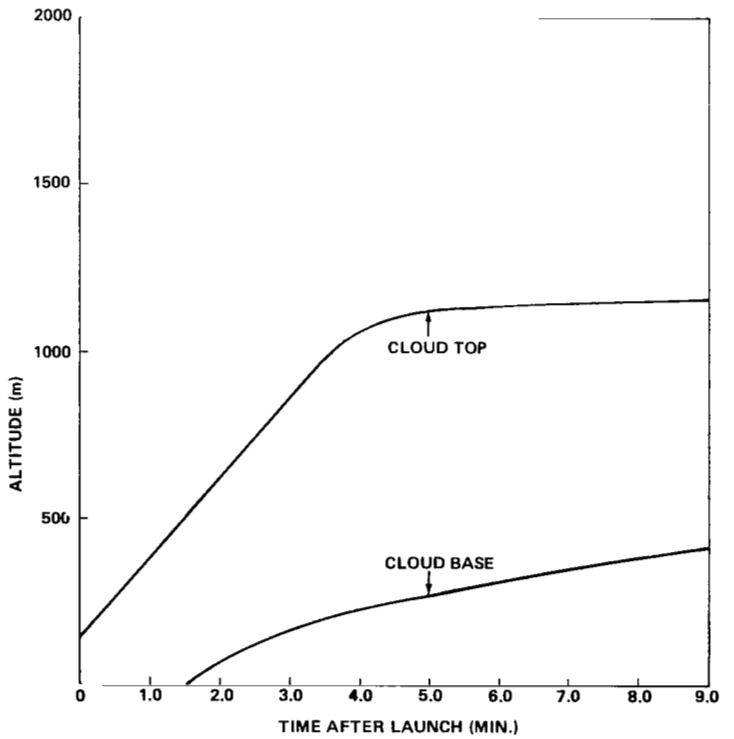

Figure IIIe-4. Height of exhaust cloud base and cloud top as functions of time after the STS-3 launch. The curves are based on analysis of KSC photographs taken at 30 sec intervals.

IV. SUMMARY AND CONCLUSIONS

This study was initiated to determine the controlling mechanism in the acidic deposition production process. The primary conclusion is that the acidic deposition results from atomization of the deluge water by the extreme shears and turbulence of the vehicle exhausts. This mechanism produces the large liquid drops which become the core of the deposition. The initial size must be at least 20 percent of the final deposition diameter, but something in excess of 70 percent is more likely. These drops rapidly coagulate with large numbers of small aluminum oxide particles and cloud drops (condensed water) which contribute to the final composition. Hydrogen chloride gas is rapidly and efficiently scavenged by both the large and small liquid drops. The entire deposition formation process is very rapid. It is essentially complete within 60 sec of SRB ignition although coagulation, evaporation, condensation, and scavenging continue to modify its properties at diminished rates. The formation process is largely independent of ambient atmospheric conditions although ambient temperature and humidity must impact the cloud density and the rate of HCl scavenging. These effects, however, are probably not discernible by measurement across the range of conditions expected for actual launches.

The definitive evidence for this concept of deposition formation was provided by the 6.4 percent model tests at MSFC. The fact that deposition forms in these very small, short-lived clouds virtually eliminates the possibility that the formation is controlled by "cloud physics" type processes in the later stages of the cloud's life cycle. Confirming evidence is provided by the following:

a) Calculation of the maximum rate of growth by a condensation/coagulation type mechanism.

b) The repeated occurrence of deposition near the pad in locations which indicate it must have spent only a short time within the exhaust cloud. Direct observation by video tape and rotating copper plate of the time of liquid deposition hitting the surface after STS-4.

c) Repeated occurrence of deposition at all launches, even on dry, windy days.

d) Laboratory data on the high affinity and rapid scavenging of HCl by water.

e) Presence of drops greater than 1 mm diameter on the first aircraft cloud pass only 4 min after the STS-3 launch.

f) The presence of large quantities of excess water, over and above the amount which can be evaporated by the heat from the exhaust, in and around the launch mount area at launch time (i.e., see Table IIIb-1).

Several additional conclusions can be drawn based on this picture of the deposition formation mechanism:

a) The location where the deposition falls will be highly dependent on the atmospheric conditions, especially winds and stability. However, since the formation is largely independent of atmospheric parameters, the problem of predicting the footprint of the deposition is greatly simplified, i.e., numerical models need only consider transport processes. Formation processes may be taken as a constant, dependent only on pad and vehicle configuration.

b) Since a substantial fraction of each deposition drop comes from the deluge water without an intervening phase transition, chemicals added to the deluge water will be well mixed into the deposition. Thus, there is a possibility of neutralizing the acid in the deposition by addition of a base to the deluge

water supply. The neutralizing chemicals would primarily be effective in the near field. Chemicals which ease the wash-down problem of the aluminum oxide residue could also be added. These possibilities are currently under study.

c) The possibilities of acidic fallout through mechanisms identified prior to this study (wash-out by precipitation from an overlying cloud, merger with a natural precipitating cloud or development into a precipitating system by natural mechanisms) are not appreciably altered by the findings of this study, although several factors have been revealed which tend to diminish the probability of a serious impact; the HCl scrubbing by the deluge water may reduce the HCl concentrations in the ground cloud by a measurable fraction, air flows may not organize quickly enough around the rising ground cloud to feed and support sustained growth.

d) Although the numerical analysis reported here is a very preliminary, quick-look study, it serves to point out that trapping the ground cloud on or near the surface is a possibility. The lifetime of the cloud and distance of travel are strongly dependent upon the meteorology and terrain so no definitive statement can be made as to whether a trapped cloud could reach civilian areas. However, it is clear that it would present a substantial hazard to those exposed. The problem is still under study.

e) The aircraft measurements of the aerosol properties in the STS-3 ground cloud indicate a very low probability that residue from the cloud would cause discernible "weather modification" effects in natural clouds by "cloud seeding." Cloud condensation nucleus counts rapidly decay to levels typical of polluted urban aerosols and the ice nuclei counts were not significantly different from the background counts in the boundary layer. However, ice nuclei are very sensitive to both counting technique and conditions of formation, and sufficient questions remain from laboratory studies that some additional work may be warranted. Other potential types of weather modification, impacts of the aerosol in the high troposphere and low stratosphere on cirrus formation, for example, have not been addressed in this study.

The two primary areas where additional work is required have already been mentioned, neutralization of the deposition by addition of chemicals to the deluge water and assessment of the potential for trapping the ground cloud against the surface. A concept test of neutralization is under consideration and another step in the assessment of cloud trapping will begin shortly. A third area where additional work is urgently needed is quantifying the HCl and water balances in the cloud, i.e., how much deposition is formed? What is the acid concentration? How is it distributed between near field and far? Considerable effort has already been made to address these questions and the effort is continuing. However, at present the data base is still too weak to allow anything but limited estimates. The measurement efforts made in this study illustrate that new measurement methods will have to be developed to completely address the problem.

REFERENCES

1. William H. Bowie: Environmental Effects of the STS-1 Flight Readiness Firing and Launch. Technology Inc., Life Sciences Div. for Medical Directorate, J. F. Kennedy Space Center, NASA, Contract Number NAS9-14880, October 1981.

2. "Environmental Impact Statement for the Kennedy Space Center," Final, October 1979.

3. William M. Knott: STS-2 Environmental Effects Final Report. Biomedical Office, J. F. Kennedy Space Center, February 15, 1982.

4. D. L. Johnson, G. Jasper, and S. C. Brown: Atmospheric Environment for Space (STS-1) Launch. NASA TM-82436, July 1981.

5. D. L. Johnson and S. C. Brown: Atmospheric Environment for Space Shuttle (STS-2) Launch. NASA TM-82463, December 1981.

6. R. Dawbarn, M. Kinslow and D. J. Watson: Analysis of the Measured Effects of the Principal Exhaust Effluents From Solid Rocket Motors. NASA CR-3136, January 1980.

7. D. L. Johnson, S. C. Brown, and G. W. Batts: Atmospheric Environment for Space Shuttle (STS-3) Launch. NAAS TM-82480, April 1982.

8. Lala, G. G., and J. E. Jiusto: An Automatic Light Scattering CCN Counter. J. Appl. Meteor., Vol. 16, 1977, pp. 413-418.

9. NASA Conference Publication 2212: The Third International Cloud Condensation Nuclei Workshop, October 6-17, 1980, Reno, Nevada, 1981, 288 pp.

10. Langer, G.: Evaluation of NCAR Ice Nucleus Counter, Pt. I: Basic Operation. J. Appl. Meteor., Vol. 12, 1973, pp. 1000-1011.

11. Hallett, J.: Measurement of Size, Concentration and Structure of Atmospheric Particulates by the Airborne Continuous Particle Replicator. AFGL-TR-76-0149, 1976, 92 pp.

12. Knollenberg, R. G.: Three New Instruments for Cloud Physics Measurements: The 2-D Spectrometer, the Forward Scattering Spectrometer Probe, and the Active Scattering Aerosol Spectrometer. Preprints, Intern. Conf. on Cloud Physics, Boulder, Colorado, 1976, pp. 554-561.

13. Knollenberg, R. G.: The Optical Array: An Alternate to Extinction and Scattering for Particle Size Measurements. J. Appl. Meteor., Vol. 9, No. 1, 1970.

14. Twomey, S.: Atmospheric Aerosols. Elsevier Scientific Pub. Co., New York, 1977, 302 pp.

15. "Environmental Impact Statement for the Kennedy Space Center," 1978 Edition.

16. Sheldon D. Smith: Space Shuttle Solid Rocket Motor Sea Level Exhaust Plume Prediction. Report on Contract NAS8-33719 by Lockheed Missiles & Space Co., Inc., Huntsville, Alabama, January 1981.

17. Mason, B. J.: The Physics of Clouds. Second edition, Clarendon Press, Oxford, 1971, p. 218.

18. Gomberg, R. I. and R. B. Stewart: A Computer Simulation of the Afterburning Processes Occurring Within Solid Rocket Motor Plumes in the Troposphere. NASA Technical Note D-3803, 1976.

19. Radke, L. F., et al.: Airborne Measurements of Cloud Forming Nuclei and Aerosol Particles at Kennedy Space Flight Center, Florida. Naval Weapons Center TM 3667, 1978.

20. Wisniewski, J. and G. Langer: Ice Nucleus Concentrations Measured During the 1975 Florida Area Cumulus Experiment (FACE). J. Appl. Meteor., Vol. 19, 1980, pp. 676-682.

21. Parungo, F. P.: Measurement of Lead in Urban Air for Weather Modification Research. J. Appl. Meteor., Vol. 9, 1970, pp. 468-475.

22. Super, A. B.: AgI Plume Characteristics Over the Bridger Range, Montana. J. Appl. Meteor., Vol. 13, 1970, pp. 62-70.

23. Heimbach, J. A.: A Suggested Technique for the Analysis of Airborne Continuous Ice Nucleus Data. J. Appl. Meteor., Vol. 16, 1977, pp. 225-261.

24. Langer, G. and D. Garvey: Interomparison of MEE and NCAR Ice Nucleus Counter and the CAS Isothermal Chamber. J. Weather Mod., Vol. 12, 1980, pp. 24-33.

25. Parungo, F. P., and P. A. Allee: Rocket Effluent: Its Ice Nucleation Activity and Related Properties. J. Appl. Meteor., Vol. 17, 1978, pp. 1856-1863.

26. Hindman, E. E., II, D. M. Garvey, G. Langer, F. K. Odencrantz, and G. L. Gregory: Laboratory Investigations of Cloud Nuclei from Combustion of Space Shuttle Propellant. J. Appl. Meteor., Vol. 19, 1980, pp. 175-184.

27. Hindman, E. E., II, L. F. Radke, and M. W. Eltgroth: Measurements of Cloud Nuclei in the Effluents from Launches of Liquid- and Solid-Fueled Rockets. J. Appl. Meteor., Vol. 21, 1982, pp. 1323-1331.

28. Orville, H. D.: A Numerical Study of the Initiation of Cumulus Clouds Over Mountainous Terrain. J. Atmos. Sci., Vol. 22, 1965, pp. 684-699.

29. Liu, J. Y., and H. D. Orville: Numerical Modeling of Precipitation and Cloud Shadow Effects on Mountain-Induced Cumuli. J. Atmos. Sci., Vol. 26, 1969, pp. 1283-1298.

30. Orville, H. D. and K. G. Hubbard: On the Freezing of Liquid Water in a Cloud. J. Appl. Meteor., Vol. 12, 1973, pp. 671-676.

31. Orville, H. D. and F. J. Kopp: Numerical Simulation of Life History of a Hailstorm. J. Atmos. Sci., Vol. 34, 1977, pp. 1596-1618.

32. Chen, C-H., and H. D. Orville: Effects of Mesoscale Convergence on Cloud Convection. J. Appl. Meteor., Vol. 19, 1980, pp. 256-274.

33. Orville, H. D., P. A. Eckhoff, J. E. Peak, J. H. Hirsch, and F. J. Kopp: Numerical Simulation of the Effects of Cooling Tower Complexes on Clouds and Severe Storms. Atmos. Environ., Vol. 15, 1981, pp. 833-836.

BIBLIOGRAPHY

Bjorklund, J. R., R. K. Dumbauld, C. S. Cheney, and H. V. Geary: User's Manual for the REEDM Rocket Exhaust Effluent Diffusion Model Computer Program. NASA Contractor Report 3646, 1982.

Bosart, L., J. E. Jiusto, G. G. Lala, V. A. Mohnen, V. J. Schaefer, and E. Bollay: Position paper on the potential of inadvertent weather modification of the Vandenberg area resulting from the Space Shuttle Solid Rocket Booster exhaust clouds. Prepared for NASA Langley Research Center, Contract NAS1-15948, 1980.

Goldford, A. I., S. I. Adelfang, J. S. Hickey, S. R. Smith, R. P. Welty, and G. L. White: Environmental Effects from SRB Exhaust Effluents – Technique Development and Preliminary Assessment. NASA Contractor Report 2923, 1977.

Hermsen, R. W.: Aluminum Oxide Particle Size for Solid Rocket Motor Performance Prediction. J. Spacecraft, Vol. 18, No. 6, 1981, pp. 483-490.

Hindman, E. E., II, and G. G. Lala: Comments on Rocket Effluent: Its Ice Nucleation Activity and Related Properties. J. Appl. Meteor., Vol. 19, 1980, pp. 122-128.

Knutson, E. O. and D. L. Fenton: Atmospheric Scavenging of Hydrochloric Acid. NASA Contractor Report CR-2598, 1975.

Lala, G. G.: Measurements of Ice Nucleus Concentrations in Titan Rocket Exhaust Clouds. Final Report on Contract NAS9-15538, NASA Johnson Space Flight Center, Houston, Texas, 1978.

Pellett, G. L.: Analytic Model for Washout of HCl(g) from Dispersing Rocket Exhaust Clouds. NASA Technical Paper 1801, 1981.

Pellett, G. L., D. I. Sebacher, R. J. Bendura, and E. E. Wornom, 1983: HCl in Rocket Exhaust Clouds: Atmospheric Dispersion, Acid Aerosol Characteristics, and Acid Rain Deposition. JAPCA, Vol. 33, No. 4, 1983, pp. 304-311.

Pellett, G. L., R. J. Bendura, and R. W. Storey: Near-Field Deposition of Acidic Droplets from Titan III Space Shuttle Launches. Presented at 1981 Annual Meeting JANNAF Safety and Environmental Protection Subcommittee, November 17-20, 1981, Kennedy Space Center, Florida.

Pellett, G. L. and W. R. Cofer, III: Effect of Metastable Alumina Dissolution on Water Vapor Pressure Over Aqueous HCl and Modification of Warm Rain Processes by Chlorided Alumina from Space Shuttle Exhaust. Presented at the Shuttle Environmental Effects, NASA, Johnson Space Center, 1978.

Radke, L. F., P. V. Hobbs, and D. A. Hess: Aerosols and Trace Gases in the Effluents Produced by the Launch of Large Liquid- and Solid-Fueled Rockets. J. Appl. Meteor., Vol. 21, 1982, pp. 1332-1345.

Radke, L. F., P. V. Hobbs and M. W. Eltgroth: Airborne Measurements in the Column and Ground Cloud from a Titan III Rocket. Department of Atmospheric Sciences, University of Washington, Seattle, Washington, Technical Report prepared for Naval Weapons Center, China Lake, California, 1979.

Stephens, J. B. and R. B. Stewart: Rocket Exhaust Effluent Modeling for Tropospheric Air Quality and Environmental Assessments. NASA Technical Report TR R-473, 1977.

Susko, M.: Electrets Used to Measure Exhaust Cloud Effluents from Solid Rocket Motor (SRM) During Demonstration Model (DM-2) Static Test Firing. NASA TM 78171, 1978.

Varsi, G.: Particulate Measurements. Proceedings of the NASA Atmospheric Effects Working Group Meeting, Vandenberg Air Force Base, 1976.

Woods, D.: Rocket Effluent Size Distributions Made with a Cascade Quartz Crystal Microbalance. Proceedings of 4th Joint Conference on Sensing of Environmental Pollutants. Amer. Chem. Soc., 1978, pp. 716-718.

Woods, D. C., R. J. Bendura, and D. E. Wornom: Launch Vehicle Effluent Measurments During the August 20, 1977, Titan III Launch at Air Force Eastern Test Range. NASA Technical Memorandum 78778, 1979.

APPENDIX I

Computer listings of our current Fortran IV deposition trajectory model, TRAJM, and associated plot program, VPLOT, are given below. Details of their development and operation are discussed in Section III.E.

```
0001  FTN4X,L
0002  $FILES(0,2)
0003        PROGRAM TRAJM
0004  C
0005  C     UPDATE:  2:30 PM  FRI., 22  JULY, 1983
0006  C
0007  C
0008  C ---DEFINITIONS
0009  C     CLBS=CLOUD BASE(M), CLTP=CLOUD TOP(M), CLCTR=CLOUD CENTER(M)
0010  C     TT=TIME AFTER LAUNCH(SECS)
0011  C     XCLP=X COORDINATE OF CLOUD POSITION(M)
0012  C     YCLP=Y COORDINATE OF CLOUD POSITION(M)
0013  C     DT=TIME BETWEEN CLOUD HEIGHT OBSERVATIONS(SECS)
0014  C     WZCL=CLOUD RISE RATE(M/S)
0015  C     HT=HEIGHT ABOVE GROUND(M)
0016  C     U=WIND SPEED AT THAT HEIGHT(M/S)
0017  C     DIR=DIRECTION WIND IS COMING FROM AT THAT HEIGHT(DEGREES MEASURED
0018  C     CLOCKWISE FROM NORTH)
0019  C     TC=TEMPERATURE(CELSIUS) AT THAT HEIGHT
0020  C     TD=DEW POINT TEMPERATURE (C) AT THAT HEIGHT
0021  C     RH=RELATIVE HUMIDITY AT THAT HEIGHT (%)
0022  C     TOFI=TIME(L+MIN) OF DROP IMPACT ON GROUND
0023  C     DIAIN=INITIAL DROP DIAMETER (UM)
0024  C     FDIA=FINAL DROP DIAMETER (UM)
0025  C     FXC=X-COORDINATE OF FINAL DROP IMPACT (M)
0026  C     FYC=Y-COORDINATE OF FINAL DROP IMPACT (M)
0027  C     FDIST=FINAL DISTANCE OF DROP FROM PAD (M)
0028  C     FANG=FINAL ANGLE OF DROP FROM PAD (DEGREES)
0029  C     XIA=DROP FALLS FROM (XIA=1 CLOUD BASE) OR (XIA=2 CLOUD TOP)
0030  C     XWOD=TELLS IF DROP IS WET, DRY OR EVAPORATED
0031  C     PRAT=DRY PARTICLE DIAMETER (UM)
0032  C
0033        DIMENSION XCLP(100),YCLP(100),          WZCL(100),CLCTR(100)
0034        DIMENSION UXC(90),UYC(90),D(10),LABL(8),WD(100)
0035        DIMENSION ZL(90),UXA(90),UYA(90),TDBF(90),RH(100)
0036        DIMENSION TOFI(100),DIAIN(100),FDIA(100),FXC(100),FYC(100)
0037        DIMENSION FDIST(100),FANG(100),XIA(100),PRAT(100),XWOD(100)
0038        COMMON /D/ CLBS(100),CLTP(100),TT(100),HT(100),U(100),DIR(100)
0039       1 ,TC(100),TD(100)
0040        WRITE(1,9999)
0041  9999  FORMAT("ENTER FILE NAME&")
0042        READ(1,9998) (LABL(I),I=1,8)
0043  9998  FORMAT(8A2)
0044        WRITE(1,9997)
0045  9997  FORMAT("ENTER CART NO.& _")
0046        READ(1,*) ICART
0047        OPEN(ICART,FILE=LABL,STATUS='NEW',IOSTAT=IOS,ERR=99)
0048  C
0049  C----INITIALIZATION OF VARIABLES
0050  C
0051  C     NCHO=NUMBER OF CLOUD HEIGHT OBSERVATIONS ENTERED
0052  C     M=NUMBER OF SOUNDING LEVELS USED
0053  C
0054  C**************************************
0055  C  CHANGE NCHO AND M APPROPRIATELY
0056  C
0057        NCHO=19
0058        M=21
```

```
0059  C****************************************
0060  C
0061        N=NCHO+1
0062  C
0063  C---CONVERT SOUNDING HEIGHT AND WIND SPEED TO METRIC UNITS
0064  C
0065        DO 10 ME=1,M
0066        HT(ME)=HT(ME)*0.3048
0067        U(ME)=U(ME)*0.3048
0068     10 CONTINUE
0069  C
0070  C---COMPUTE RELATIVE HUMIDITY
0071  C
0072        DO 20 IG=1,M
0073        TCK=TC(IG)+273.16
0074        TDK=TD(IG)+273.16
0075        RH(IG)=(10.**(2353.*(1./TCK-1./TDK)))*100.
0076     20 CONTINUE
0077  C
0078        N1 = N - 1
0079        WRITE(ICART,8999) N1
0080  8999  FORMAT(" N1="I3)
0081        CLCTR(1)= (CLBS(1) + CLTP(1))/2.
0082        XCLP(1)=1.
0083        YCLP(1)=500.
0084        WZCL(1)=10.
0085        PI=4.0*ATAN(1.0)
0086        DO 30 I=1,M
0087        WD(I)=DIR(I)
0088  30    DIR(I)=DIR(I)*PI/180.
0089  C
0090  C---COMPUTE CLOUD POSITION AS A FUNCTION OF TIME
0091  C
0092    250 DO 500 II=2,N
0093    260 CLCTR(II)=(CLBS(II)+CLTP(II))/2.
0094    270 IJ=II-1
0095    320 WZCL(II)=(CLCTR(II)-CLCTR(IJ))/(TT(II)-TT(IJ))
0096        K=1
0097        KW=1
0098        DO 400 I=M,1,-1
0099        IF(CLTP(II).LE.HT(I)) KW=I-1
0100        IF(CLBS(II).LE.HT(I)) K=I
0101    400 CONTINUE
0102        IF(KW.LT.K+1) GO TO 435
0103        L=1
0104  C
0105  C---AVERAGE WEIGHTED WIND BETWEEN CLOUD BASE AND
0106  C     CLOUD TOP ACTS ON CLOUD CENTER
0107  C
0108        DO 410 ID=K+1,KW
0109        ZL(L)=(HT(ID)-HT(ID-1))
0110        UXC(ID-1)=U(ID-1)*COS(3.*PI/2.-DIR(ID-1))
0111        UYC(ID-1)=U(ID-1)*SIN(3.*PI/2.-DIR(ID-1))
0112        UXC(ID)=U(ID)*COS(3.*PI/2.-DIR(ID))
0113        UYC(ID)=U(ID)*SIN(3.*PI/2.-DIR(ID))
0114        UXA(L)=(UXC(ID-1)+UXC(ID))/2.
0115        UYA(L)=(UYC(ID-1)+UYC(ID))/2.
0116        L=L+1
0117    410 CONTINUE
0118        UXL=0.
```

```
0119          UYL=0.
0120          ZTOT=0.
0121          DO 415 JV=1,L-1
0122          UXL=UXA(JV)*ZL(JV)+UXL
0123          UYL=UYA(JV)*ZL(JV)+UYL
0124          ZTOT=ZL(JV)+ZTOT
0125      415 CONTINUE
0126          UX=UXL/ZTOT
0127          UY=UYL/ZTOT
0128          GO TO 440
0129      435 UX=U(K)*COS(3.*PI/2.-DIR(K))
0130          UY=U(K)*SIN(3.*PI/2.-DIR(K))
0131      440 CONTINUE
0132          DT=TT(II)-TT(IJ)
0133      460 XCLP(II)=UX*DT+XCLP(IJ)
0134      470 YCLP(II)=UY*DT+YCLP(IJ)
0135      500 CONTINUE
0136    C
0137    C---PRINT SOUNDING DATA
0138    C
0139          WRITE(6,2800)
0140     2800 FORMAT(42X,"SOUNDING DATA",/)
0141          WRITE(6,2810)
0142     2810 FORMAT(/,3X,"HEIGHT (M)",5X,"WIND SPEED (M/SEC)",
0143         1 5X,"WIND DIR (CW FROM N)",5X,"TEMPERATURE (C)",5X,
0144         2 "REL HUMID (%)",5X,"DEW PT TEMP (C)",2X)
0145          DO 525 LZ=1,M
0146          WRITE(6,2820) HT(LZ),U(LZ), WD(LZ),TC(LZ),RH(LZ),TD(LZ)
0147     2820 FORMAT(3X,F10.1,10X,F5.1,17X,F5.1,20X,F6.1,14X,F5.1,14X,F6.1)
0148      525 CONTINUE
0149    C
0150    C---PRINT CLOUD POSITION VERSUS TIME
0151    C
0152          WRITE(6,2900)
0153          WRITE(ICART,2900)
0154     2900 FORMAT(1H1,    40X,26HCLOUD POSITION VERSUS TIME,/)
0155      550 WRITE(6,3000)
0156          WRITE(ICART,3000)
0157     3000 FORMAT(/,3X,10HTIME (MIN),5X,10HCLBASE (M),5X,10HCLDTOP (M),5X,
0158         1 10HCLDCTR (M),5X,8HXCLP (M),5X,8HYCLP (M),5X,8HRCLP (M),5X,
0159         2 5HTHETA,2X)
0160      560 DO 700 IK=1,N-1
0161      570 RCLP=(XCLP(IK)*XCLP(IK) + YCLP(IK)*YCLP(IK))**.5
0162    C     COMPUTER GIVES ANGLES IN QUADRANTS I AND IV
0163      580 ALP=ATAN(YCLP(IK)/XCLP(IK))
0164    C     STANDARD NOTATION MEASURES ANGLES COUNTERCLOCKWISE FROM EAST
0165            IF(XCLP(IK).LT.0.) ALP=PI+ALP
0166    C     MAP DIRECTIONS GIVE ANGLES CLOCKWISE FROM NORTH
0167            THETA=PI/2.-ALP
0168            IF (THETA.LT.0.) THETA=2.*PI+THETA
0169    C     CHANGE FROM RADIANS TO DEGREES
0170            THETA=THETA*180./PI
0171            TM=TT(IK)/60.
0172      600 WRITE(6,3010) TM     ,CLBS(IK),CLTP(IK),CLCTR(IK),XCLP(IK),
0173         1 YCLP(IK),RCLP,THETA
0174            WRITE(ICART,3010) TM     ,CLBS(IK),CLTP(IK),CLCTR(IK),XCLP(IK),
0175         1 YCLP(IK),RCLP,THETA
0176     3010 FORMAT(3X,F10.1,5X,F10.1,5X,F10.1,5X,F10.1,5X,F8.1,5X,F8.1,5X,
0177         1 F8.1,5X,F5.1)
0178      700 CONTINUE
```

```
0179  C
0180  C---COMPUTE DROP TRAJECTORIES
0181  C
0182  C      DELT=TIME FOR DROP TO FALL FROM HEIGHT ZN TO HEIGHT ZNM1(SECS)
0183  C      D=DROP DIAMETER(MICRONS)
0184  C      V=DROP TERMINAL VELOCITY(M/SEC)
0185  C      TT=TIME AFTER SHUTTLE LAUNCH (SECS)
0186  C      XN=X COORDINATE MEASURED EAST FROM PAD (M)
0187  C      YN=Y COORDINATE MEASURED NORTH FROM PAD (M)
0188  C      ZN=HEIGHT OF DROP ABOVE GROUND (M)
0189  C      ZNM1=HEIGHT OF NEXT LOWER SOUNDING (M)
0190  C      NDS=NUMBER OF DROP SIZES BEING ALLOWED TO FALL
0191  C      DIAMIN=MINIMUM PARTICLE DIAMETER. SMALLER PARTICLES "EVAPORATE"
0192  C      IV=A COUNTER
0193  C      TDBF=TIME AFTER LAUNCH WHEN DROP BEGINS FALLING (MIN)
0194  C
0195  C  -INITIAL DROP SIZES
0196  C
0197     750 NDS=10
0198  C
0199         D(1)=2000.
0200         D(2)=1500.
0201         D(3)=1250.
0202         D(4)=1000.
0203         D(5)=750.
0204         D(6)=500.
0205         D(7)=400.
0206         D(8)=300.
0207         D(9)=200.
0208         D(10)=150.
0209         DIAMIN=100.
0210         IV=1
0211         JB=1
0212  C
0213  C  -DROPS FALLING FROM CLOUD; FIRST FROM CLOUD BASE THEN FROM CLOUD TOP
0214  C
0215     800 DO 1500 IA=1,2
0216         IF(IA.GT.1) GO TO 900
0217     810 WRITE(6,4000)
0218    4000 FORMAT(/////,39X,"  DROPS FALLING FROM CLOUD BASE"
0219        1,/)
0220         GO TO 950
0221     900 CONTINUE
0222     910 WRITE(6,4010)
0223    4010 FORMAT(/////,39X,"  DROPS FALLING FROM CLOUD TOP"
0224        1,//)
0225     950 CONTINUE
0226  C    COMPUTE TRAJECTORY FOR EACH SELECTED DROP SIZE
0227     955 DO 1500 JA=1,NDS
0228  C    COMPUTE TRAJECTORY FOR DIFFERENT POINTS ALONG CLOUD PATH
0229     960 DO 1500 I=2,N,4
0230         DIA=D(JA)
0231         RATIO=(.3*(DIA**3.))**(1./3.)
0232         IF(IA.EQ.1) ZN=CLBS(I)
0233         IF(IA.EQ.2) ZN=CLTP(I)
0234         IF(ZN.EQ.0.) GO TO 970
0235     965 WRITE(6,4020)
0236    4020 FORMAT(/,3X,10HTIME (MIN),3X,13HDROP DIA (UM),3X,11HVTERM (M/S),
0237        1 3X,10HHEIGHT (M),3X,12HDISTANCE (M),3X,17HANGLE (CW FROM N),
0238        2 3X,11HX-COORD (M),3X,11HY-COORD (M),2X)
```

```
0239     970 CONTINUE
0240         NN=1
0241     975 DO 1000 J=1,N
0242         IF(ZN.LE.HT(J)) GO TO 1001
0243    1000 CONTINUE
0244    1001 NN=J-1
0245         IF(NN.EQ.0) NN=1
0246         ZNM1=HT(NN)
0247         IF(ZNM1.GE.ZN) GO TO 1500
0248         TDBF(JB)=TT(I)/60.
0249         JB=JB+1
0250         MM=NN+1
0251         UZN=U(MM)
0252         THN=DIR(MM)
0253         RHZN=RH(MM)
0254         TCZN=TC(MM)
0255         UZNM1=U(NN)
0256         THNM1=DIR(NN)
0257         RHZNM1=RH(NN)
0258         TCZNM1=TC(NN)
0259         X=XCLP(I)
0260         Y=YCLP(I)
0261         TM=TT(I) /60.
0262         DELT=0.
0263         A=.00447
0264         B=-.191
0265    C
0266    C    DROP TERMINAL VELOCITY VERSUS DROP DIAMETER
0267    C
0268    1050 IF(DIA.LE.300) GO TO 1070
0269         V=9.65-10.30*EXP(-.0006*DIA)
0270         GO TO 1080
0271    C    NOT GOOD EQUATION FOR DIAMETERS LESS THAN 100 UM
0272    1070 V=A*DIA+B
0273    1080 CONTINUE
0274    C
0275    C   -RADIAL DISTANCE AND DIRECTION FROM LAUNCH PAD
0276    C
0277         R=(X*X+Y*Y)**.5
0278         ALPHA=ATAN(Y/X)
0279         IF(X.LT.0.) ALPHA=PI+ALPHA
0280         THET=PI/2.-ALPHA
0281         IF(THET.LT.0.) THET=2.*PI+THET
0282         THET=THET*180./PI
0283    1082 WRITE(6,4030) TM,DIA,V,ZN,R,THET,X,Y
0284    4030 FORMAT(3X,F10.3,3X,F13.2,3X,F11.2,3X,F10.1,3X,F12.1,3X,F17.1,
0285        1 3X,F11.1,3X,F11.1,2X)
0286         IF (ZN.NE.0.) GO TO 1086
0287    1085 CONTINUE
0288         FDIA(IV)=DIA
0289         TOFI(IV)=TM
0290         DIAIN(IV)=D(JA)
0291         FXC(IV)=X
0292         FYC(IV)=Y
0293         FDIST(IV)=R
0294         FANG(IV)=THET
0295         XIA(IV)=IA
0296         PRAT(IV)=RATIO
0297         IV=IV+1
0298         IF (DIA.EQ.RATIO) WRITE(6,4040)
```

```
 4040 FORMAT(16X,"**** DRY PARTICLE ****",/)
      GO TO 1500
 1086 DELT=(ZN-ZNM1)/V
C
C---DETERMINE AVERAGE WIND SPEED IN EACH SUCCESSIVELY LOWER
C   HORIZONTAL LAYER (M/S)
C
      UZNX=UZN*COS(3.*PI/2.-THN)
      UZNY=UZN*SIN(3.*PI/2.-THN)
      UZNXM1=UZNM1*COS(3.*PI/2.-THNM1)
      UZNYM1=UZNM1*SIN(3.*PI/2.-THNM1)
      UXAVE=(UZNX+UZNXM1)/2.
      UYAVE=(UZNY+UZNYM1)/2.
      TM=TM+DELT/60.
      XM1=X+UXAVE*DELT
      YM1=Y+UYAVE*DELT
      X=XM1
      Y=YM1
      ZN=ZNM1
      UZN=UZNM1
      THN=THNM1
C
C---DETERMINE AMOUNT OF EVAPORATION IN THIS LAYER
C
C     DELR=CHANGE IN DROP RADIUS (CM)
C     RDROP=RADIUS OF DROP (CM)
C     TK=TEMPERATURE (KELVIN)
C     AL=LATENT HEAT OF CONDENSATION (ERG/G)
C     AK=THERMAL CONDUCTIVITY OF AIR (ERG/CM S K)
C     RHOL=DENSITY OF WATER (G/CM3)
C     RW=GAS CONSTANT FOR MOIST AIR (ERG/G K)
C     PRESS=AIR PRESSURE AT GIVEN TEMPERATURE IN
C           U.S. STANDARD ATMOSPHERE (MB)
C     DIFF=DIFFUSIVITY OF WATER VAPOR THROUGH AIR (CM2/S)
C     RHOST=SATURATED VAPOR DENSITY OF WATER (G/CM3)
C     SIG=SATURATION RATIO MINUS ONE
C
      RHAVE=(RHZN+RHZNM1)/2.
      SIG=(RHAVE/100.-1.)
      TCAVE=(TCZN+TCZNM1)/2.
      TKAVE=TCAVE+273.16
      AL=(2.501-.0024*TCAVE)*(10.**10.)
      AK=(5.69+.0168*TCAVE)/2.39E-3
      RHOL=1.0
      RW=4.615E6
      RDROP=DIA/2.E4
      PRESS=1013.25*((TKAVE/288.16)**5.256)
      DIFF=(1.87E-6)*PRESS*(TKAVE**2.072)/1013.25
      RHOST=((1.3239E-3)*(10.**(7.5*TCAVE/(TKAVE-35.86))))/TKAVE
      VAPOR=(RHOL/(DIFF*RHOST))
      HEAT=(((AL*RHOL)/(AK*TKAVE))*(AL/(RW*TKAVE)-1.))
      DELR=(SIG*(1.+(V*100.*RDROP/(2.*PI*DIFF))**.5)*DELT/RDROP)
     1 *(1./(HEAT+VAPOR))
 1088 DIA=DIA+2.*DELR*(10.**4.)
      TCZN=TCZNM1
      RHZN=RHZNM1
 1089 IF (DIA.LE.RATIO) DIA=RATIO
      IF(DIA.LT.DIAMIN) GO TO 1090
      NN=NN-1
      IF(NN.LE.0) ZNM1=0.
```

```
0359          IF(NN.LE.0) UZNM1=0.
0360          IF(NN.LE.0) GO TO 1100
0361          ZNM1=HT(NN)
0362          UZNM1=U(NN)
0363          THNM1=DIR(NN)
0364          TCZNM1=TC(NN)
0365          RHZNM1=RH(NN)
0366          GO TO 1100
0367     1090 CONTINUE
0368          JB=JB-1
0369     1095 WRITE(6,4050)
0370     4050 FORMAT(    14X,"***** DROP EVAPORATED *****",//)
0371          GO TO 1500
0372     1100 CONTINUE
0373          GO TO 1050
0374     1500 CONTINUE
0375     1600 WRITE(6,5000)
0376          WRITE(ICART,5000)
0377     1610 WRITE(6,5010)
0378          WRITE(ICART,5010)
0379     5000 FORMAT(1H1,2X,"INIT TIME",3X,"FINAL TIME",4X,"INITIAL DIA",3X,
0380         1 "FINAL DIA",3X,"X-COORD",3X,"Y-COORD",3X,"DISTANCE",6X,"ANGLE",
0381         2 6X,"BASE OR",3X,"WET OR",3X,"DRY DIA")
0382     5010 FORMAT(4X,"(MIN)",8X,"(MIN)",9X,"(UM)",9X,"(UM)",7X,"(M)",7X,
0383         1 "(M)",8X,"(M)",5X,"(CW FROM N)",5X,"TOP?",6X,"DRY?",5X,"(UM)",/)
0384     1650 DO 1700 IB=1,IY-1
0385          IF(XIA(IB).EQ.1.) ORG=2HB
0386          IF(XIA(IB).EQ.2.) ORG=2HT
0387          XWOD(IB)=1.
0388          IF(FDIA(IB).LE.PRAT(IB)) XWOD(IB)=2.
0389          IF(FDIA(IB).LT.DIAMIN) XWOD(IB)=3.
0390          IF(XWOD(IB).EQ.1.) WOD= 2HW
0391          IF(XWOD(IB).EQ.2.) WOD= 2HD
0392          IF(XWOD(IB).EQ.3.) WOD= 2HE
0393     1660 WRITE(6,5050) TDBF(IB),TOFI(IB),DIAIN(IB),FDIA(IB),
0394         1FXC(IB),FYC(IB), FDIST(IB),FANG(IB),ORG,WOD,PRAT(IB)
0395          WRITE(ICART,5050) TDBF(IB),TOFI(IB),DIAIN(IB),FDIA(IB),
0396         1 FXC(IB),FYC(IB),FDIST(IB),FANG(IB),ORG,WOD,PRAT(IB)
0397     5050 FORMAT(4X,F6.2,7X,F6.2,5X,F8.1,5X,F8.1,3X,F8.1,2X,F8.1,3X,F7.1,
0398         1 7X,F5.1,10X,1A2,7X,1A2,4X,F8.1)
0399     1700 CONTINUE
0400          CLOSE(ICART,STATUS='KEEP',IOSTAT=IOS,ERR=99)
0401          STOP
0402     99   WRITE(1,9995) IOS
0403     9995 FORMAT("I/O ERROR NUMBER& _"I4)
0404          STOP
0405          END
0406          BLOCK DATA
0407          COMMON /D/CLBS(100),CLTP(100),TT(100),HT(100),U(100),DIR(100)
0408         1 ,TC(100),TD(100)
0409          DATA TT/0.,30.,60.,90.,120.,150.,180.,210.,240.,270.,300.,330.,
0410         1 360.,390.,420.,450.,480.,510.,540./,
0411         2CLBS/0.,0.,0.,0.,75.,130.,170.,200.,230.,255.,275.,292.,310.,
0412         3 330.,348.,368.,385.,402.,420./,
0413         4CLTP/145.,265.,388.,510.,630.,750.,875.,988.,1070.,1115.,1135.,
0414         5 1142.,1148.,1150.,1155.,1160.,1165.,1169.,1171./,
0415         6HT/21.,100.,200.,300.,400.,500.,600.,700.,800.,900.,1000.,
0416         7 1500.,2000.,2500.,3000.,3500.,4000.,4500.,5000.,5500.,6000./,
0417         8U/13.,15.,15.,16.,17.,9.,10.,16.,21.,20.,20.,18.,14.,20.,22.,
0418         9 22.,21.,17.,17.,17.,21./
```

```
0419          DATA DIR/60.,70.,79.,75.,96.,89.,80.,88.,100.,113.,118.,
0420         1 140.,143.,136.,162.,188.,207.,228.,245.,246.,213./
0421          DATA TC/22.8,22.4,22.0,21.5,21.1,20.6,20.2,19.7,19.3,18.8,
0422         1 18.4,17.5,16.5,15.5,14.5,13.4,12.3,12.5,12.8,12.5,12.1/,
0423         2 TD/13.3,13.2,13.2,13.1,13.0,13.0,12.9,12.8,12.7,12.7,12.6,
0424         3 11.5,10.3,10.3,10.4,10.6,10.9,3.0,-4.9,-5.6,-6.4/
0425    C
0426    C---DATA FROM STS-6
0427    C
0428    C---CLOUD HEIGHTS FROM STS-3
0429    C
0430          END
```

```
0001  FTN4X,L
0002  $FILES(0,2)
0003        PROGRAM VPLOT
0004        DIMENSION IPL(192),IPAR(5),LABL(8)
0005        COMMON ICART
0006        DATA XL/19.8/, YL/27.4/, IW/2HW /, ID/2HD /, IT/2HT /, IB/2HB /
0007        CALL RMPAR(IPAR)
0008  C
0009  C---------------------------
0010        ICART = IPAR(1)
0011        IPLT = IPAR(2)
0012  C---------------------------
0013  C
0014        WRITE(1,9999)
0015  9999  FORMAT("ENTER FILE TO BE OPENED␣")
0016        READ(1,9998) (LABL(I),I=1,8)
0017  9998  FORMAT(8A2)
0018        WRITE(1,9986)
0019  9986  FORMAT("ENTER FRACTIONS FXL,FYL␣")
0020        READ(1,*) FXL,FYL
0021        XORG = FXL*XL
0022        YORG = FYL*YL
0023        XMIN = -XORG
0024        YMIN = -YORG
0025        XMAX = XL + XMIN
0026        YMAX = YL + YMIN
0027        CALL PLOTR(IPL,2,1,IPLT)
0028        CALL VIEWP(IPL,10.2,76.5,10.2,102.4)
0029        CALL WINDW(IPL,XMIN,XMAX,YMIN,YMAX)
0030        CALL PEN(IPL,1)
0031        CALL FRAME(IPL)
0032        CALL AXES(IPL,1.,1.,0.,0.,50.,50.)
0033        OPEN(ICART,FILE=LABL,STATUS='OLD',IOSTAT=IOS,ERR=99)
0034        READ(ICART,9997) N1
0035  9997  FORMAT(" N1="I3)
0036        CALL JUNK(4)
0037        DO 100 I=1,N1
0038          READ(ICART,9996) XC,YC
0039  9996    FORMAT(63X,F8.1,5X,F8.1)
0040          CALL MOVE(IPL,XC/1000.,YC/1000.)
0041          CALL PENDN(IPL)
0042          CALL PENUP(IPL)
0043  100   CONTINUE
0044        CALL JUNK(3)
0045        CALL PEN(IPL,2)
0046        DO 200 I=1,32000
0047          READ(ICART,9995,END=250,IOSTAT=IOS,ERR=99) XD,YD,IBORT,IWOD
0048  9995    FORMAT(52X,F8.1,2X,F8.1,32X,A2, 7X,A2)
0049          IF(IBORT.EQ.IT) CALL PEN(IPL,1)
0050          IF(IWOD.EQ.IW) THEN
0051            CALL CIRCL(IPL,XD/1000.,YD/1000.)
0052          ELSE
0053            CALL CROSS(IPL,XD/1000.,YD/1000.)
0054          ENDIF
0055  200   CONTINUE
0056  250   CALL PEN(IPL,0)
0057        STOP
0058  99    WRITE(1,9994) IOS
```

```
0059  9994  FORMAT("I/O ERROR IOSTAT =Δ"I4)
0060        STOP
0061        END
0062        SUBROUTINE CIRCL(IPL,XC,YC)
0063        DIMENSION IPL(1)
0064        PI = 3.14159
0065        CALL MOVE(IPL,XC+0.5,YC)
0066        DO 100 I=0,36
0067          THETA = I*10.*PI/180.
0068          X = XC + 0.5*COS(THETA)
0069          Y = YC + 0.5*SIN(THETA)
0070          CALL DRAW(IPL,X,Y)
0071  100     CONTINUE
0072        CALL PENUP(IPL)
0073        RETURN
0074        END
0075        SUBROUTINE CROSS(IPL,XC,YC)
0076        DIMENSION IPL(1)
0077        CALL MOVE(IPL,XC-.5,YC)
0078        CALL DRAW(IPL,XC+.5,YC)
0079        CALL MOVE(IPL,XC,YC-.5)
0080        CALL DRAW(IPL,XC,YC+.5)
0081        CALL PENUP(IPL)
0082        RETURN
0083        END
0084        SUBROUTINE JUNK(N)
0085        COMMON ICART
0086        DO 100 I=1,N
0087          READ(ICART,9999) IJ
0088  9999    FORMAT(A2)
0089  100   CONTINUE
0090        RETURN
0091        END
0092        END$
```

1. REPORT NO.	2. GOVERNMENT ACCESSION NO.	3. RECIPIENT'S CATALOG NO.
NASA TP-2258		

4. TITLE AND SUBTITLE	5. REPORT DATE
Space Shuttle Exhaust Cloud Properties	December 1983
	6. PERFORMING ORGANIZATION CODE
7. AUTHOR(S)	8. PERFORMING ORGANIZATION REPORT #
B. J. Anderson and V. W. Keller (See Note)	
9. PERFORMING ORGANIZATION NAME AND ADDRESS	10. WORK UNIT NO.
George C. Marshall Space Flight Center Marshall Space Flight Center, Alabama 35812	M-433
	11. CONTRACT OR GRANT NO.
	13. TYPE OF REPORT & PERIOD COVERED
12. SPONSORING AGENCY NAME AND ADDRESS	Technical Paper
National Aeronautics and Space Administration Washington, D.C. 20546	14. SPONSORING AGENCY CODE

15. SUPPLEMENTARY NOTES

Prepared by Atmospheric Sciences Division
Systems Dynamics Laboratory, Science and Engineering

16. ABSTRACT

A data base describing the properties of the exhaust cloud produced by the launch of the Space Transportation System and the acidic fallout observed after each of the first four launches was assembled from a series of ground and aircraft based measurements made during the launches of STS 2, 3, and 4. Additional data were obtained from ground-based measurements during firings of the 6.4 percent model of the Solid Rocket Booster at the Marshall Center. Analysis indicates that the acidic fallout is produced by atomization of the deluge water spray by the rocket exhaust on the pad followed by rapid scavenging of hydrogen chloride gas and aluminum oxide particles from the Solid Rocket Boosters. The atomized spray is carried aloft by updrafts created by the hot exhaust and deposited down wind. Aircraft measurements in the STS-3 ground cloud showed an insignificant number of ice nuclei. Although no measurements were made in the column cloud, the possibility of inadvertent weather modification caused by the interaction of ice nuclei with natural clouds appears remote.

NOTE

Contributions to specific sections were made by M. T. Reischel, R. A. Sarma, G. D. Emmitt, and G. Langer under the auspices of the Universities Space Research Association, and by G. G. Lala of the State University of New York at Albany.

17. KEY WORDS	18. DISTRIBUTION STATEMENT
Space transportation system Exhaust cloud Aluminum oxide Hydrochloric acid Environmental effects	Unclassified - Unlimited Subject Category 46

19. SECURITY CLASSIF. (of this report)	20. SECURITY CLASSIF. (of this page)	21. NO. OF PAGES	22. PRICE
Unclassified	Unclassified	116	A06

For sale by National Technical Information Service, Springfield, Virginia 22161

NASA-Langley, 1983

National Aeronautics and
Space Administration

Washington, D.C.
20546

Official Business
Penalty for Private Use, $300

THIRD-CLASS BULK RATE

Postage and Fees Paid
National Aeronautics and
Space Administration
NASA-451

S

S 1 IU,E, 831206 S009,00S
DEPT OF THE AIR FORCE
AF WEAPONS LABORATORY
ATTN: TECHNICAL LIBRARY (SUL)
KIRTLAND AFB NM 87117

NASA

POSTMASTER: If Undeliverable (Section 158 Postal Manual) Do Not Return